Final Report

AMPC
AUSTRALIAN MEAT PROCESSOR CORPORATION

Plasma-Activated Water

A Cold Plasma Wash Water Technology for Meat Safety and Shelf-Life Extension

Project Code
2016-1326

Prepared by
Koentadi Hadinoto, Javiera Barrales Astorga and Francisco J. Trujillo

Date Submitted
19/09/22

Published by
Australian Meat Processor Corporation

Date Published
19/09/2022

Contents

1.0 Executive Summary

In this study, plasma activated water (PAW) was evaluated as a meat decontamination method. Project 2016-1326 developed and validated a novel non-thermal plasma (NTP) technology to improve the industry capability to achieve food safety and reduce microbial spoilage of fresh meat. PAW showed an efficient removal of pathogens suspended in water. When PAW is applied correctly on meat surfaces, it improved not only the safety of beef but also retained and in some cases improved quality parameters, particularly those of importance for consumer acceptability such as limiting the extent of lipid oxidation, limiting the rise in pH during storage and improving beef tenderness. For instance, spraying PAW on meat surfaces at 55 ^{o}C for 30 s followed by an additional water spraying at 25 ^{o}C for 60 s achieved higher inactivation compared to the same sequence of washing with water instead of PAW. This PAW washing sequence minimised the detrimental effect on the redness of the meat while achieving a significantly higher inactivation of *Salmonella*. It is important to note that the inactivation of *Salmonella* on meat surfaces required to heat PAW to 55 ^{o}C, and that failing to wash with water after the PAW application negatively affected the meat colour. Hence, a correct PAW application is required to achieve significantly higher inactivation levels while protecting the meat quality.

At the start of this project, 50 mL of PAW was produced. The PAW production was subsequently scaled up to 200 mL, 250 mL, 500 mL, 1 L and finally 2 L, which is an important achievement because most of reported studies produced PAW in mL to achieve similar decontamination efficiencies. In the scaling up process, different reactor configurations were evaluated. We firstly optimized the performance of the air pin-to-liquid discharge achieving the highest efficacy in the destructions of *Escherichia coli* and *Salmonella* Typhimurium. Secondly, we studied the performance of plasma-bubble discharge. Thirdly, we designed a novel hybrid plasma discharge (HPD) reactor, which produced both the pin-to-liquid and plasma-bubble discharges within one power source, increasing the volume of PAW by one-fold to 2 L. PAW produced by the HPD reactor exhibited the dual benefits of exceptional energy efficiencies and high bacterial removal at 30 seconds compared to literature studies, which take several minutes or hours to achieve same level of inactivation. This reactor design is another important achievement that was published in the Chemical Engineering Journal (Impact Factor = 16.744),

PAW can offer benefits because of its simple operation, as it is produced from water and electrical discharges, and its potential to be integrated in meat processing industries. Based on the findings in this project, meat washing with PAW can save water by up to 40.4%. However, the production of PAW at a commercial scale and the effect of PAW technology on carcasses in commercial facilities needs to be studied for the commercialisation of this technology. Furthermore, the capital cost related to implementing the scale-up PAW technology, estimated as AU$ 362,767 and AU$ 1,252,051 for small and medium scale producers, respectively, needs to be optimized for the successful implementation of this technology at industrial scale.

The objectives of this project were executed on 4 phases and the key findings are summarized below.

- **Phase 1: System Design and Optimisation of the Antimicrobial Efficacy**
  - The presence of aqueous reactive species (NO_2^-, NO_3^-, H_2O_2) in water, formed by air discharge plasmas at the gas-liquid interface, was quantified under varying conditions including discharge time, availability of working gas, treated water volume and surface area, storage time and storage temperature.
  - Various volumes of plasma-activated water (PAW) at 0.05, 0.1, 0.15, 0.2 and 0.25 L were produced at various discharge times of 5, 10, 20, 25 and 30 min.
  - PAW was optimised and it subsequently was used to study the effect of PAW on known spoilage and pathogenic organisms including *Lactococcus lactis subsp. Lactis*, *Pseudomonas fluorescens, Salmonella enterica* serovar Typhimurium and *Escherichia coli* serovar O157:H7.

- The antimicrobial effects of PAW were conducted and significant reductions in microbial population were observed. Maximum log_{10} reduction of 0.67 (*E. coli* O157:H7); 2.24 (*S.* Typhimurium); 1.32 (*L. lactis)* and 1.37 (*P. fluorescens)* was recorded for PAW generated in a closed system with a 30min discharge time and a microbial time of 390 seconds.

- **Phase 2: Optimisation of Processing Conditions for Microbial Decontamination of Meat by Non-Thermal Plasma Treatment**
  - The efficacy of PAW against pathogenic microorganisms (Salmonella, verocytotoxin producing *E. coli* and *Listeria monocytogenes*) inoculated onto cuts of raw beef and lamb were determined.
  - Results showed favourable reductions in pathogenic species inoculated onto beef and lamb cuts with PAW water bath and wash water treatments.
  - An overall log_{10} reduction of 2.66 was reported for *S.* Typhimurium and 2.67 for *E. coli* O157 on beef topside samples while a 3.63-log_{10} reduction was seen for *L. monocytogenes* on lamb shoulder samples.
  - PAW also exhibited a significant antimicrobial effect on spoilage microorganism, *B. thermosphacta,* with 3.12-log_{10} reduction.
  - PAW treatment at an applied temperature of 55 °C doubled PAW's efficacy.
  - When compared to wash water treatments, PAW also showed a continued antibacterial effect for up to 35 min and thereby reducing risks of cross contamination through water run-off.
- **Phase 3: Assessment of the Effect of Plasma Treatment on the Nutritional and Organoleptic Properties of Meat**
  - This phase investigated the effect of plasma-activated water (PAW) treatment on the quality attributes of raw and cooked beef.
  - For comparison, beef was treated with 2% lactic acid, a common decontamination chemical used within the meat industry. Quality parameters including protein, mineral and vitamin B6 content, colour (Lightness L*, redness a*, yellowness*), pH, myoglobin redox forms, lipid oxidation, and texture profile in beef treated with PAW solutions were analysed.
  - No significant reduction in mineral, vitamin, protein (% N and myoglobin) were observed with PAW.
  - PAW did not significantly change the lightness (L*) and yellowness (b*) of beef sample and a reduction in redness (a*) was comparable to that observed when treated with lactic acid.
  - The extent of lipid oxidation indeed improved with PAW treatment compared to water and lactic acid.
  - PAW improved raw beef tenderness.
  - Unsealed PAW treated beef at day 8 showed no significant difference in colour coordinate values (L*, a*, and b*) when compared to water-treated and untreated control.
  - PAW-treated samples retained a low pH of pH 5.26 during storage compared to the untreated control, which had a pH of 5.44 by day 8.
  - Vacuum packaged PAW treated beef increased lightness (L*) and redness (b*) at week 4 compared to control, suggesting a good retention in colour during storage.
  - Shelf-life studies were carried out on unsealed (PAW treated and stored without vacuum sealing) and vacuum-packed beef stored under refrigeration. Throughout storage, PAW treatment resulted in a

lower anaerobic population when compared to water. At the end of storage, final bacterial population was lower in PAW treated samples compared to control.

- PAW treatment greatly improved not only the safety of beef but also retained and in some cases improved quality parameters, particularly those of importance for consumer acceptability such as limiting the extent of lipid oxidation, limiting the rise in pH during storage and improving beef tenderness.

- **Phase 4: Scale up and application of Plasma-Activated Water (PAW) to Meat Surfaces**
  - The HPD reactor is energy efficient with the input power less than 100 W and it can kill *Escherichia coli* within seconds.
  - The generated PAW demonstrated the dual benefits of exceptional RONS energy efficiencies (up to 11 $g \cdot kW^{-1} \cdot h^{-1}$) and high bacterial removal (99%) at 30 seconds compared to literature studies, which take several minutes or hours to achieve same level of inactivation.
  - The HPD reactor was combined with ultrasound to maximise the production of RONS. This scaled system showed a remarkable efficiency, it can kill pathogenic species within seconds, and is the base for larger systems to be integrated into commercial processing lines.
  - We studied and compared two washing methods: spraying and immersion with the contact times of 15, 30 and 60 s. The effects of meat storage after washing for 1 day and 7 days were also investigated. Overall, PAW increased the bacterial inactivation and preserved the lightness, pH, water holding capacity and TBARS (thiobarbituric acid reactive substance) value of beef compared to untreated and water-treated beef samples.
  - The electric field in the HPD reactor was simulated, showing the simultaneous formation of regions of high electric field intensity around both the HV electrode and the ground electrode within one power source, which explains the remarkable performance of this reactor. This work was just published in the highest impact factor journal of *Elsevier* in chemical engineering, the Chemical Engineering Journal (Impact Factor = 16.744),
  - Lastly, an economic analysis of PAW technology was performed for small and medium scale enterprise producers. The capital cost related to implementing the scale-up PAW technology for the small and medium scale enterprise producers were estimated to be AU$ 362,767 and AU$ 1,252,051, respectively.

The application of PAW on meat and meat products is limited within the literature. This project reports for the first time, the use of PAW against specific bacterial species on a meat surface including *Escherichia coli O157:H7*, *Salmonella enterica* serovar Typhimurium, *Listeria monocytogenes* and *Brochothris thermosphacta.* This project also demonstrated the potential for induced bacterial resistance through exposure to PAW over several generations. Furthermore, this work determined, for the first time, the impact of PAW against the nutritional composition of beef and its quality attributes, providing the tools for larger scale designs that can be implemented in the Australia's red meat processing facilities.

2.0 Introduction

The processing of highly perishable heat sensitive foods, such as fresh meat and meat products, poses many challenges in the control of biological hazards. There are increasing concerns over the growth of pathogenic species including Salmonella, Escherichia Coli and Listeria which are estimated to cause over 5 million cases of food borne illnesses in Australia per year [1]. Several emerging non-thermal technologies are considered to meet industry standards and assist in the management and control of food safety hazards. The control of microbial growth and contamination of fresh meats proves far more challenging due to the complexity of its food matrix. Fresh meat has a favourable nutritional composition and water availability that promotes the growth of both spoilage and pathogenic microorganisms thereby limiting its shelf life. Fresh meats are likely to undergo further preservation hurdles (i.e heat processing, drying etc.) and so the focus lies on the control of cross-contamination arising from affected fresh meat as well as the survival of heat resistant microorganisms including spore-formers.

After slaughter, beef carcasses are exposed to excessive numbers of spoilage and pathogenic bacteria. The meat industry is currently facing challenges with the control of bacterial growth and risks associated with cross contamination down the process line. Traditional methods including hot water washing and steam pasteurization can impart unfavorable physical changes such as the discoloration of meat surfaces. Chemical disinfectants, including organic acids and chlorine-based chemicals are commonly integrated in carcass spray cabinets, however due to recent studies on the potential harmful impacts of these chemicals, and the rise in disinfectant resistant bacterial strains caused by their overuse, the industry is now seeking alternative non-thermal technologies.

Non-thermal plasma (NTP) inactivation technologies have gained a lot of attention over the past decades especially within the food and agricultural industries. NTPs are characterized as a mixture of highly reactive species generated through the ionization of a gas, typically air. These highly reactive species, comprising of electrons, ions and radicals, have been applied to food surfaces such as fruit, vegetables, goat and chicken to achieve sterilization and preservation. Despite its many advantages, the use of direct NTP treatment can negatively impact the physiochemical properties of food surfaces, inducing oxidation and destroying light sensitive compounds. The antimicrobial capacity of NTP is also reduced due to the complexity of the surface topography of food products making it difficult for the plasma to reach microorganisms that may be hidden. This has led to the generation of plasma activated water (PAW) whereby water is exposed to a NTP leading to several physiochemical changes including a reduction in pH, an increase in solution conductivity and the formation of aqueous reactive species. The efficiency of PAWs antimicrobial activity is dependent on the parameters during plasma generation including voltage, frequency, NTP activation time and working gas, the microorganism species and the treatment method including treatment volume and time. Until recently, works on the antimicrobial properties of PAW has primarily focused on the sanitization of fresh produce and processing equipment surfaces. As a sustainable and environmentally friendly treatment, the use of non-thermal plasma activated water shows potential as a novel meat decontaminant. However, the impact of PAW on meat safety and quality has yet to be determined.

3.0 Project Objectives

This project was conducted through the following four phases:

- Phase 1: System Design and Optimisation of the Antimicrobial Efficacy
    - The first phase was to design and construct a non-thermal plasma system, which infuses the plasma afterglow into the wash water. The technology prototype was designed to facilitate control over various plasma control parameters. The system facilitated monitoring and subsequent diagnostics of the plasma discharge with a view to future process control. The prototype was designed to be scalable in nature, with the transformer operating at only1-2% of its duty cycle for the prototype.
    - The lifetime of the active species within the water was tested to determine the window of treatment.
    - Antimicrobial optimisation of the prototype was conducted against major pathogens including Salmonella, verocytotoxigenic E. coli, lactic acid bacteria and Pseudomonas, with pathogens spiked into the wash water itself and subsequently on model surfaces prior to testing on meat surfaces.
- Phase 2: Optimisation of Processing Conditions for Microbial Decontamination of Meat by Non-Thermal Plasma Treatment
    - The second phase applied the most effective antimicrobial plasma conditions, as determined in Phase 1, to meat carcasses and cuts in various direct and indirect ways. Particular attention was paid to the complexity of meat surfaces with regard to microbial protection against the antimicrobial approaches.
    - Efficacy of the technology against the various microbial strains and investigation of any potential resistance were performed. In order to document the reduction of pathogens, meat from different species (beef, lamb or goat) was inoculated on the surface, using approximately 105 bacteria/cm^2. The pathogen reduction was documented for pathogens including Salmonella, verocytotoxin producing E. coli, Campylobacter and Listeria monocytogenes, being the most important contaminants present in meat. From each species, different types of cuts was selected representing different surface characters, i.e. lean meat, fat and skin.
        - Effects on background microflora was also be assessed as well as brochothrix thermosphacta, a spoilage organism of particular concern to spoilage of meat products in long term refrigerated MAP storage. Challenge inoculation studies on a range of red meat product surfaces was used to enumerate the microbial reduction following treatment protocol determined.
        - To ensure the system will be challenged appropriately, the recovery of sub-lethally injured cells using appropriate enrichment protocols was included in the analyses. Although it was not expected that NTP led to an adaptive or stress response by the microorganisms of concern, it was nonetheless important to rule this out. It was anticipated that the NTP process would form a key part of an overall hurdle approach to food safety and quality retention within the plant, but for any novel technology, it was warranted to investigate potential for induction of a stress response. Therefore, to simply investigate the potential for key challenge microorganisms to develop resistance to NTP, resistance studies was performed to evaluate any potential for induced resistance to plasma compared to untreated controls utilising

optimised conditions and also a more extreme and less extreme treatment. Samples was exposed to plasma treatments and any surviving organisms was cultured and exposed to plasma. This process was carried out repeatedly to determine if resistance to the treatment could be generated.

- For comparison, non-treated meat and meat treated with commonly used decontamination methods (i.e. lactic acid, steam etc.) was evaluated in a similar way to obtain a direct comparison of the pathogen reducing effect. Each meat species/type of cut was examined in triplicate, and the whole study was repeated at two different days using two different batches of meat in order to estimate the "between treatment" variability. In each of the studies, replicate samples was taken from each treated meat cut (i.e. from the top, bottom, front and back) in order to evaluate the "within treatment" variability,
- Testing the antimicrobial effect of plasma concentration, application time, temperature, humidity, etc., was carried out to find the optimal conditions and process variability.

- The potential to combine the approach with freezing was investigated.

- Phase 3: Assessment of the Effect of Plasma Treatment on the Nutritional and Organoleptic Properties of Meat

  This phase assessed:

  - Changes to the chemical and nutritional composition of meat including proteins, fat, vitamins and minerals.
  - Changes to the colour and pigment of meat.
  - Changes to physical properties such as tenderness and water holding capacity.
  - Effect on protein denaturation and lipid oxidation.
  - Effect on vacuum packed meat. as specified by consultation with the red meat industry.
  - Cooking properties when subjected to various methods of cooking, e.g., roasting, grilling, stirring frying, boiling.
  - Sensory properties such as appearance, tenderness, juiciness, texture, aroma and flavour.
  - Quantification of shelf-life of treated product. For the shelf-life analysis the treated meat was stored under 'real-life' conditions resembling typical retail display storage. The shelf-life analysis comprised sensory, chemical and microbial analysis in order to determine sensory changes with focus on odour, chemical changes in terms of progress in oxidation and microbial growth. All analysis was carried out in UNSW's sensory, chemical and microbiological laboratories.

- Phase 4: Scale up and application of Plasma-Activated Water (PAW) to Meat Surfaces

  - This phase designed a rig for an efficient PAW production. The rig was scaled from laboratory scale to a 2L pilot scale. During the design stage, in keeping with the needs and user requirement specifications which was well researched during the industry-driven approach in Phase 1, and in order to contribute to the mainstreaming and future uptake of the system, considerable effort was dedicated to ensure that the system is:

    - Easily and readily integrated into existing commercial meat processing lines in order to ensure that the system will lead to as little installation time and cost as possible.

- Capable of treating meat in the order of seconds, or few minutes, to ensure its feasibility for industrial scale treatments.
- Simple and easy to use. The system approach was based upon electricity meaning that steam, heat or chemicals are not required, facilitating a more hygienic, energy efficient and controlled manufacturing process.
- Versatile in that the system will be readily scalable to treat different volumes of products. Moreover, the system may be employed for many product types and categories. The potential for expansion of existing processing facility usage to process organic produce may be a factor enhancing the cost-benefit of this technology, in that direct chemical interventions are not employed for produce treatment. Therefore, the same facility could be used for processing conventionally farmed meat and organically farmed meats.
- Sufficiently low cost to ensure its uptake and use by small/medium enterprise producers within the sector. An economic analysis was conducted to assess the costs of implementing this PAW technology for small/medium scale enterprise producers.

- To optimise processing conditions for microbial decontamination of meat by PAW, including plasma species, treatment time, discharge frequency, electrical conductivity, etc.
- Four reactor configurations, scaling up the final two options to 2 L, were studied and optimized: (1) the air pin-to-liquid discharge, (2) the plasma-bubble reactor, (3) the hybrid plasma-bubble discharge (HPD) reactor, and the HPD reactor with ultrasound.
- The HPD system achieved a remarkable RONS energy efficiency (up to 11 $g \cdot kW^{-1} \cdot h^{-1}$) and up to 5-$log_{10}$ reduction of *Escherichia coli* in 30s of PAW contact time.
- Modelling the electrical field in the HPD reactor during the generation of PAW.
- Studying the antimicrobial efficacy of PAW on microorganisms adhered to beef surfaces by applying PAW using two application methods, spraying and immersion, at the contact times of 15, 30 and 60 s and the storage times of beef at 0, 1 and 7 days. This determined the best application method for an effective industrial implementation.
- Asessing the colour, myoglobin, water holding capacity, pH, lipid and weight gain of meat with the storage times of beef at 0, 1 and 7 days.
- Performing an economic analysis to assess the costs of implementing this PAW technology for small/medium scale enterprise producers.

4.0 Methodology

4.1 Phase 1

This phase focused on the development of a non-thermal plasma system capable of generating plasma activated water (PAW) and optimizing its activity for maximum efficacy against spoilage and pathogenic microorganisms by exploring the parameters that influence the generation of long-lived reactive species within PAW and their concentrations. These parameters comprised discharge time, water volume, availability of working gas and agitation.

4.1.1 Generation and Analysis of Plasma-Activated Water

Generation of PAW

PAW was produced through the generation of non-thermal plasma discharges above a water surface operating at atmospheric pressure with air used as the working gas. The electrical discharge used to drive the plasma was produced by a high voltage power supply (Phenix 6Cp120/60-7.5) operating at a frequency of 50 Hz with a maximum voltage output of 120 kV.

The plasma generator consists of a medium-carbon steel needle electrode with the tip fixed at a distance of approximately 5 mm from the water surface and an applied voltage of 20kV, a round stainless-steel ground electrode and a Plexiglas base as illustrated in **Fig. 1**. In this study, water samples of varying volumes (50 ml, 100 ml, 150 ml, 200 ml and 250 ml) were treated with spark discharge plasma for varying discharge times (5 min, 10 min, 15 min, 20 min. 25 min and 30 min). Operating conditions were varied between an open and enclosed system thereby limiting the working gas as well as the introduction of agitation. Concentrations of long-lived reactive species, nitrite (NO_2^-) nitrate (NO_3^-) and hydrogen peroxide (H_2O_2) was measured in water samples after treatment with spark discharge plasma.

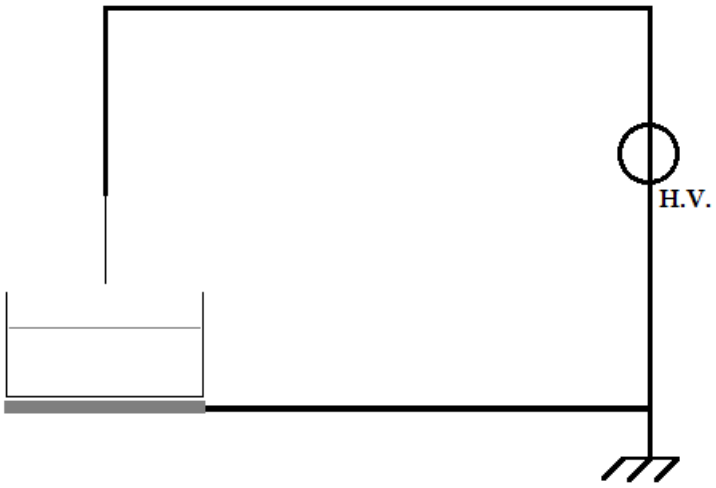

Figure 1. Schematic diagram of air spark discharge in contact with water.

Optical Emissions Spectra (OES) Detection of Major Excited Species in PAW

A fiber optics spectrometer was employed to record the emissions of major excited reactive species during the spark air-plasma discharge.

Detection of Reactive Species in PAW

Concentrations of H_2O_2 and NO_2^- in PAW samples were measured by spectrophotometry. H_2O_2 was determined using reagent Titanium(IV) oxysulfate-sulfuric acid solution (Sigma-Aldrich® 89532). A calibration curve was generated using standard solutions of 30% H_2O_2 at concentrations of 100 µM, 200 µM, 400 µM, 80 0µM and 1000 µM. 150 µl of reagent was added to 1.5ml standard sample and absorbance was read at 405 nm after 10 min.

NO_2^- was determined using Griess reagent (Sigma-Aldrich® 03553). A calibration curve was generated using standard solutions of $NaNo_2$ at concentration of 0 µM, 5 µM, 10 µM, 15 µM and 20 µM. 750 µl of reagent was added to 750µl standard sample and absorbance was read at 548 nm after 30 min.

NO_3^- was determined using an ion selective electrode (Cole Parmer model no. 27504-22). Probe was calibrated daily using standard solutions of KNO_3 at concentrations of 10 ppm, 100 ppm and 1000 ppm. 400 µl of ionic strength adjuster, 2M $(NH_4)_2SO_4$, was added to each 20ml standard and test samples thereby reducing the margin of error due to ionic strength variations between samples.

4.1.2 Generation and analysis of plasma-activated water

Concentration of Reactive Species with Increasing Discharge Time in an Open and Closed System

Spark discharge plasma was generated within a closed system (sealed plastic container) filled with 50ml MilliQ® water and treated for up to 30 min before concentrations of reactive species were measured, this was termed PAW-C. Procedure was repeated using an open system termed PAW-O.

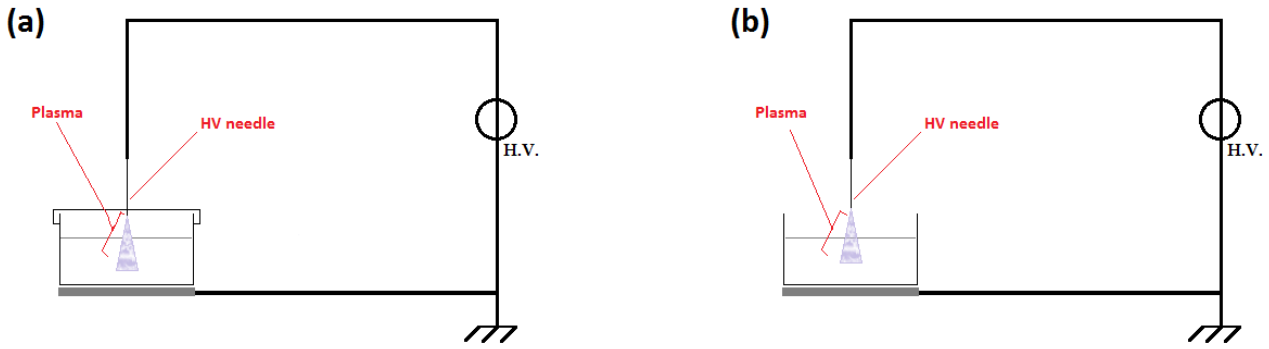

Figure 2. Schematic diagram of PAW generation in (a) closed (PAW-C); (b) open system (PAW-O).

Concentration of Reactive Species with Increasing Volume

Sealed plastic containers of up to 250ml MilliQ® water were treated with spark discharge plasma for 10 min before concentrations of reactive species were measured.

Concentration of Reactive Species with Increasing Agitation in an Open and Closed System

Spark discharge plasma was generated within a sealed plastic container filled with 50ml MilliQ® water and stirred using a magnetic stirrer at 0, 400 and 600 rpm. Samples were treated for 10 min with plasma and termed PAW-A-C. Procedure was repeated using an open system PAW-A-O.

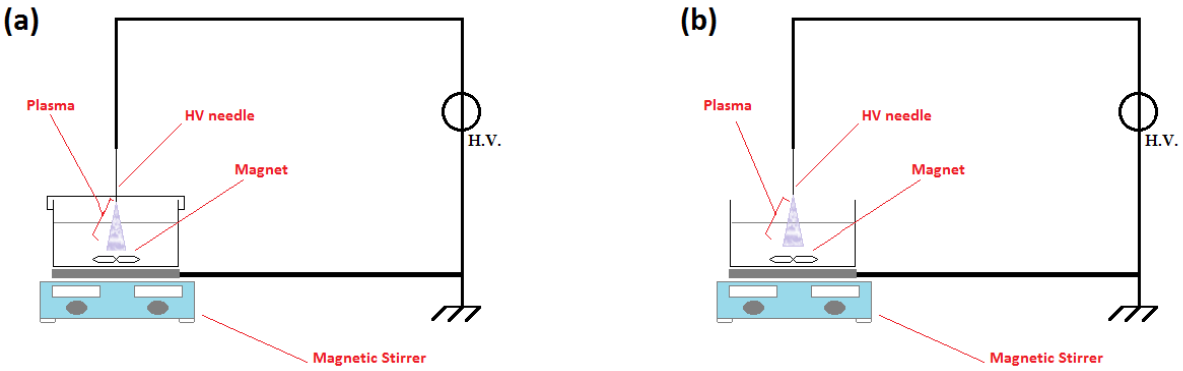

Figure 3. Schematic diagram of PAW generation with agitation in an (a) closed (PAW-A-C); (b) open system (PAW-A-O).

Concentration of Reactive Species with Water Surface Area

Spark discharge plasma was generated within a sealed glass container of varying sizes (Diameter 43mm, 70mm) filled with equal volumes of MilliQ® water (50ml) thereby altering the available water at the gas-liquid interface. Samples were treated with 20kv air-plasma for 30 min and reactive species measured.

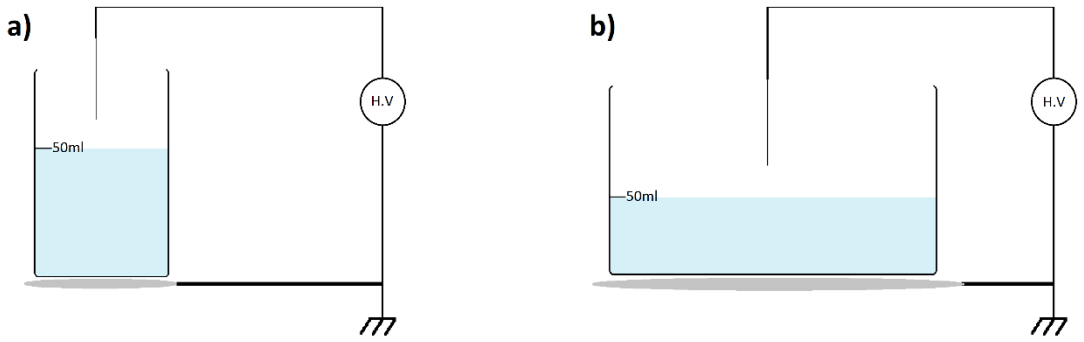

Figure 4. Schematic diagram of PAW generated in (a) D=43mm and (b) D=70mm glass container.

Statistical Analysis

Results were measured in triplicates and experiments were replicated three times. Values are expressed as mean ± standard deviation (SD).

4.1.2 Window of Activity

Concentration of Reactive Species with Storage Time and Temperature

Spark discharge plasma was generated within a sealed plastic container filled with 50ml MilliQ® water and treated for 10 min before storage at room temperature and under refrigeration (approximately 2 °C) completely sealed. Reactive species were measured every day for up to 30 days. Procedure was repeated using an open system as previously described.

Concentration of Reactive Species with Storage Methods

Spark discharge plasma was generated within a sealed plastic container filled with 50ml MilliQ® water and treated for 10 min before storage at room temperature without sealing container. Experiment was repeated with agitation created with a magnetic stirrer. Containers were stored up to 5 days without agitation and 24 h with agitation.

4.1.3 Bacterial Strains, Cell Suspension and Antimicrobial Activity of PAW

Bacterial Strains and Cell Suspension Preparation

Spoilage microorganisms, *Lactococcus lactis subsp. lactis* (ATCC®9936™) and *Pseudomonas fluorescens* (ATCC®13525™) as well as pathogenic species *Salmonella enterica* serovar Typhimurium (NCTC 74) and *Escherichia coli* serovar O157:H7 (ATCC®700728™) were sub-cultured onto Nutrient Agar No 2, Vegitone (Sigma-Aldrich® 04163). Single colonies were isolated, transferred into peptone water (Sigma-Aldrich® 94217) and incubated for 24 h at 37 °C for *L.lactis*, *S.*Typhimurium and *E.coli* O157:H7 and 26 °C for *P.fluorescens*, to generate a cell suspension to be used for the remainder of this study.

Preparation of Model Surfaces

Silicon wafers were cut into 10x10mm pieces. 50 µl of 10%wt beef fat (in ethyl acetate) was spin coated (at 1500 rpm for 15 s) onto silicon wafers with a thickness of approximately 115nm. Un-coated Silicon wafers and glass were also used as model surfaces.

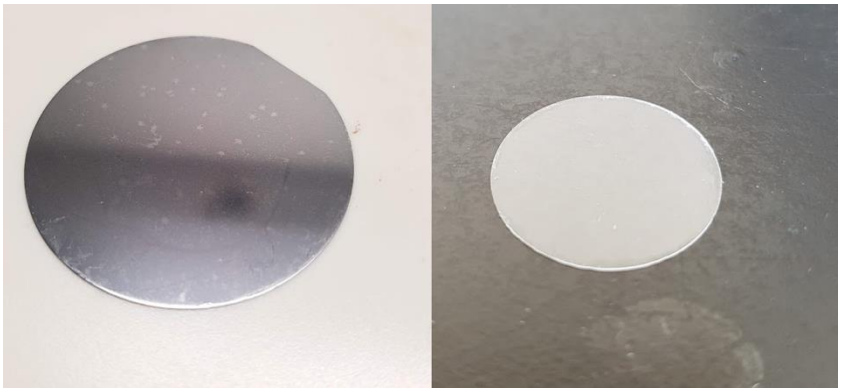

Figure 5. Images of spin coated silicon wafer (left) and spin coated glass slide (right).

PAW Treatment of Free-Living Cells

Cell suspensions (50 µl) were added to PAW (4.95 ml) and left in contact at room temperature for 30, 180 and 390 s. A tenfold serial dilution was performed at each sampling time and 100 µl spread onto nutrient agar plates. Cultivable cells were counted after a 24h incubation period at 37 °C for *L. lactis*, *S.* Typhimurium and *E. coli* O157:H7 and 26 °C for *P. fluorescens*.

PAW Treatment of Adhered Cells

Model surfaces were first submerged in acetone before 50 µl of *Escherichia coli* serovar O157:H7 (ATCC®700728™) cell suspension was added and left to dry in a sterile container at 37 °C. After 24 h, the surface samples were treated with PAW (5 ml) for 390 s before the addition of approximately 0.7g acid washed glass beads (106 µm; Sigma-Aldrich® G4649). Containers were vortexed for 60 s at maximum intensity. A ten-fold serial dilution was performed and 100 µl spread onto nutrient agar plates. Cultivable cells were counted after a 24h incubation period at 37 °C. Procedure was repeated with water as a control.

Analysis of Antimicrobial Activity of PAW

The antimicrobial activity of PAW was expressed as Log reduction calculated from the number of bacteria in an untreated sample (N_0) and treated sample (N), according to equation (1).

$$\text{Log reduction} = \text{Log}\left(\frac{N_0}{N}\right) \quad (1)$$

Statistical Analysis

All experiments were replicated three times. Values are expressed as mean ± standard deviation (SD).

4.2 Phase 2

This phase focuses on PAW's ability to reduce pathogenic (*E. coli* O157, *S.* Typhimurium and *L. monocytogenes*) and spoilage (*B. thermosphacta*) microorganisms on beef and lamb samples along with investigating the potential for induced resistance. Finally, the potential of coupling PAW treatment with freezing will be explored.

4.2.1 Generation and Analysis of Plasma-Activated Water

The design and procedure for PAW generation has been described previously in Phase 1. Briefly, PAW was produced through the generation of non-thermal plasma discharges above a water surface operating at atmospheric pressure with air used as the working gas. The electrical discharge used to drive the plasma was produced by a high voltage power supply (Phenix 6Cp120/60-7.5) operating at a frequency of 50 Hz with a maximum voltage output of 120 kV.

In this phase of the project, MilliQ® water of varying volumes were exposed to approximately 20 kV RMS plasma discharge for varying exposure times and subsequently used to treat raw meat samples. The following PAW solutions were prepared for subsequent treatment of inoculated beef and lamb samples.

	MilliQ® water volume prior to discharge	Plasma discharge time
PAW10	50ml	10min
PAW30	50ml	30 min
PAW60	50ml	60 min
PAWA	25ml	30 min

4.2.2 Microbial Reduction with PAW Treatment of Inoculated Beef and Lamb Samples

Preparation of Beef and Lamb

Fresh beef topside and rump (< 72h post-mortem) without any antimicrobial treatment was obtained from a commercial beef processing facility (Northern Co-operative Meat Company Ltd, NSW). Lamb shoulder and leg of lamb (< 72h post-mortem) was obtained from a lamb processing facility (Gundagai Meat Processors, NSW). Boneless beef and lamb samples were obtained fresh, cut into 20x20x10mm size once received and stored at -20 °C until required.

Preparation of inoculum *Salmonella* enterica serovar Typhimurium (NCTC 74), *Escherichia coli* serovar O157:H7 (ATCC®700728™), *Listeria monocytogenes* (ATCC®15313™) and *Brochothrix thermosphacta* (ATCC®11509™) were sub-cultured onto nutrient agar (No 2 Vegitone, Sigma-Aldrich® 04163). *Campylobacter jejuni* (ATCC®33560™) was sub-cultured onto Campylobacter Agar (Thermofisher PP2005). Listeria was incubated aerobically for 48 h at 30 °C. *Salmonella* and *E. coli* were also incubated aerobically for 24 h at 37 °C. Campylobacter was incubated in a microaerophillic environment (generated using Oxoid™ CampyGen™ CN0025A) for 24-48 h at 37 °C – 42 °C.

A single colony was isolated, transferred into peptone water (Sigma-Aldrich® 94217) and incubated to generate a cell suspension to be used for the remainder of this study. Suspensions were incubated for 24 h at 37 °C, for *S.* Typhimurium and *E. coli* O157:H7, and for 48 h for *L. monocytogenes*. *B. thermosphacta* suspensions were incubated at 27°C for 48 h and *C. jejuni* suspensions at 37 °C for up to 48 h.

Efficacy of PAW on Inoculated Beef and Lamb Samples through Water Bath Treatment

Boneless beef topside and rump as well as lamb shoulder and leg were cut into 20x20x10mm samples and frozen until required. Once required, samples were thawed and allowed to stand for at least 60 minutes to reach room temperature. Samples were then washed with 70% ethanol and stored at room temperature for 20 min to allow alcohol to evaporate from the surface. 50 µl of bacterial suspensions was spread on the top of each sample surface. Following inoculation, samples were stored in a sterile environment at room temperature for 20 min, allowing surface to dry.

Beef and lamb samples were subjected to PAW water baths as per method illustrated in **Fig. 6**. Briefly, samples were treated with PAW30, PAW60, or PAW30 at volumes of either 10 or 20 ml and with treatment times of 5 and 10 min. PAW30 treatments were applied at either room temperature or at approximately 55 °C. After treatment, samples and treatment solution was stomached for 2 min and serial dilutions preformed before surviving cells were spread onto the following selective media.

	Selective Media	CODE
E. coli O157	Sorbitol MacConkey agar	Thermofisher PP2092
L. monocytonges	PALCAM agar	Thermofisher PP2142
S. Typhimurium	XLD agar	Thermofisher PP2004
B. thermosphacta	STAA agar	OXOID CM0881B

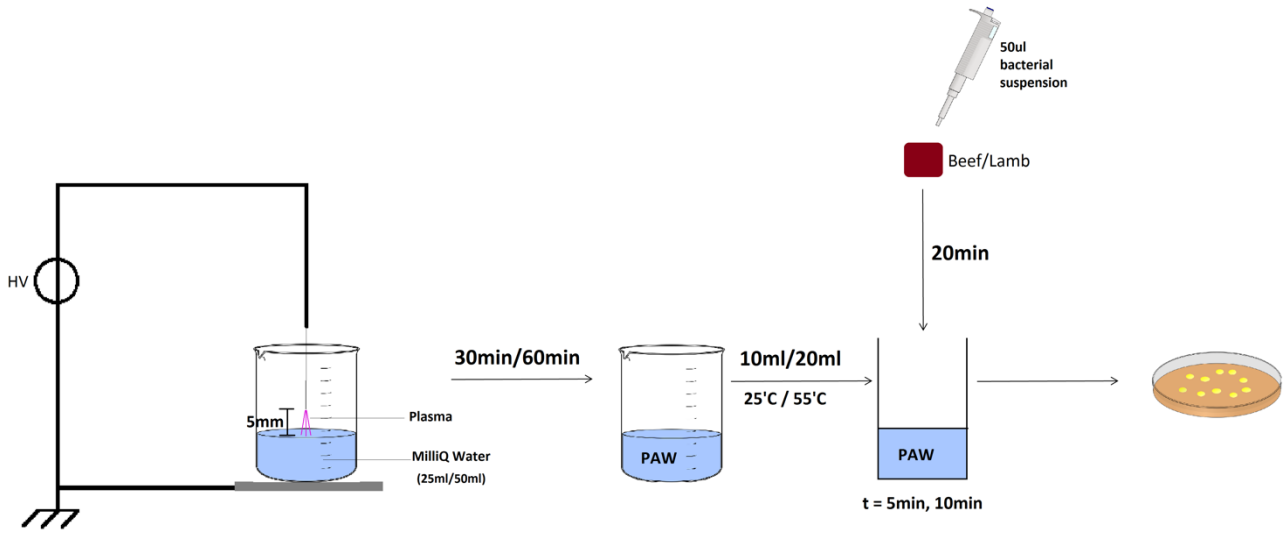

Figure 6. Schematic diagram of plasma activated water generation and the experimental method including inoculation of beef and lamb samples with bacterial suspensions and subsequent PAW water bath treatment.

4.2.3 Investigating the Potential for Continued Antimicrobial Effects of PAW after Water Wash Treatment

Beef rump samples were cut into 20x20x10mm samples and frozen until required. Once required, samples were thawed and allowed to stand for at least 60 minutes to reach room temperature. Samples were then washed with 70% ethanol and stored at room temperature for 20 min to allow alcohol to evaporate from the surface. Samples were inoculated with either *E. coli* O157 ($1.1x10^8$ CFU/cm^2) or *L. monocytogenes* (4.3×10^7 CFU/cm^2). Following inoculation, samples were stored in a sterile environment at room temperature for 20 min, allowing surface to dry. Once dry, samples were subjected to a warm PAW30 washing treatment as illustrated in **Fig. 7**. Beef samples were removed from wash solution and remaining attached cells were analysed. The remaining wash solution was continuously sampled for up to 35 min.

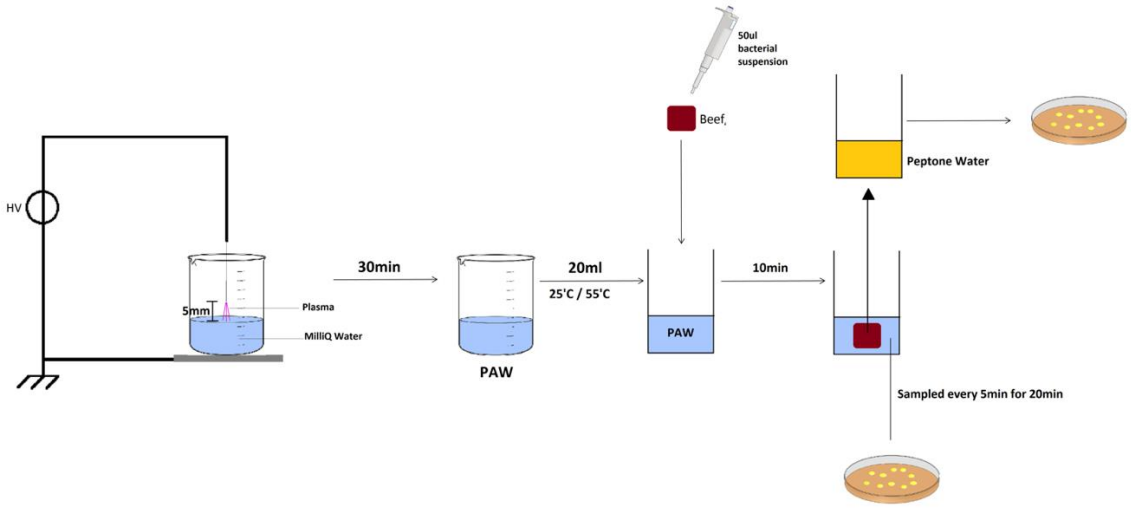

Figure 7. Schematic diagram of plasma activated water generation and the experimental method including inoculation of beef samples with E. coli/L. monocytogenes and subsequent PAW water wash treatment.

4.2.4 Investigating the Potential for Induced Resistance to PAW

The potential for microorganisms to develop resistance to PAW treatment was investigated through resistance studies carried out over several generations. *E. coli* and *L. monocytogenes* suspensions were subjected to PAW10 and PAW30 for 180 s and 390 s with surviving organism cultured and re-treated with PAW. This was repeated over several generations

4.2.5 PAW Treatment Coupled with Freezing

PAW30 solutions were generated and immediately frozen for up to 4 days. PAW of varying storage times (1-4 days) was thawed and allowed to reach room temperature before treatment. 50 µl of *P. fluorescens* was added to 5ml thawed PAW30. A tenfold serial dilution was performed after 390 s and 100 µl streaked onto agar plates.

4.2.6 Analysis of antimicrobial activity of PAW

The antimicrobial activity of PAW was expressed as Log reduction calculated from the number of bacteria in an untreated sample (N_0) and treated sample (N), according to equation (1).

4.2.7 Statistical Analysis

Data was obtained from at least three replicate experiments performed on at least three independently grown cultures ($n \geq 9$) and expressed as mean ± standard deviation (SD).

4.3 Phase 3

4.3.1 Generation and Analysis of Plasma-Activated Water

The design and procedure for PAW generation has previously been described in Phase 1 and 2. Briefly, PAW was produced through the generation of a non-thermal plasma discharge above a water surface operating at atmospheric pressure with air used as the working gas, illustrated in **Fig. 8**. In this study, two types of non-thermal plasma discharges, namely Pin-to-Plate and Pin-to-Dielectric Barrier (DBD), were employed. Each plasma discharge was achieved in a 250ml reagent bottle, as the reactor, a 316L stainless steel round bar, as the high-voltage electrode, and a 10-mm copper tape as the ground electrode. To create a pin-to-plate discharge, the ground electrode was placed inside the beaker; in the Pin-to-DBD discharge, the grounded electrode was attached outside the reactor (**Fig. 8**).

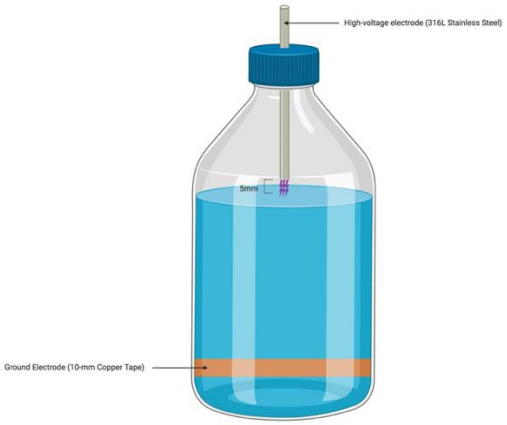

Figure 8. Schematic of experimental setup for PAW generation by pin discharge.

Pin-to-Plate discharge is hereafter referred to as “Copper In” and Pin-to-DBD as “Copper Out”.

A high-voltage power supply, Leap100 (PlasmaLeap Technologies, Sydney, Australia), was used to generate the non-thermal plasma, and atmospheric air acted as the working gas, with a resonance frequency and duty cycle of 60 kHz and 50 microSec, respectively. The discharge frequency varied from 1000 Hz to 2000 Hz. The discharge time changed from 10 to 30 min in increments of 10 min. The reactor contained 200ml MilliQ® water of varying conductivity. For this study conductivity of MilliQ® water was raised from 0 S/m to 0.02 S/m and 0.2 S/m with the addition of sodium chloride (NaCl, Sigma Aldrich).

Detecting the Physical Properties of Plasma-Activated Water

The physical properties of each generated PAW solution (such as power, conductivity, pH, oxidation-reduction potential and temperature) were measured. The consumed power was measured by a plug-in power meter (Reduction Revolution, Australia). The conductivity of PAW was measured using a conductivity meter (FiveEasyTM Plus FP30, Mettler-Toledo Ltd., Port Melbourne, Australia) at ambient temperature of 25ºC. The conductivity meter was calibrated using three standards at 84 microS/cm, 1413 microS/cm and 12.88 mS/cm.

The pH and oxidation-reduction potential (ORP) of each sample were measured by a benchtop pH/ORP meter kit (edge, Dedicated pH/ORP Meter HI2002, Hanna Instruments, Australia). The pH probe was calibrated using three buffer solutions of pH at 4, 7 and 10. The ORP probe was calibrated using an ORP test solution at 470 mV. Additionally, the temperature of PAW was measured using a digital thermometer (Acurite, Wisconsin, U.S.).

Reactive Oxygen and Nitrogen Species (RONS) Detection in PAW

Three long-lived reactive species of PAW, including NO_2^-, NO_3^- and H_2O_2, were quantified. A spectrometer-based microplate reader (SPECTROstar Nano, BMG Labtech, Australia) with a 96-well microplate (82.1581, Sarstedt Inc., Australia) was used to perform a colorimetric technique for fast and reliable absorbance measurements of NO_2^- and H_2O_2 in PAW. Titanium (IV) oxysulfate-sulfuric acid reagent (Sigma Aldrich® 89532) was used to determine the concentration of H_2O_2 in each sample. Subsequently, 20 µL of the reagent was added to 200µL sample/standard thereby forming a yellow-coloured complex with absorbance read at 403 nm after 10 min. To calculate the concentration of H_2O_2 in PAW, a calibration curve of H_2O_2 was required. Nine standard solutions at concentrations of 0, 12.5, 25, 50, 100, 200, 400, 800 and 1000µM were prepared from the hydrogen peroxide solution (30% (w/w) in H_2O, Sigma Aldrich® H1009) to produce the calibration curve.

The concentration of NO_2^- in PAW was quantified by microplate spectrometer via the colorimetric Griess assay (Sigma Aldrich® 03553). A total of 100µL of the Griess reagent was added to 100µL sample/standard, forming a magenta-coloured azo dye. The absorbance of the sample at 548nm was read after 30 minutes. Six $NaNO_2$ standard solutions at 0, 15.63, 31.25, 62.5, 125 and 250 µM were prepared to generate the NO_2^- calibration curve. The concentration of NO_3^- in PAW was determined using an ion selective electrode (EW-27504-22, Cole-Parmer, Australia). The electrode was calibrated daily using three KNO_3 standards at 10, 100 and 1000 ppm. Sulfamic acid was added prior to measurement, thereby eliminating potential NO_2^- interference. An ionic strength adjuster, 2M $(NH_4)_2SO_4$, was also used to minimise the margin of error due to variations in ionic strength between samples.

Energy Yield Calculation

The energy yield of NO_2^-, NO_3^- and H_2O_2 was calculated using the equation below:

$$EY = \frac{C\ x\ V\ x\ MM}{P}$$

where,

- EY is the energy yield in g.kWh^{-1},
- C is the concentration of NO_2^-, NO_3^- and H_2O_2 in µM,
- V is the volume of sample in L (which was 0.2L),
- MM is the molar mass of NO_2^-, NO_3^- and H_2O_2 in g.µmol^{-1}, and
- P is the consumed power to generate non-thermal plasma.

4.3.2 Bacterial Strains, Cell Suspension and Antimicrobial Activity of PAW on Planktonic Cells

Escherichia coli serovar 0157:H7 (ATCC®700728™) and *Salmonella enterica* serovar Typhimurium (NCTC74) were grown individually onto nutrient agar plates (Nutrient Agar No. 2, Vegitone, Sigma Aldrich® 04163) for 24 h at 37 ˚C. To produce a cell suspension, a single colony of *E. coli* and *S.* Typhimurium was isolated and inoculated into 5 mL of peptone water (Sigma Aldrich® 94217) for 24 h of incubation at 37 ˚C. In this study, 50 µL of each prepared bacterial suspension was added to 4.95 mL of sterile water (as a control) or prepared PAW at ambient temperature for treatment times ranging from 1 to 16 min. After treatment with sterile water or PAW, the *E. coli* and *S.* Typhimurium sample were serially diluted into peptone water and 100 µL of the suitable dilution was spread onto nutrient agar plates. Bacterial colonies were counted after 24 hours of incubation at 37 ºC and the results were termed as $\log_{10}$ CFU/ml.

Modelling of Microbial Inactivation

Two theoretical inactivation models, which are log-linear regression and Weibull [2-4], were applied to the mean numbers of survived bacterial colonies for all PAW treatments using GInaFiT, a freeware add-in for Microsoft© Excel [5]. The log-linear regression model was expressed as:

$$\log_{10} N = \log_{10} N_0 - \frac{k_{max} t}{\ln 10}$$

where,

- N is the microbial cell count after the PAW treatment (in CFU/mL),
- N_0 is the microbial cell count after control treatment (in CFU/mL),
- k_{max} is the inactivation rate (in s^{-1}), and
- t is the treatment time (in s).

The Weibull distribution, a non-linear model, was expressed as [2-4]:

$$\log_{10} N = \log_{10} N_0 - (\frac{t}{\delta})^p$$

where,

- N is the microbial cell count after the PAW treatment (in CFU/mL),
- N_0 is the microbial cell count after control treatment (in CFU/mL),
- p is the shape parameter (concave upward if p<1, concave downward if p>1, straight line if p=1),
- δ is the scale parameter (in s), and
- t is the treatment time (in s).

4.3.3 Preparation of Meat Samples and PAW Treatment

Fresh beef rump whole cuts were collected from local butchers within three weeks of slaughter and stored either at 4 ± 1 ºC prior to the analysis of nutrient composition, colour, pH, lipid oxidation, and textural profile or frozen at -20 ± 1 ºC to be used at a later date for further chemical and microbial analysis.

Beef was cut into 30x25x10mm pieces weighing approximately 10 g for quality analysis unless specified otherwise and subsequently treated with optimised PAW solutions (PAW(x) x=1,2,3 and 4). PAW treatment volumes of 0.14 mlPAW/g beef (PAW(x)V_{min}) and 0.57 mlPAW/g beef (PAW(x)V_{max}) was used and allowed to air dry for 20 min before analysis. Controls were either untreated samples or treated with ultrapure water. Treated beef was stored either unsealed at 4 ± 1 ºC and -20 ± 1 ºC or vacuum packaged at 4 ± 1 ºC prior to analysis.

4.3.4 Measurement of Quality Attributes

Refrigerated unsealed beef samples were analysed for colour, pH, lipid oxidation, myoglobin content, texture profile and microbial population. In addition, colour, pH, water holding capacity, cooking loss, thermal shrinkage and textural

properties of unsealed cooked beef was also determined. Frozen unsealed beef samples were lyophilised over 48 h and blended into a powder for mineral, % nitrogen and vitamin analysis. Vacuum packaged beef was sampled for colour, pH and drip loss as well as anaerobic and aerobic microbial population during storage.

Nutritional Composition

Powdered beef was digested with nitric acid and hydrogen peroxide by microwave enhanced digestion and digests were analysed for Iron (Fe), zinc (Zn) and selenium (Se) by ICP-OES and ICP-MS with assistance from Microscopy Australia at the Electron Microscope Unit (EMU) within the Mark Wainwright Analytical Centre (MWAC) at UNSW Sydney. % Nitrogen was determined using an Elementar Vario Cube analyser with assistance from the XRF laboratory, SSEAU, Mark Wainwright Analytical Centre.

Vitamin B6 (pyridoxine) was determined through HPLC analysis. Pyridoxine was extracted from beef samples according to Bognar and Ollilainen [6] with some modifications. 1 g of lyophilised beef powder was mixed with 0.1N Sulfuric acid and autoclaved at 120 ºC for 15 min and allowed to cool before pH was adjusted to 4.8 using 2.5M sodium acetate buffer. A quantity of 50 mg of Takadiastase was then added to facilitate the separation of protein bound vitamins and samples were stored overnight at 37 ºC before being centrifuged with the supernatant filtered through a 0.2u PTFE filter into an 300ul amber vial for HPLC analysis.

HPLC analysis of pyridoxine was performed according to Chatzimichalakis et al. [7] with minor modifications. A phenomenex column, Luna 3µ C18(2) (150x4.6mm, 3µm) coupled with a Phenomenex guard column was used at ambient temperature. The mobile phase consisted of A: 0.05M ammonium acetate/methanol (99/1) and B:water/methanol (50/50). A multi-step gradient was used with initial conditions set to A:B v/v 99:1 and remaining isocratic for 4 min. Composition was changed linearly until solvent B reached 100% after 18 min and remained isocratic for 8 min. A 25-min equilibration time was observed between injections.

Colour

The effect of PAW treatment on surface colour was measured with a ChromaMeter (CR-400 Konica Minolta Optics, INC) and applying the L*a*b* system where colour coordinate values for brightness (L*) redness/greenness (a*) and yellowness/blueness (b*) were measured for each sample. The difference in colour coordinate values against untreated control were determined by the following equation:

ΔL* (L* sample minus L* standard) = difference in lightness and darkness (+ = lighter, – = darker)
Δa* (a* sample minus a* standard) = difference in red and green (+ = redder, – = greener)
Δb* (b* sample minus b* standard) = difference in yellow and blue (+ = yellower, – = bluer)

pH

pH measurements were determined using a portable pH probe (Testo, Inc USA testo-205).

Lipid Oxidation

Lipid oxidation was determined through the TBARS value of treated samples represented as g MDA/kg sample. TBARS content was determined according to method described by Zeb and Ullah [8] with modifications. Treated unsealed beef samples were homogenised in 20ml glacial acetic acid for 2 min with an addition of 1% BHT to prevent further oxidation. Homogenised solution was centrifuged with the supernatant filtered and reacted with 20mM TBA 1:1 v/v. Samples with reagent were placed in a 95 ºC water bath for 60 min before absorbance was read at 532 nm.

Myoglobin Redox Forms

The composition of myoglobin in beef samples was determined according to method described by Tang et al [9]. Briefly, 1 g of treated beef was homogenised with 10ml phosphate buffer (pH 6.8) for 2 min and centrifuged at 3,000 rpm for 10 min. The absorbance of the supernatant was measured at 503, 525, 557 and 582 nm. Deoxymyoglobin (DeoMb), oxymyoglobin (OxyMb), and metmyoglbobin MetMb content was determined by the following equation

DeoMb (%) = -0.543R1 + 1.594R2 + 0.552R3 – 1.329

OxyMb (%) = 0.722R1 – 1.432R2 – 1.659R3 + 2.599

MetMb (%) = -0.159R1 – 0.085R2 + 1.262R3 – 0.520

Where

- R1 = Absorbance at 582nm / Absorbance at 525nm
- R2 = Absorbance 557nm / Absorbance at 525nm
- R3 = Absorbance 503nm / Absorbance 525nm

Water Holding Capacity

Water holding capacity (WHC) was determined by a centrifugal method described by Zhang et al [10] with modifications. Meat samples were treated with a known volume of PAW. weighed and placed in a filter bag attached to the inside of a centrifugal container. Sample was then centrifuged at 3,000 rpm for 30 min. After centrifugation, free water in the container was collected and weighed. WHC % was calculated by the following equation

WHC (%) = (weight of treatment solution added (g) – free water in container (g))/meat sample mass (g) x 100

Textural Profile

Unsealed chilled and cooked beef samples were allowed to come to room temperature (25 °C) and sectioned into 60x60x10mm pieces, cut parallel to the muscle fibre. Maximum Warner-Bratzler shear force (WBSF) analysis was determined using a Texture Analyser (Stable Micro Systems, TA.XT.plus texture analyser) with a Warner-Bratzler V-notch blade. Sample was sheared perpendicularly to the long axis of the muscle fibres. Further textural properties of treated cooked beef samples were calculated by the following equations

Weight gain (%)
= (meat sample after treatment (g) – initial meat sample (g)) / initial meat sample mass (g) x 100

Cooking loss (%)
= (meat sample before cooking (g) – meat sample after cooking (g))/ meat sample before cooking (g) x1 00

Cooking yield (%)
= 100 – cooking loss (%)

Thermal shortening
= (meat length before cooking (mm) – meat length after cooking (mm)) / meat length before cooking (mm) x 100

4.3.5 Shelf-Life Analysis

Beef rump was cut to a size of 20x30x10mm in a laminar flow cabinet and tumbled in a sterile container for 5 min to evenly distribute microorganisms on beef surfaces. Meat samples were sealed in vacuum packages and stored at 4 °C for 4 weeks and sampled at weekly increments. pH and colour were measured as described above. Drip loss was calculated by the following equation:

Drip loss (%)

= (weight of bag with meat removed (g) - initial weight of bag (g))/initial weight of meat x100

Meat samples were sampled for aerobic and anaerobic microbial growth at weeks 1, 2 and 3. Vacuum packaged beef samples were homogenised in 20ml peptone water and a 10-fold serial dilution was performed before 100 ul was spread onto nutrient agar in duplicates. Plates were separated and incubated aerobically and anaerobically at 37 ºC for 48 h.

For shelf-life analysis of unsealed beef, meat was cut into 10x20x10mm pieces and treated with PAW and stored for up to eight days with colour, pH, lipid oxidation, texture profile and total plate count determined in duplicates on each sampling day. Microbial analysis was conducted by homogenising beef samples in 20ml peptone water and performing a 10-fold serial dilution before 100 ul was spread onto nutrient agar and incubated at 37 ºC for 48 h.

4.3.6 Statistical Analysis

Results were presented as the mean of experimental data with at least three replicates. The error bars shown in the figures represent the standard deviations of the data, unless stated otherwise. Samples were then statistically analysed via ANOVA using Prism 8, to check whether there was a significance difference between the mean of two or more groups. The significance level was set at 0.05. A post-hoc analysis by Tukey's Test was also performed in this study.

4.4 Phase 4

4.4.1 PAW Generation

4 different plasma reactors were employed to generate PAW with a plasma generator (Leap100, PlasmaLeap Technologies, Australia), voltage probe (P6015A, Tektronix, U.S.), current probe (4100, Pearson Electronics, U.S.), digital oscilloscope (DS-6104, RIGOL, China), optical emission spectra (OES) system (B&W Tek, USA).

PAW Generation by Pin-to-liquid Discharge

PAW was produced through a pin-to-liquid discharge reactor (**Fig. 9**) consisting of a 316-stainless-steel rod (with better corrosion resistance compared to 304 type) with an 8-mm outer diameter, which acted as the high-voltage (HV) electrode, placed at the centre of a polypropylene screw cap and inside a 250-mL laboratory bottle (Duran®). The distance between the end of the rod and the water surface was kept at ~5 mm. Two ground electrode configurations, made from an adhesive and electrically conductive copper tape with a 10-mm width (Advance Tapes AT526, RS Components Pty. Ltd.©, Australia), were investigated (**Fig. 9**). The first one, labelled as ground out (GO), placed the copper tape outside of the bottle wall. The second one, labelled as ground in (GI), placed the copper tape inside the bottle, partially submerged in the water. Atmospheric air was utilised as the working gas in the reactor. The following operational parameters were used: resonance frequency – 60 kHz; duty cycle – 50 µsec; discharge time – 30 min; maximum output voltage – 4.01 kV; maximum output current – 1.56 A. The plasma discharges occurred in 0.2 L of MilliQ® water.

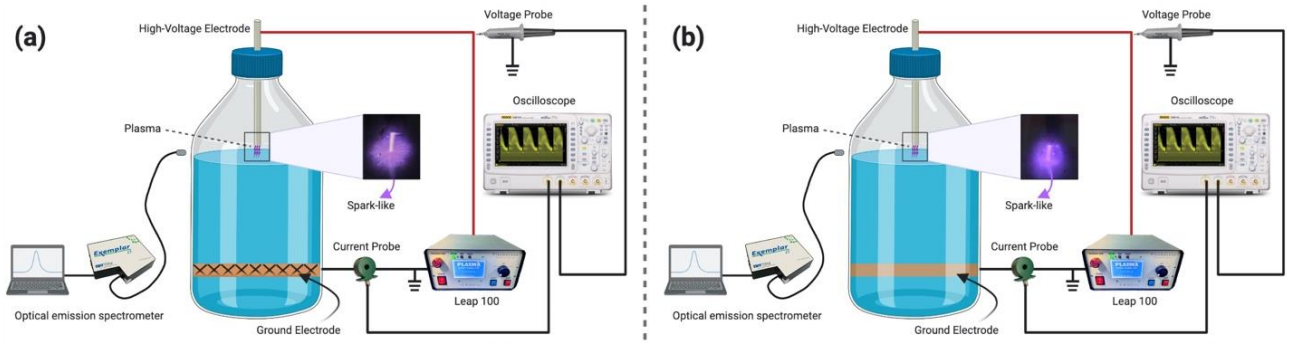

Figure 9. Schematic of the experimental configuration for the atmospheric plasma generator to produce a pin-to-liquid discharge with the ground electrode placed (a) outside (GO) and (b) inside (GI) the reactor.

For investigating the impacts of discharge frequency, at constant operational conditions described above with GO, the discharge frequency was varied from 1000 Hz to 2000 Hz.

For investigating the impacts of initial electrical conductivity, three different initial electrical conductivities (0.05 μS·cm^{-1}, which was labelled as 0 S·m^{-1} in this study, 0.02 S·m^{-1} and 0.2 S·m^{-1} by adding NaCl into MilliQ® water) were used to generate PAW by the pin-to-liquid discharge reactor at 2000 Hz with both GO and GI.

PAW Generation by Plasma-Bubble Discharge

PAW was produced through a plasma discharge in a bubble reactor with a single hole (2-mm diameter, **Fig. 10**). The detail of its design has been previously described [11]. The reactor was modified by submerging ~5 mm from the base of the generator under water in a 250 mL laboratory bottle. The ground electrode used in the bubble reactor was kept the same as the pin-to-liquid discharge reactor (as per above) using 10-mm copper tape. Compressed air was used as the working gas via a gas flow controller (198-2981, RS Components, Australia). The following operational parameters were used: resonance frequency – 60 kHz; discharge frequency varied from 1000 to 2000 Hz; duty cycle – 50 μsec; discharge time varied from 10 min to 30 min; maximum output voltage – 4.19 kV; maximum output current – 1.07 A.

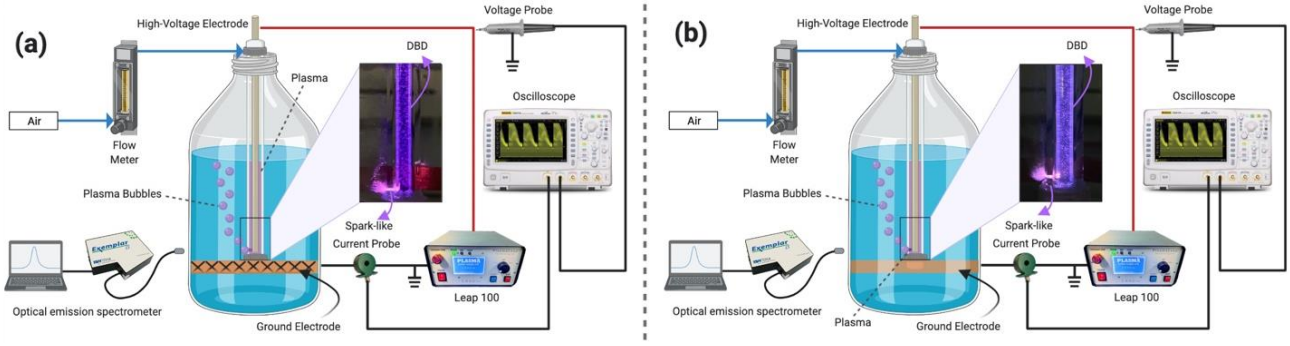

Figure 10. Schematic of the experimental configuration for the atmospheric plasma generator to produce plasma-bubble discharge with the ground electrode placed (a) outside (GO) and (b) inside (GI) the reactor.

For investigating the impacts of air flowrate, at constant operational conditions described above with GO, the air flowrate was varied from 0.2 to 1 L·min^{-1} in increments of 0.2 L·min^{-1} to generate PAW at 10-min discharge time and the discharge frequencies of 1000 Hz and 2000 Hz.

For investigating the impacts of discharge frequency, at constant operational conditions described as above with GO, the discharge frequency was varied from 1000 Hz to 2000 Hz.

For investigating the impacts of initial electrical conductivity, three different initial electrical conductivities (0.05 μS·cm^{-1}, which was labelled as 0 S·m^{-1} in this study, 0.02 S·m^{-1} and 0.2 S·m^{-1} by adding NaCl into MilliQ® water) were used to generate PAW by the pin-to-liquid discharge reactor at 2000 Hz and 0.8 L·min^{-1} with both GO and GI.\

PAW Generation by Hybrid Plasma Discharge

PAW was produced through a hybrid plasma-bubbles discharge (HPD) reactor that combine the two types of plasma discharges previously studied (pin-to-liquid discharge and plasma-bubble discharge). The HPD reactor vessel consisted of a wide-mouth borosilicate reagent bottle, a sharpened-point metal rod and a specially designed bubble reactor [**Fig. 11**(a)]. The rod and bubble reactor were placed inside the bottle. The rod, made from 316 stainless steel with an outer diameter of 8 mm and a length of 179 mm, was insulated with a rubber tube and connected to the

negative terminal. The distance between the surface of the liquid and the end of the rod in all experiments was maintained at 6 mm as shown in **Fig. 11**(a). Compressed air kept at a flowrate of 0.8 L.min^{-1} via a flow controller was supplied to the plasma-bubble reactor, which was connected to the positive terminal [**Fig. 11**(a)]. The following operational parameters were used: resonance frequency – 60 kHz; discharge frequency – 2500 Hz; duty cycle – 50 µsec; discharge time – 30 min; maximum output voltage – 8.91 kV; maximum output current – 1.79 A.

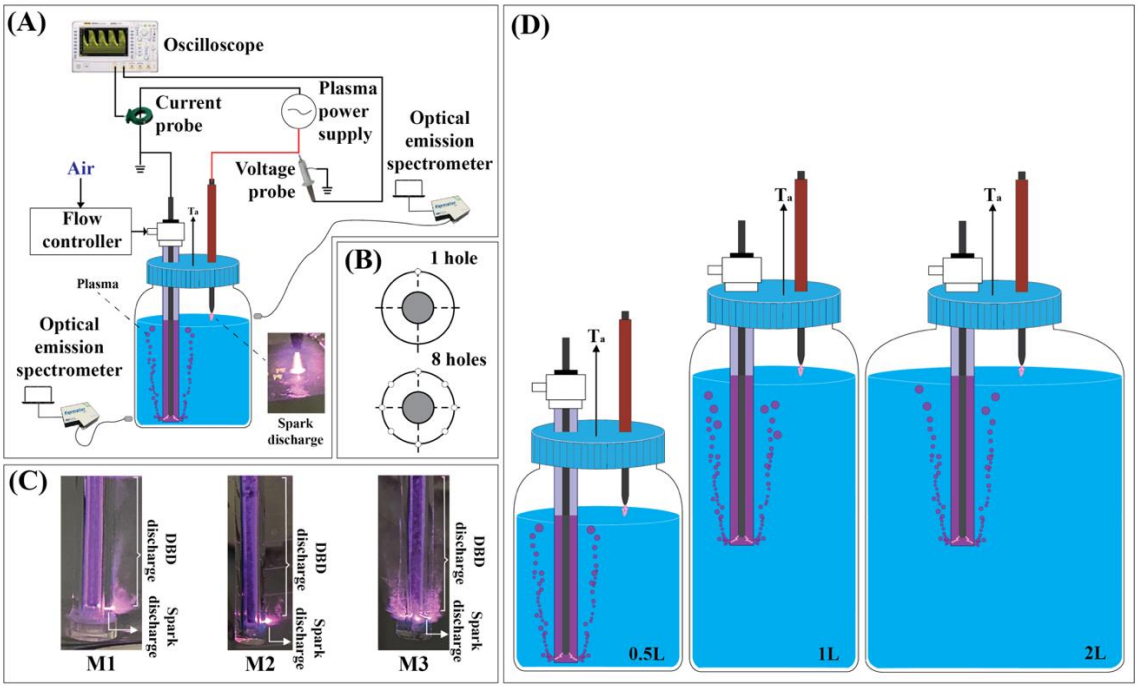

Figure 11. a) Schematic illustration of the experimental setup of non-thermal plasma reactor for hybrid plasma discharge (HPD); (b) images of plasma-bubble columns with a single hole (M1, 2 mm); a single hole (M2, 400 µm) and eight holes (M3, 400 µm); (d) schematics representing hybrid-mode plasma discharge reactors with 0.5, 1 and 2 L of liquid. T_a represents gas out to the atmosphere.

For investigating the effect of input voltage and different HPD reactors, at constant operational conditions described as above, the input voltage was varied between 100-200 V in 20 V increments. The plasma discharges occur in 0.5 L of MilliQ® water stored in a 0.5 L glass bottle (Pyrex®) via three HPD reactors: (a) single orifice (M1, 2 mm diameter), (b) single orifice (M2, 400 µm diameter), and (c) eight orifices (M3, 400 µm diameter) [**Fig. 11**(a)-(c)]. The best performing input voltage based on the total reactive oxygen and nitrogen species (RONS) concentration was then chosen for the microbial inactivation of PAW generated by all HPD reactors.

For investigating the impacts of liquid volume, three different reactor vessels with differing volumes of MilliQ – 0.5 L glass bottle (Pyrex) with 0.5 L MilliQ, 1 L glass bottle (Duran) with 1 L MilliQ, and 2 L glass bottle (Duran) with 2 L MilliQ were used to generate PAW [**Fig. 11**(d)].

For investigating the impacts of liquid composition, increasing the salinity of the water prior plasma treatment has been observed to improve the physicochemical properties of PAW, particularly in NO_2^- generation [12-14]. Experiments that result in the least bacterial inactivation efficiencies are chosen to evaluate if increasing the salinity of water prior plasma treatment improved bacterial inactivation efficiency. Four NaCl concentrations were chosen – 2, 4, 6, and 8 mM, and the outcomes were benchmarked against the control sample which had 0 mM NaCl.

PAW Generation by Hybrid Plasma Discharge and Ultrasound

PAW was produced by a hybrid plasma-bubbles discharge (HPD) with the addition of ultrasound. The sharpened-point metal rod and the bubble reactor, utilised to produce the pin-to-liquid discharge and the plasma-bubble discharge in

above, were used in this study. A schematic experimental setup is shown in **Fig. 12**. The body of reactor vessel was made from a cylindrical acrylic pipe with the inner diameter, thickness and height of 123, 5 and 190 mm, respectively. In order to generate ultrasonic waves, a vibration plate made of 316 stainless steel with the diameter and thickness of 190 and 2 mm, respectively, was placed at the bottom of the acrylic pipe. A transducer with the frequency of 28 kHz and the power of 100 W (HS-4SH-4528, Hesentec Ultrasonic Transducer, China) was glued below the vibration plate with an epoxy glue (8265S, J-B Weldz™, U.S.). A power transformer (Model SUT 2K LF-7, T&C Power Conversion, U.S.) was connected to the transducer and driven by power generator (AG 1021, T&C Power Conversion, U.S.).

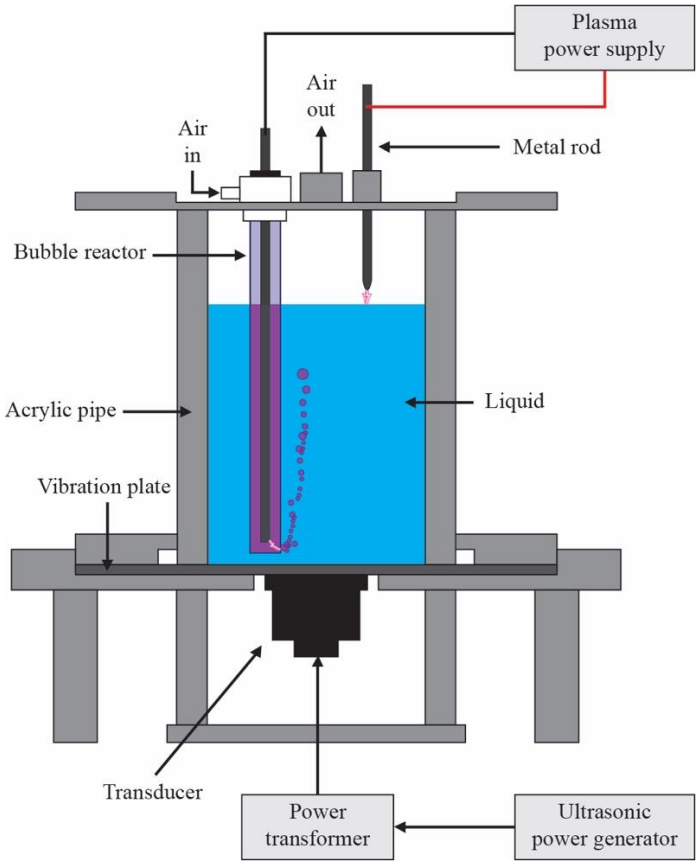

Figure 12. Experimental setup of a hybrid plasma-bubbles discharge (HPD) reactor combined with ultrasound.

1.5 L of MilliQ with the addition of salt (8mm NaCl) were used to generate PAW instead of 2 L. This is because based on our preliminary study, we observed that big flames were generated from the tip of the metal rod in the HPD reactor with the liquid volume of 2 L after 10 min of plasma discharge. For plasma generation, the operational parameters as above were used. For the generation of ultrasonic waves, the following operational parameters were used: drive frequency – 25 kHz; input power – 50 W; drive power – 45 W.

PAW Generation by Hybrid Plasma Discharge for the Investigations of Beef Quality and Bacterial Inactivation on Beef

The newly designed hybrid plasma discharge (HPD) reactor was fabricated as shown in **Fig. 13**. The HPD reactor was powered using a high voltage AC power source (Leap100, PlasmaLeap Technologies, Australia). The HPD reactor vessel consisted of a cylindrical acrylic pipe, a flat-end metal rod and a specially designed bubble reactor with a single orifice (400µm diameter) and a gas flow controller (198-2981, RS Components, Australia). The reactor vessel in **Fig. 13**(a) was made from a cylindrical acrylic pipe with the inner diameter, thickness and height of 123, 5 and 190 mm, respectively. The rod and bubble reactor were placed inside the acrylic pipe as shown as **Fig. 13**(a). The rod, made from 316 stainless steel with an outer diameter of 4 mm and a length of 179 mm, was insulated with a rubber tube and

connected to the positive terminal of the power supply. We refer to this as the HV electrode of the HPD reactor. The distance between the surface of the liquid and the end of the rod (high-voltage electrode) in all experiments was maintained at 6 mm as shown in **Fig. 13**(a). The bubble reactor contains a metallic rod enclosed on a quartz tube and the design of plasma-bubble reactor has been reported in the literature [11, 15, 16]. Compressed air, retained at a flowrate of 0.8 L.min^{-1} via a flow controller, was supplied to the plasma-bubble reactor. The metal rod inside the bubble reactor was connected to the negative terminal of the power supply to complete the circuit.

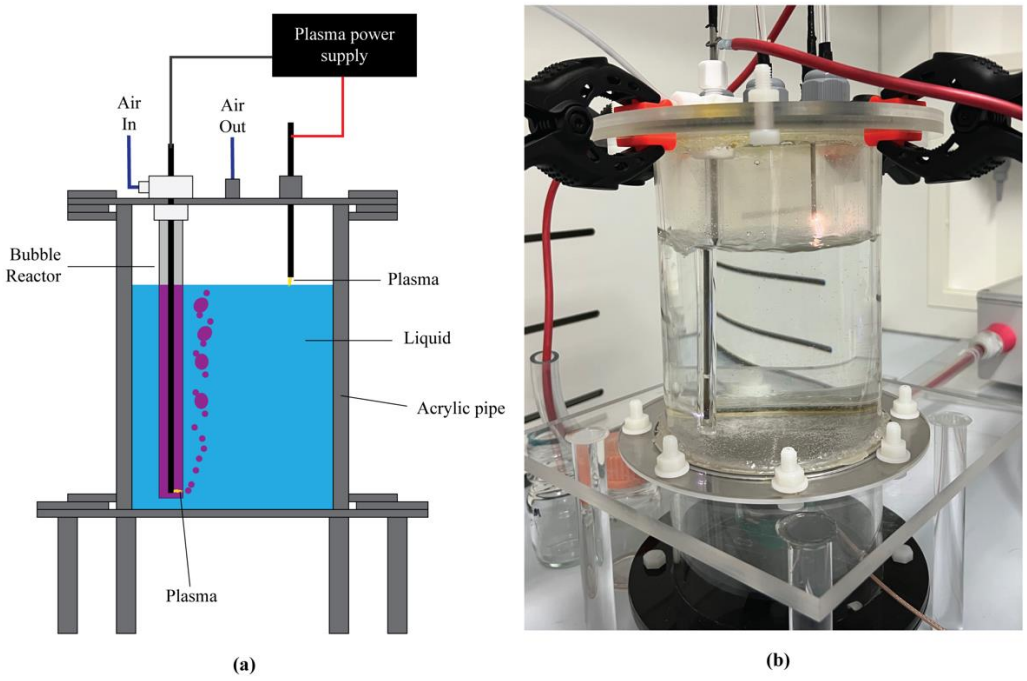

Figure 13. (a) Experimental setup of a hybrid plasma discharge (HPD) reactor; (b) image of the HPD reactor.

Plasma-activated water (PAW) was produced using the HPD reactor in this section. 1.5 L of MilliQ with the addition of salt (8mm NaCl). The following operational parameters were used: resonance frequency – 60 kHz; input voltage – 200 V; discharge frequency – 2500 Hz; duty cycle – 50 µsec; discharge time – 30 min.

4.4.2 Physical properties of PAW

Electrical conductivity, pH and oxidation-reduction potential (ORP) were measured using a conductivity meter (Mettler-Toledo Ltd., Australia), and a benchtop pH/ORP meter kit (Hanna Instruments, Australia) [17]. Measurements were conducted at the end of the discharge prior to bacterial inactivation on every sample.

4.4.3 Physical properties of PAW

The OES of plasma discharges were performed to identify the RONS in plasma [18]. The OES of plasma discharges were measured during plasma discharge using a spectrometer (Exemplar® LS, B&W Tek, USA) and the BWSpec™ software with a ruled grating of 600/250, a resolution of 1.5 nm, and a round-to-slit optical fiber (B&W Tek, USA) for an exposure time of 1s in the 200-800 nm range [19].

The energy efficiency of RONS (g·kW^{-1}·h^{-1}) was evaluated based on the average discharge power and the accumulation of the NO_2^-, NO_3^- and H_2O_2 energy efficiencies by recording the applied voltage and current across the plasma reactor using voltage and current probes that were connected to a digital oscilloscope. The following expressions were used to determine the energy injection and discharge power, via the OriginPro® software [20, 21]:

$$\text{Energy injection (J.pulse}^{-1}\text{)}, E = \int_{t_0}^{t_0+T} u(t)i(t)dt$$

$$\text{Discharge power (W)}, P = E\ f$$

where, $u(t)$ is the voltage (V), $i(t)$ is the current (A) and f is the pulse repetition frequency (Hz).

The energy efficiency of NO_2^-, NO_3^- and H_2O_2 was calculated using the equation below:

$$Energy\ efficiency\ = \frac{C\ x\ V\ x\ MM}{P}$$

where, C is the concentration of NO_2^-, NO_3^- and H_2O_2 in μM,
V is the volume of sample in L,
MM is the molar mass of NO_2^-, NO_3^- and H_2O_2 in g·μmol^{-1}, and
P is discharge power (kW·h).

4.4.4 Analysis of RONS concentration

Reactive oxygen and nitrogen species (RONS) measurements were performed at the end of the discharge prior to bacterial inactivation.

NO_2^-, H_2O_2

A colorimetric method with a Griess' reagent and a titanium oxysulfate assay, respectively, using a UV-visible microplate reader (SPECTROstar Nano, BMG Labtech, Australia) at 548 nm and 403 nm, respectively were employed. Sodium azide was added to remove the NO_2^- interference with the H_2O_2 measurement [22]. 100 μL Griess' reagent was added to 100 μL of NO_2^--containing sample. After an incubation time of 30 min, the absorbance of the sample was immediately read at a 548nm absorbance, which were then corrected with the absorbance signal by MilliQ® water (blank). Six $NaNO_2$ standards at 0, 15.6, 31.3, 62.5, 125 and 250 μM were used to create the NO_2^- standard curve and produce a fitted linear equation with an R^2 value of 0.9974, as given as:

$$\text{Absorbance} = 0.007165 \times NO_2^- \text{ concentration (μM)} + 0.02374$$

Then NO_2^- concentration of the sample (μM) was calculated using the linear equation and the corrected absorbance signal. In addition, an appropriate dilution was carried out when the sample produced higher absorbance signals than the $NaNO_2$ standard at 250 μM.

The calibration curve of H_2O_2 was generated by nine standards of H_2O_2 at 0, 12.5, 25, 50, 100, 200, 400, 800 and 1000 μM, produced a fitted linear equation with an R^2 value of 0.9950, as given as:

$$\text{Absorbance} = 0.0004313 \times H_2O_2 \text{ concentration (μM)} + 0.006054$$

Then H_2O_2 concentration of the sample (μM) was then calculated using the linear equation and the corrected absorbance signal.

NO_3^-

An ion-selective technique using a NO_3^--selective electrode (Cole-Parmer, Australia), an Ionic Strength Adjuster (ISA) and sulfanic acid for the removal of NO_2^- interference was utilised.

Dissolved O_3

An indigo colorimetric assay was employed using indigo trisulfonate [14, 23-25]. Dissolved O_3 was not measured in Section 4.1.3 with increasing salinity because the high Cl^- concentrations interfered with O_3 detection via the indigo colorimetric assay.

The indigo primary stock solution and indigo reagents (IR I and IR II) were made in a brown glass bottle from MilliQ® water, potassium indigo trisulfonate, concentrated phosphoric acid and sodium dihydrogen phosphate as described in references [23, 26]. IR I and IR II were prepared fresh to provide accurate measurements. The presence of ozone in each sample caused the discolouration of the indigo reagent [23]. IR I was used for lower O_3 concentration at 0.01-0.1 mg.L^{-1} and IR II was used for higher O_3 concentration at 0.05-0.5 mg·L^{-1} [24, 26]. The O_3 measurement was only performed for the studies with MilliQ® water.

To measure the absorbance value of blank (MilliQ® water) or sample, 1 mL of indigo reagents (IR1 or IR2) was added to a glass-stoppered 25 mL volumetric flask followed by filling to mark with blank or sample. The absorbance measurement of the mixed solution at an 600nm absorbance was performed by a fiber-optic spectrometer (Ocean Optics, USB4000) and a semi-micro cuvette with a 10mm path length (Sarstedt, Inc.). The equation below was then used to calculate the concentration of dissolved O_3, via the "Spectrophotometric, volumetric method":

$$\text{Dissolved } O_3 \text{ (mg.L}^{-1}) = \frac{(A_b - A_s)V_f}{fbV_s}$$

where A_b is absorbance of the blank at 600 nm, A_s is absorbance of the sample at 600 nm, V_f is the final volume of the flask (mL), V_s is the volume of the sample added into the flask (mL), b is the optical path length of UV cells (cm), and f is the sensitivity factor (0.42 L·mg^{-1}·cm^{-1}).

ClO^-

Due to the presence of chloride ions in PAW during the addition of NaCl, the concentration of ClO^- was measured. A UV-Vis spectrometer (USB4000, Ocean Optics, U.S.) and a UV cuvette (759170, BrandTech® Scientific, U.S.) at 292 nm were utilised [27]. The Beer-Lambert law was used to corelate the measured absorbance with the molar extinction coefficient of ClO^- (362 M^{-1}·cm^{-1}) [27].

Total RONS Concentration

The total concentration of RONS was expressed as the sum of NO_2^-, NO_3^-, H_2O_2 as below:

$$\text{Total concentration of RONS (mg·L}^{-1}) = [NO_2^-]\ (\text{mg·L}^{-1}) + [NO_3^-]\ (\text{mg·L}^{-1}) + [H_2O_2]\ (\text{mg·L}^{-1})$$

4.4.5 Simulation of Electrical Field

The electric field in the HPD reactor was simulated using COMSOL Multiphysics AC/DC module version 6 (COMSOL Inc., MA, USA) as described in the literature [28], with some modifications. The HPD reactor in **Section 4.4.1** was modelled in a three-dimensional system and a physics-controlled mesh of extra finer elements was used to accomplish the simulation. The voltage of the high-voltage electrode was set as 5.94 kV and the voltage of the ground electrode was set as zero.

4.4.6 Bacterial analysis post-PAW treatment

Evaluating bacterial inactivation efficiency

Bacterial inactivation efficiency was evaluated via the plate counting method [11, 29]. *Escherichia coli* 0157:H7 (ATCC®700728™) and *Salmonella* Typhimurium (NCTC74) were grown individually on nutrient agar plates for an incubation time of 24 h at 37 °C to obtain isolated colonies. To produce cell suspension, single colony was isolated and inoculated into 5 mL of peptone water (10 g/L, Thermo Fisher Scientific, Inc. CM0009). The cell suspension was incubated for 24 h at 37 °C. Subsequently, 50 μL of the prepared bacterial suspension was added to 4.95 mL of sterile water (as a control) or PAW: (i) at ambient temperature for the contact times from 60 to 960 s for the pin-to-liquid discharge and plasma-bubble discharge (ii) at 55 °C for the contact times from 10 to 30 s for the hybrid plasma

discharge and (iii) at 55 °C for the contact times from 20 to 30 s for the hybrid plasma discharge with ultrasound. Three replicates were performed independently for each treatment.

After treatment, samples were serially diluted in peptone water and 100 μL spread onto nutrient agar in triplicates. Plates were incubated for 24 h at 37 °C. Bacterial colonies were counted, and results reported as $\log_{10}$ CFU/mL. $\log_{10}$ reduction was calculated using the following equation:

$$\log_{10} reduction = \log_{10} N_0 - \log_{10} N$$

here, N is the microbial cell count after treatment (CFU/mL), N_0 is the microbial cell count after control treatment (CFU/mL).

For PAW generation by the pin-to-liquid discharge and plasma-bubble discharge, two theoretical inactivation models, log-linear regression [30] and Weibull [3, 4], were applied to mean values of survived bacterial colonies for all PAW treatments using GInaFiT [5]. The parameters and goodness of fit for the log-linear and Weibull model were tabulated in **Table S1** and **Table S2**.

The log-linear regression model was expressed as [30]:

$$\log_{10} N = \log_{10} N_0 - \frac{k_{max} t}{\ln 10}$$

where, k_{max} is the inactivation rate (s^{-1}), and t is the treatment time (s).

The Weibull distribution, a non-linear inactivation model, was defined as [3, 4]:

$$\log_{10} N = \log_{10} N_0 - (\frac{t}{\delta})^p$$

where, p is the shape parameter (concave upward if p<1, concave downward if p>1 and straight line if p=1), δ is the scale parameter (s).

Morphological changes in bacteria and detecting DNA leakage from bacteria

TEM analysis was used to investigate the morphological changes in *E. coli* after PAW treatment. Immediately after *E. coli* treatment with water (control) or plasma-activated water at the contact time of 30 s, bacterial samples were fixed in a solution comprising 2.5% w·v^{-1} glutaraldehyde and 1 mg·mL^{-1} ruthenium red in 0.2 M sodium phosphate buffer over night at 4 °C as per **Rezaeimotlagh, Resch, Kuchel, Biazik, Ziuzina, Bourke, Cullen and Trujillo [31]**. Fixed cells were rinsed with 0.1 M sodium phosphate buffer and post stained with 1% osmium tetroxide in 0.1 M sodium phosphate buffer using a BioWave Pro+ Microwave Tissue Processor (Ted Pella, USA). The samples were then washed with MilliQ® water, dehydrated with a graded series of ethanol, infiltrated with resin (Procure, 812), and polymerized using an oven at 60 °C for 24 h. A diamond knife (Diatome) was used to cut ultrathin sections (70 nm), which were collected onto carbon-coated copper TEM grids. Uranyl acetate (2%) and lead citrate was used to post stain the grids. The stained grids were then examined using a transmission electron microscope (JEM-1400, JEOL, Tokyo, Japan) operating at 100 keV and 500 nm. The cell pellets obtained from the inactivation study of *E. coli* in Figure 15 were not enough to perform TEM analysis. Therefore, in order to obtain enough cell pellets, the ratio of bacterial suspension and sample (including control and PAW) was modified to 10 % of the bacterial suspension and 90 % of the sample **[32]**.

Similarly**,** in the experiment of the hybrid plasma discharge that had the highest bacterial inactivation efficiency, DNA leakage from *E. coli* cells post-PAW treatment was investigated by measuring the concentrations of DNA molecules released from the cells in the treated solution as a function of treatment time, described previously [33]. Sterile water treatment was used as the control. Immediately after 10, 20 and 30-s contact times, the DNA concentrations in the

samples were measured at 485 nm excitation and 520 nm emission maxima according to the manufacturer's protocols using the Quanti-iT™ High-Sensitivity dsDNA Assay Kit (Invitrogen, U.S.) and a fluorescence spectrometer (FLUOstar Omega, BMG Labtech, Germany) and a sterile 96-well black polystyrene microplate (CLS3603, Corning®). A standard DNA calibration method (**Fig. 14**) was used the calculate the DNA concentration.

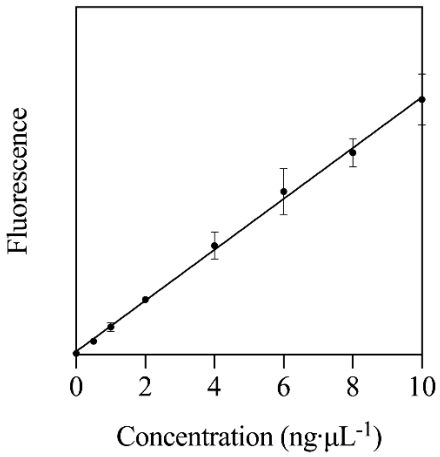

Figure 14. Standard curve for DNA leakage.

4.4.7 Bacterial inactivation on beef surface

Preparation of beef samples

Fresh grass-fed beef rump cuts were collected from a meat distrubutor within a week of slaughter and store at 4 °C prior to treatment. Beef was cut with a weight of approximately 10 g for the evaluation of bacterial inactivation. *Salmonella* Typhimurium (NCTC74) were grown individually on nutrient agar plates for an incubation time of 24 h at 37 °C to obtain isolated colonies. To produce cell suspension, single colony was isolated and inoculated into 4.5 mL of peptone water (10 g/L, Thermo Fisher Scientific, Inc. CM0009). The cell suspension was incubated for 24 h at 37 °C. The prepared beef cut was then inocculated with 100 μL of *S.* Typhimurium suspension. To enable the *S.* Typhimurium to attach to the meat, all samples were placed on a clean bench and air dried for 30 min at room temperature.

Treatment Process

Prior to treatment, all prepared beef samples with *S.* Typhimurium were chilled in a cold room at 4 °C for 24 h. Then, the chilled samples were exposed to either PAW or sterile water at 55 °C via two meat washing methods, such as spraying and immersion. A water bath (Grant Instruments, U.K.) was used to heat PAW and water to 55 °C.

For the spraying method, a handheld mist sprayer (Illu-Mist Mist Battery Powered Sprayer, U.S.) with a liquid flowrate of 3.37 $mL \cdot s^{-1}$ was used. Prior to treatment, the chilled meat sample with *S.* Typhimurium was placed on top of a stainless-steel filter (737-4096, RS Components Pty Ltd, Australia) with 4 round head bolts and nuts, which was placed in a 500mL borosilicate beaker, as shown in **Fig. 15**. The distance between the meat surface and the water outlet of the mist sprayer was kept at 70 mm. 3 contact times of the meat and spraying with PAW or liquid were used, such as 15, 30 and 60 s. To investigate the effect of storage time on the bacterial inactivation via the spraying method, all treated samples were stored in a flat-bottom container (S5527SU, Techno Plas Pty Ltd, Australia) at 4 °C for 0, 1 and 7 days as shown in **Fig. 15**.

For the immersion method, the chilled meat sample with *S.* Typhimurium was immersed in 101 mL of water or PAW, which was firstly prepared in a flatbottom container (P246SU, Techno Plas Pty Ltd, Australia) and placed in a water

bath at 55 °C for 30 min, as shown in **Fig. 15**. The value of 101 mL was chosen based on the amount of liquid consumed for the spraying method at 30 s. Similar to the spraying method, 3 contact times were used, such as 15, 30 and 60 s. To investigate the effect of storage time on the bacterial inactivation via the immersion method, all treated samples were stored in a flat-bottom container (S5527SU, Techno Plas Pty Ltd, Australia) at 4 °C for 0, 1 and 7 days. Furthermore, at a constant storage time, the treated samples by spraying and immersion, were compared with the untreated sample (control) as shown in **Fig. 15**.

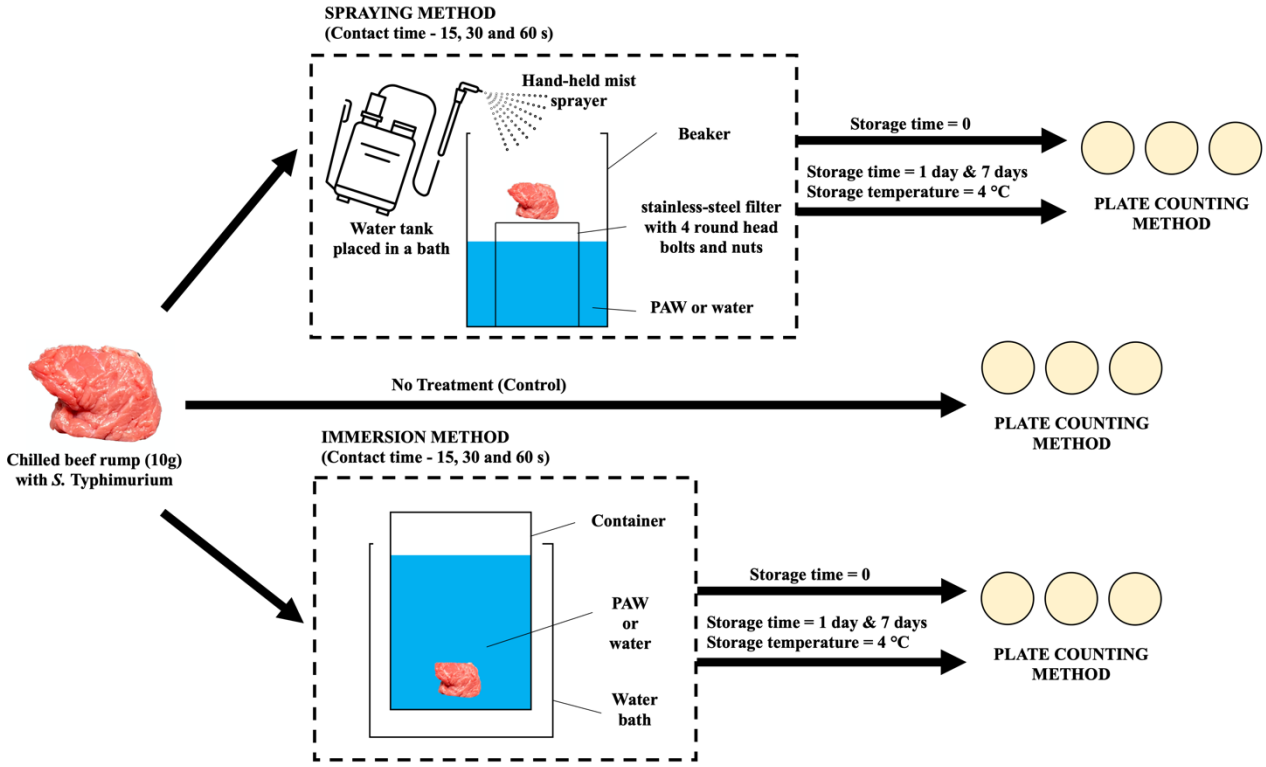

Figure 15. (a) Experimental setup of beef samples treated with spraying and immersion methods.

Bacterial evaluation

The plasma-treated, water-treated and untreated beef samples were homogenised with 90mL D/E neutralising broth (Remel, U.S.) in a stomacher bag using a stomacher (Stomacher® 400 Circulator Lab Blender, Seward Ltd., U.K.) for 2 min. A serial dilution using sterile peptone water was then performed. Then, 100 µL of each dilution was spread onto XLD agar plates (PP2004, Thermo Fisher Scientific, Australia) in triplicates. Plates were incubated for 24 h at 37 °C. Bacterial colonies were then counted.

4.4.8 Evaluating bacterial inactivation efficiency

After plate counting, the results obtained in Section 4.4.1 were reported as $\log_{10}$ CFU/mL. $\log_{10}$ reduction and calculated using the following equation:

$$\log_{10} reduction = \log_{10} N_0 - \log_{10} N$$

here, N is the microbial cell count after PAW/water treatment (CFU/mL), N_0 is the microbial cell count after control treatment (CFU/mL).

4.4.9 Quality Analysis of Beef

Water Holding Capacity

Water holding capacity (WHC) was conducted via a centrifugation method [34], with some modifications. About 10 g of plasma-treated, water-treated or untreated beef sample was mixed with 16 mL of sodium chloride solution (NaCl, 0.6 M) and homogenised using a stomacher (Stomacher® 80 Biomaster, Seward Ltd., U.K.) for 1 min. The meat slurry was then incubated at 4 °C for 30 min, followed by stirring for 1 min and centrifugation using a centrifuge (Centrifuge 5702, Eppendorf, Australia) at 4,400 rpm for 20 min. After centrifugation, the supernatant layer was then collected and measured by volume. The amount of added solution held by the beef is described as the water holding capacity in mL per 100g meat as shown as the equation below:

$$WHC\ \left(\frac{mL}{100g}\right) = \frac{Volume of\ added\ solution\ (mL) - Volume\ of\ released\ solution\ (mL)}{Weight\ of\ sample\ (g)} x\ 100$$

pH

About 10 g of plasma-treated, water-treated or untreated beef sample was homogenised for 30s with 90mL of MilliQ® water using a stomacher (Stomacher® 400 Circulator Lab Blender, Seward Ltd., U.K.). The pH of the sample was measured using a benchtop pH meter kit (Hanna Instruments, Australia) [34, 35].

Lipid Oxidation

Lipid oxidation of plasma-treated, water-treated and untreated beef samples were evaluated using the thiobarbituric acid reactive substance (TBARS) value according to the method described in the literature [35], expressed in mg of malondialdehyde (MDA) per kg of sample. About 10 g of each beef sample was homogenised with 20mL glacial acetic acid and 1% butylated hydroxytolune (BHT) using a stomacher (Stomacher® 80 Biomaster, Seward Ltd., U.K.) for 2 min. The homogenised solution was then centrifuged using a centrifuge (Centrifuge 5702, Eppendorf, Australia) at 3,000 rpm for 10 min. After centrifugation, the supernatant was filtrated and mixed with thiobarbituric acid (TBA, 20mM) and placed in a water bath (Grant Instruments, U.K.) at 90 °C for 60 min before absorbance was read using a spectrometer (SPECTROstar Nano, BMG Labtech, Australia) at 532nm.

Myoglobin Redox Forms

Similar to **Section 4.3.4**, 5 g of treated beef was homogenised with 10ml phosphate buffer (pH 6.8) for 2 min and centrifuged at 3,000 rpm for 10 min. The absorbance of the supernatant was measured at 503, 525, 557 and 582 nm.

Colour

Colour of plasma-treated, water-treated and untreated beef samples (10g) were measured using a ChromaMeter (CR-400, Komica Minolta Optics, Inc., Japan), expressed as L^* (lightness), a^* (redness) and b^* (yellowness) [35, 36]. The colour change (ΔE), which represents the degree of colour difference during treatment at each storage time was calculated using the following equation:

$$\Delta E\ = \sqrt{(L_c^* - L_t^*)^2 + (a_c^* - a_t^*)^2 + (b_c^* - b_t^*)^2}$$

where, L_c^*, a_c^* and b_c^* are the colour values of untreated beef at each storage time; and L_t^*, a_t^* and b_t^* are the colour values of plasma- or water-treated beef at each storage time [37].

Chroma (C, saturation index) was calculated to indicate vivid or dull colour via the following equation [38]:

$$C\ = \sqrt{(a^*)^2 + (b^*)^2}$$

Hue angle (h^*) was calculated using the following equation [39]:

$$h^*\ = \tan^{-1}(b^*/a^*)$$

Weight Gain

Weight gain of beef samples after each treatment was measured using the following calculation [35]:

$$Weight\ gain\ (\%) = \frac{meat\ sample\ after\ treatment\ (g) - intial\ meat\ sample\ (g)}{initial\ meat\ sample\ (g)} x\ 100$$

4.4.10 Economic Analysis

The six-tenth power rule via the equation below was implemented to estimate the approximate capital cost related to the implemention of the PAW technology for the small and medium scale enterprise producers [40].

$$C_B = C_A(\frac{S_B}{S_A})^{0.6}$$

where C_B is the approximate capital cost (AU$) for size S_B (the required volume of PAW for the small/medium scale enterprise producers) and C_A is the known capital cost (AU$) corresponding to size S_A (the current volume of PAW produced in this study or 13.5 L per day).

Assumptions below were used to calculate the approximate capital costs of PAW production for the small and medium scale enterprise producers:

- The annual cattle production is 200 head for small producers and 1576 head for medium producers [41].
- 1 head is equivalent to 340 kg of hot standard carcass [42].
- 1 ton of hot standard carcass requires 10.6 kL of town water and 4% of the water is used for carcass washing [43].
- The operating day is 251 days and the daily operation is 9 h [44].
- The total capital cost with our current PAW production (13.5 L per day) is $AU 34,900. This cost includes the costs for plasma generator, mist spray with pump and liquid tank, heating equipment.

4.4.11 Statistical Analysis

All experimental data were presented as the mean ($\overline{X}$) in three independent reproductions. For all figures, error bars represent standard deviation (SD). Analysis of variance (ANOVA), using the Prism 8 software, with a 5% level of significance was performed to statistically analyse the difference in the samples. Furthermore, significant differences were identified by Tukey's honest significance difference (HSD) test.

5.0 Project Outcomes

5.1 Phase 1 Findings

The objectives outlined in Phase 1 were achieved and presented in this section. The construction of a non-thermal plasma system was achieved as described in Section 4.1.1 above and the characterization of excited species was determined through the use of optical emission spectrometer with results presented in **Fig. 16**. OES measurements were performed to investigate the major excited species generated in PAW by air spark discharge plasma ranging from 200 to 600 nm (**Fig. 16**). Plasma was generated above the water surface at an operating frequency of 50 Hz and voltage of 20 kV with OES measurements taken after 1 min of discharge time. The results of OES indicate the presence of N_2 species with peaks observed in the UV region at 315.9 nm, 337.1 nm, 357.7 nm, 375.5 nm and 380.5 nm corresponding to the (1,0), (0,0), (0,1), (1,3) and (0,2) vibronic transitions of the second positive band system of N_2. OH ($A^2\Sigma^+ - X^2\Pi_i$) transitions were also observed at 295nm with a vibrational band (3,2).

This study further explored variables affecting such reactive species including plasma discharge time (**Fig. 17**), which saw reactive species nitrite and nitrate increase with discharge time, treated volume which saw reactive species decrease at higher water volumes (**Fig. 18**), as well as the reduction in reactive species with the presence of agitation during plasma discharge as presented in **Table 2**, and the increase in reactive species with water surface area (**Fig. 19**).

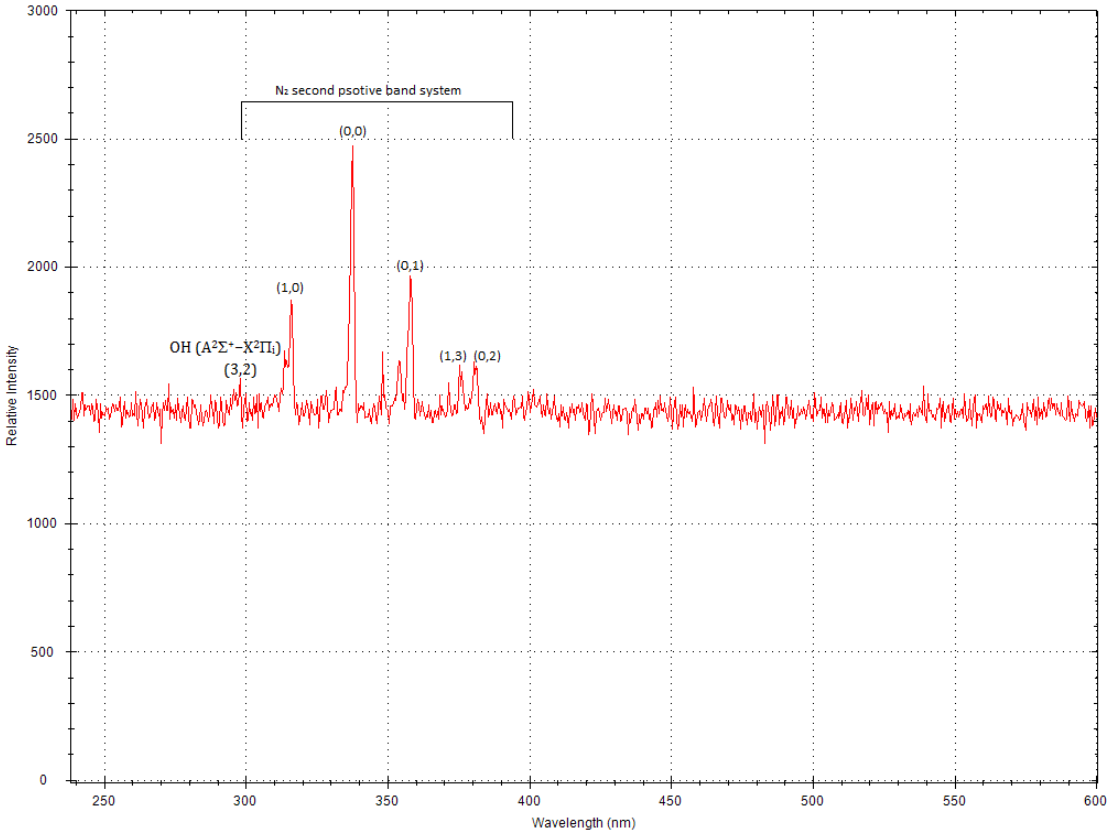

Figure 16. Optical emission spectrum of spark air-plasma discharge in contact with water.

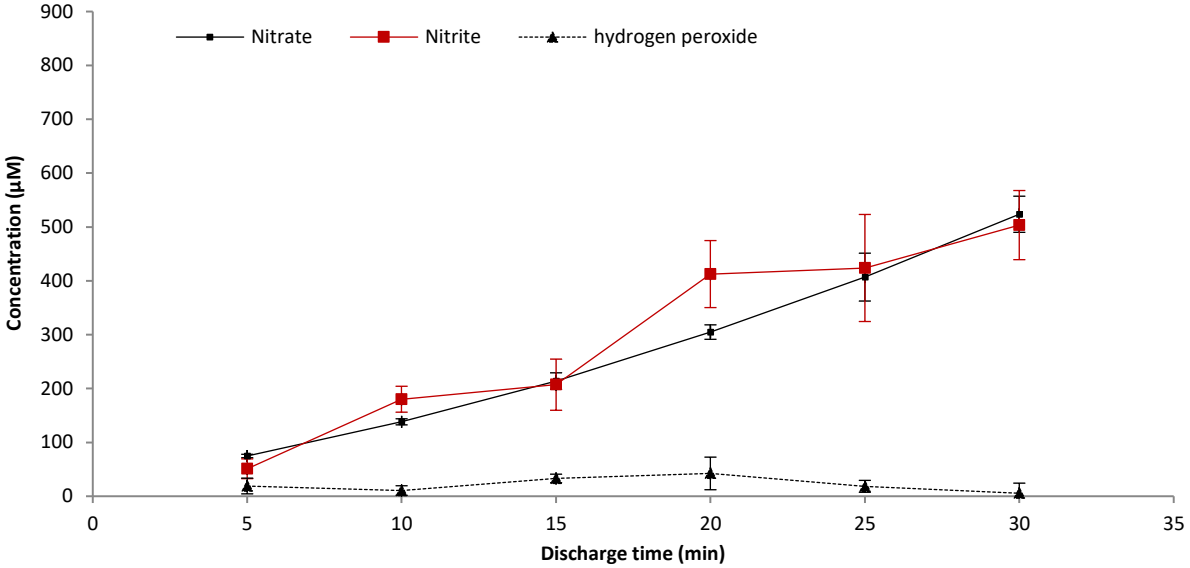

Figure 17. Concentration of reactive species (NO_3^-, NO_2^- and H_2O_2) in air-PAW in a closed system with increasing plasma discharge time.

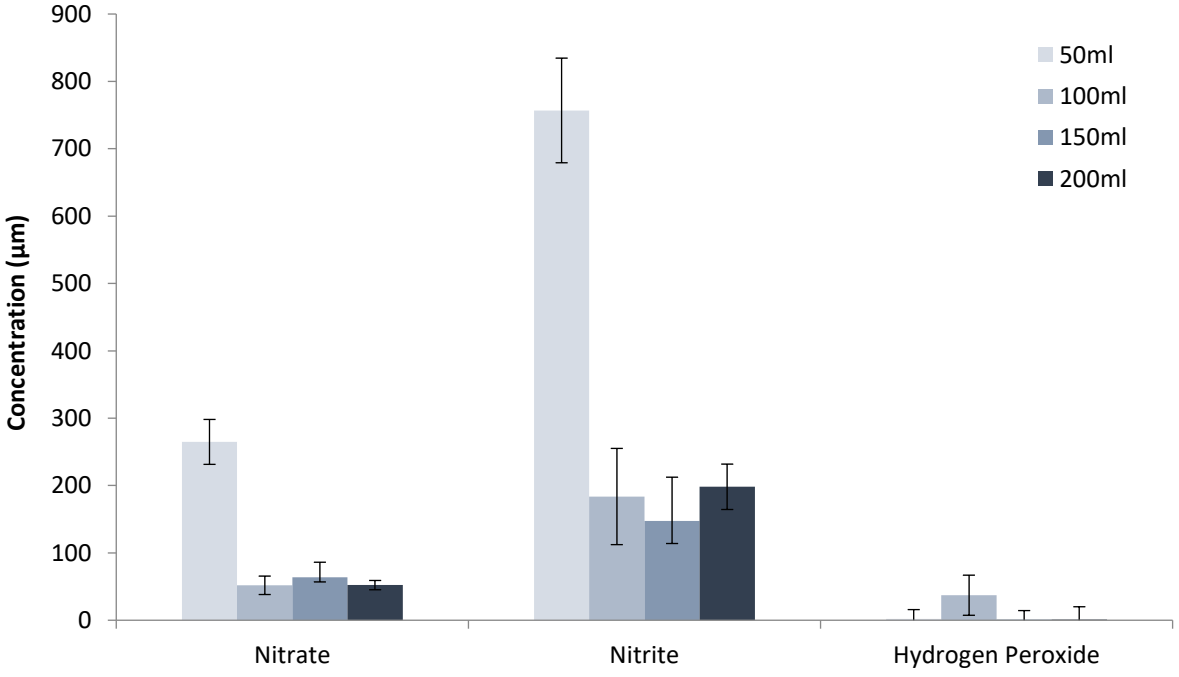

Figure 18. Nitrate, nitrite and hydrogen peroxide concentrations in air-PAW (produced in a closed system) with increasing water volume.

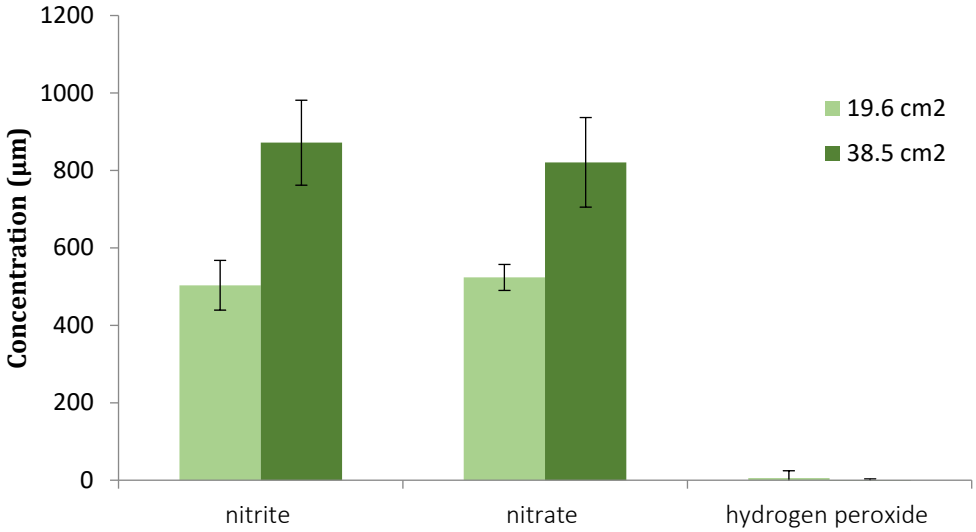

Figure 19. Concentration of nitrite, nitrate and hydrogen peroxide in air-PAW (produced in a closed system with a 10-min discharge time) with increasing water surface area.

System design was alternated between open (PAW-O) and closed (PAW-C) which allowed the availability of the working gas (air) to be controlled. PAW generated under both systems as a function of discharge time (min) are presented in **Table 1**, and as a function of agitation speed (rpm) in **Table 2**. Results show PAW-C to contain higher concentrations of nitrate and nitrite when compared to PAW-O.

Table 1. Concentration of nitrites, nitrates and hydrogen peroxide in air-PAW in a closed and open system with increasing plasma discharge time.

Discharge time (min)	Nitrite (µm)		Nitrate (µm)		hydrogen peroxide (µm)	
	Closed	Open	**Closed**	Open	**Closed**	Open
5	50.98 ± 18.35	39.76 ± 15.52	74.73 ± 3.17	27.95 ± 7.75	19.05 ± 14.64	2.70 ± 13.58
10	180.17 ± 24.04	48.26 ± 36.76	138.16 ± 5.65	48.38 ± 6.99	10.63 ± 8.84	39.37 ± 5.06
15	207.19 ± 47.52	104.58 ± 18.81	213.96 ± 15.19	68.01 ± 14.94	33.02 ± 7.97	56.98 ± 40.73
20	412.53 ± 62.21	143.14 ± 17.53	304.81 ± 13.38	106.17 ± 6.87	42.38 ± 30.29	65.24 ± 23.10
25	423.86 ± 99.38	164.60 ± 36.75	406.96 ± 44.39	134.67 ± 15.86	18.41 ± 11.05	58.57 ± 13.57
30	503.49 ± 64.19	158.39 ± 21.02	523.61 ± 33.56	163.97 ± 25.78	5.56 ± 18.82	70.00 ± 16.21

Table 2. Concentration of nitrites, nitrate and hydrogen peroxide in air-PAW in a closed and open system with increasing stirring speed (rpm).

RPM	nitrate (µm)		nitrite (µm)		hydrogen peroxide (µm)	
	Closed	Open	**Closed**	Open	**Closed**	Open
0	144.75 ± 9.53	53.759 ± 3.91	283.44 ± 61.12	63.246 ± 2.97	15.40 ± 4.45	39.37 ± 4.64
400	160.07 ± 25.34	47.577 ± 3.50	86.83 ± 63.69	51.547 ± 3.41	34.76 ± 11.45	36.51 ± 9.01
600	143.94 ± 13.13	40.588 ± 1.59	26.75 ± 13.10	43.769 ± 4.52	26.03 ± 12.07	29.68 ± 11.47

PAW-O and PAW-C's window of activity was explored with sealed storage up to 30 days at room temperature and under refrigeration with results presented in **Table 3**. Retention in reactive species was observed over the 30 days at both room temperature and under refrigeration as illustrated in **Fig. 20** and **Fig. 21**. PAW-C was also stored unsealed at room temperature with and without agitation (**Fig. 22**, **Table 4, Table 5**). Results showed a rapid decrease in reactive species when stored unsealed after just 24 h and even further when subjected to constant stirring.

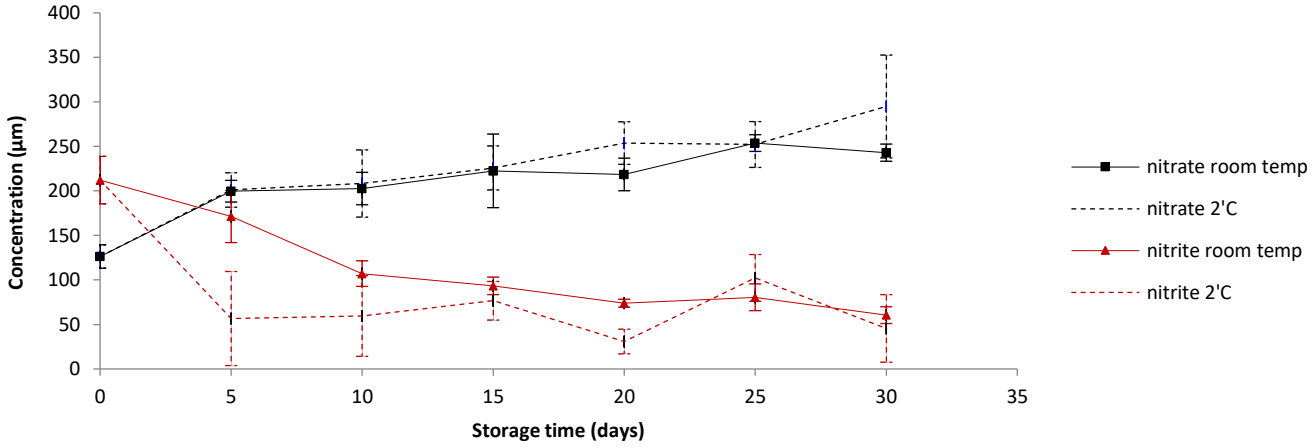

Figure 20. Concentration of nitrate and nitrite in air-PAW (produced in a closed system) stored sealed at different temperatures for up to 30 days.

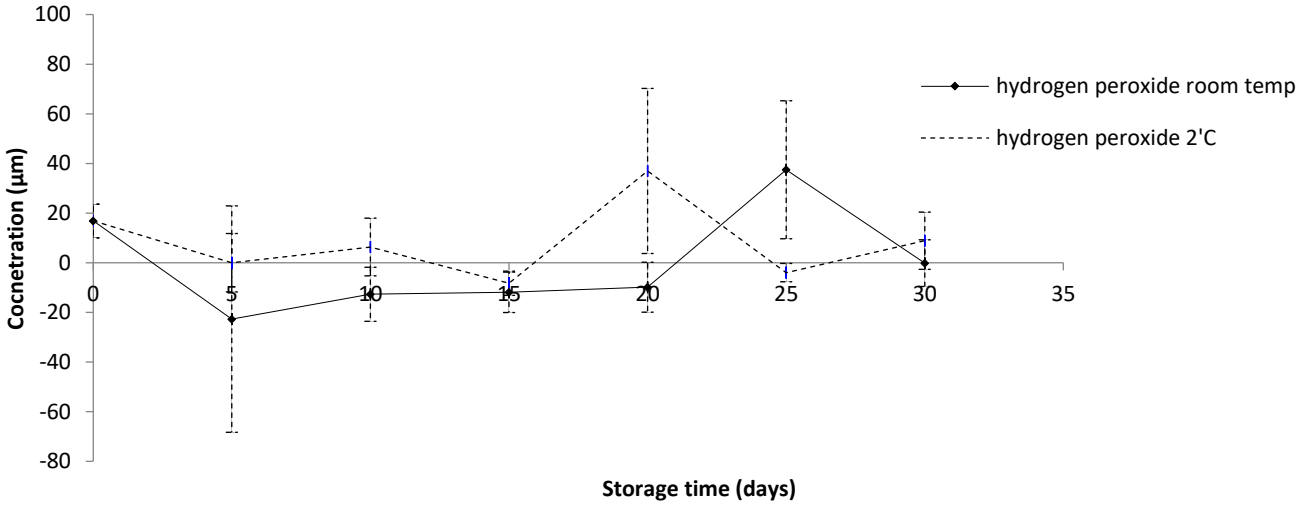

Figure 21. Concentration of hydrogen peroxide in air-PAW (produced in a closed system) stored sealed at different temperatures for up to 30 days.

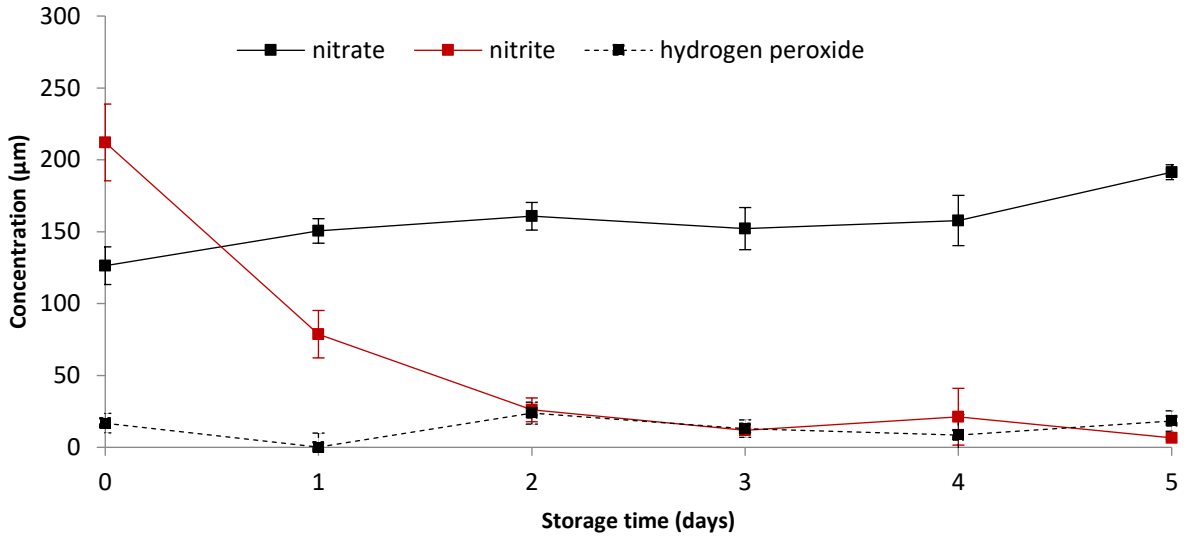

Figure 22. Concentration of nitrate, nitrite and hydrogen peroxide in air-PAW (produced in a closed system) stored open.

Table 3. Concentration of nitrites, nitrates and hydrogen peroxide in air-PAW (produced in a closed and open system) stored for up to 30 days at room temperature (RT) and at 2°C.

Closed system

Storage time (days)	nitrate (µm)				nitrite (µm)				hydrogen peroxide (µm)			
	RT	±	2°C	±	**RT**	±	2°C	±	**RT**	±	2°C	±
0	126.33	13.09	126.33	13.09	212.09	26.73	212.092	26.73	16.83	6.81	16.825	6.81
5	199.72	12.17	201.06	19.29	171.24	29.27	56.667	52.83	-22.70	45.59	0.000	11.78
10	202.67	18.21	208.32	37.69	107.12	14.36	59.542	45.32	-12.70	10.89	6.349	11.63
15	222.56	41.37	225.79	24.69	93.38	9.87	76.645	21.66	-11.90	8.14	-8.254	4.89
20	218.53	18.32	253.74	23.89	73.97	4.44	30.850	13.90	-9.84	10.06	36.984	33.25
25	253.74	9.39	252.13	25.76	80.54	15.00	102.309	26.23	37.46	27.79	-3.968	3.70
30	242.99	9.66	294.87	57.82	60.48	9.40	45.577	37.93	-0.16	9.41	8.889	11.54

Open system

Storage time (days)	nitrate (µm)				nitrite (µm)				hydrogen peroxide (µm)			
	RT	±	2°C	±	**RT**	±	2°C	±	**RT**	±	2°C	±
0	45.16	3.38	45.16	3.38	43.77	3.82	43.769	3.82	27.78	10.28	27.778	10.28
5	38.17	2.20	82.79	15.29	47.63	3.73	56.209	4.27	29.84	8.25	17.778	11.05
10	51.88	4.13	85.75	3.29	31.46	1.25	50.305	3.79	17.46	6.46	0.794	8.93
15	64.24	11.91	58.06	5.10	26.84	3.62	39.782	1.11	3.02	10.19	10.317	7.75
20	43.54	4.45	97.57	7.12	17.91	2.45	36.492	1.73	6.83	6.09	10.000	11.18
25	52.42	2.65	88.70	5.10	18.56	2.16	34.902	2.94	16.51	8.02	38.254	34.18
30	52.42	8.21	92.20	12.34	20.46	4.01	31.590	2.53	41.90	21.25	1.746	5.92

Table 4. Concentration of nitrites, nitrates and hydrogen peroxide in air-PAW (produced in a closed system) stored sealed and unsealed at room temperature.

Storage time (days)	nitrate (µm)				nitrite (µm)				hydrogen peroxide (µm)			
	Sealed	±	Unsealed	±	Sealed	±	Unsealed	±	Sealed	±	Unsealed	±
0	126.33	13.09	126.33	13.09	212.09	26.73	212.092	26.73	16.83	6.81	16.825	6.81
5	199.72	12.17	191.38	5.17	171.24	29.27	6.60	1.11	-22.70	45.59	18.25	7.10

Table 5. Concentration of nitrites, nitrates and hydrogen peroxide in air-PAW (produced in a closed system) stored unsealed at room temperature with and without agitation with magnetic stir bar.

Storage time (hrs)	nitrate (µm)				nitrite (µm)				hydrogen peroxide (µm)			
	Agitated	±	No agitation	±	Agitated	±	No agitation	±	Agitated	±	No agitation	±
0	126.33	13.09	126.33	13.09	212.09	26.73	212.092	26.73	16.83	6.81	16.825	6.81
24	161.28	3.95	150.53	8.51	14.49	0.63	78.69	16.52	7.86	7.38	0.16	9.78

PAW-C was subsequently used to treat both free-living cells (**Fig. 23**, **Fig. 24**) and adhered cells (**Fig. 25**). Higher log reductions were observed in free-living cells with PAW generated by a 30minute discharge time (PAW-C-30) as opposed to 10 min (PAW-C-10) as illustrated in **Fig. 24**. Bacteria was then treated with PAW-C-30 for up to 390 s which resulted in bacterial $\log_{10}$ reductions of 0.67, 2.24, 1.32 and 1.37 for bacterial solutions of *E. coli* O157:H7, *S.* Typhimurium, *L. lactis* and *P. fluorescens*, and a 1.2-$\log_{10}$ reduction for adhered *E. coli* cells.

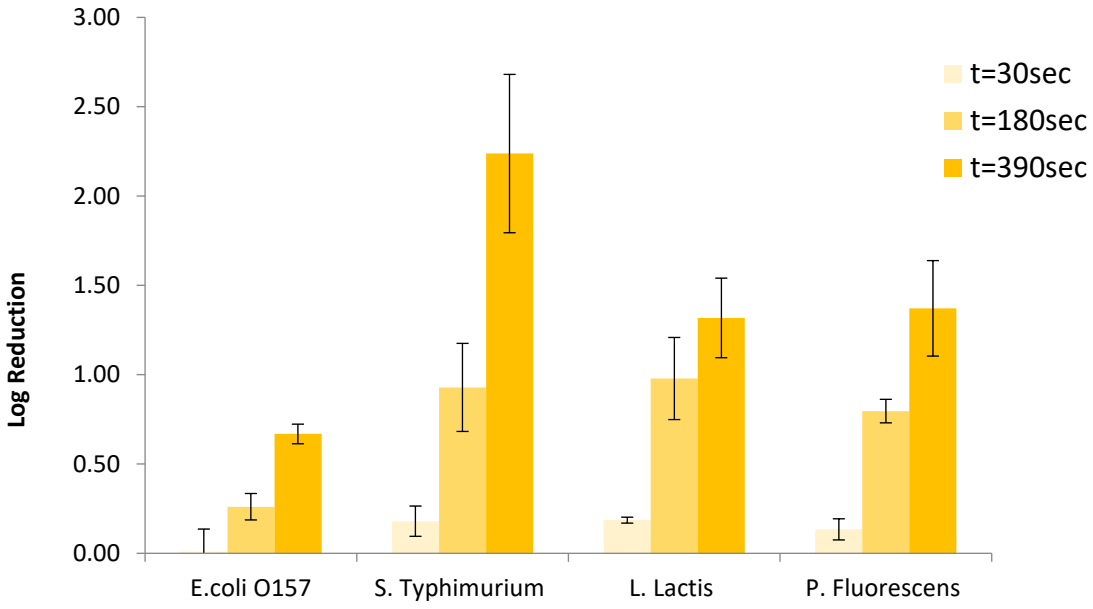

Figure 23. Inactivation rate of E. coli, S.Typhimurium, L. Lactis and P. fluorescens after treatment with PAW for 30, 180 and 390 s.

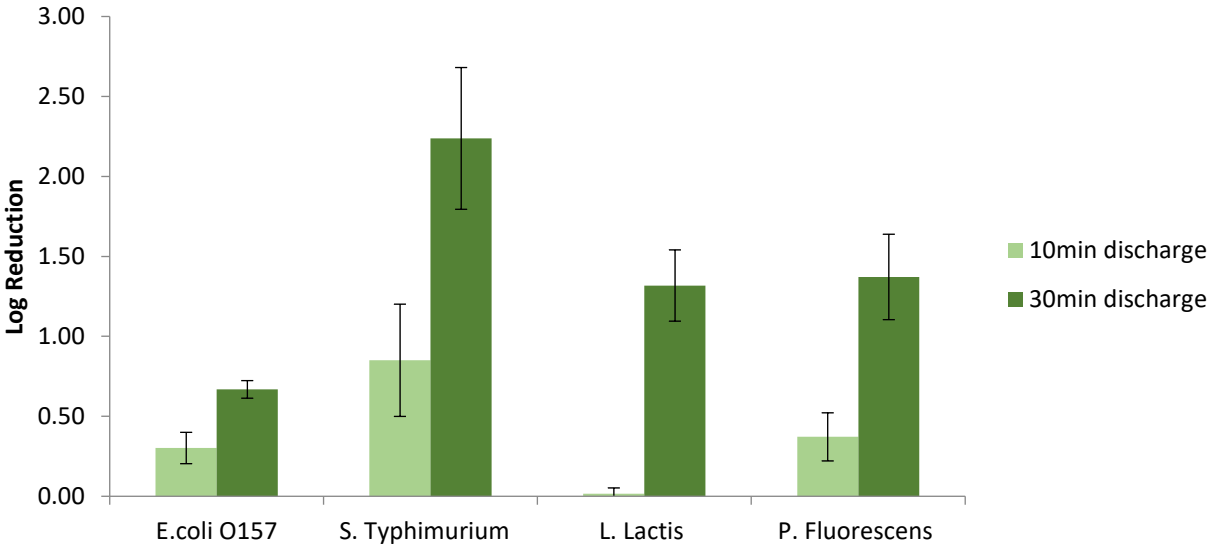

Figure 24. Inactivation rate of E. coli, S. Typhimurium, L. Lactis and P. fluorescens after treatment with PAW produced in a closed system with a 10-min and 30-min discharge time.

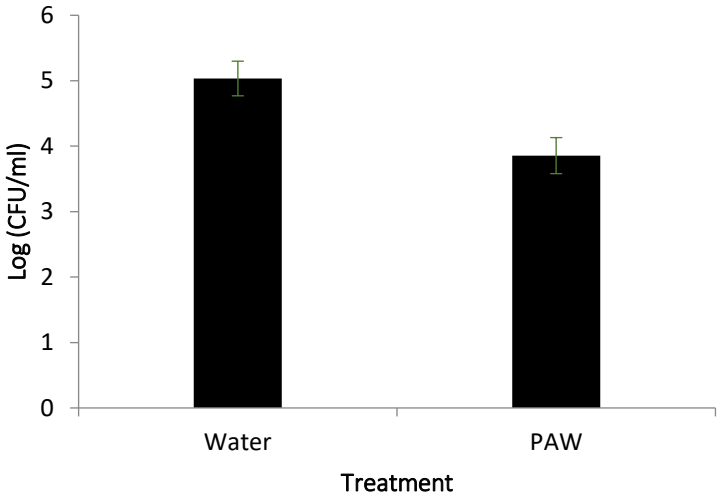

Figure 25. Antimicrobial effect of PAW (produced in a closed system with a 30-min discharge time) on E. coli cells adhered to silicon wafers with a 390s treatment time.

Table 6. Decontamination of meat containing inoculated Escherichia coli 0157:H7 by acid washes.

Tissue	Method	Decontamination potential	References
Lean beef	2% lactic acid 2% lactic acid and alginate dip	0.50-$\log_{10}$ reduction 0.74-$\log_{10}$ reduction	[45]
Lean beef and adipose tissues	1, 3, 5% lactic, acetic, citric Pilot scale washer	1- to 2-$\log_{10}$ reduction	[46]
Lean beef	1.5% lactic, citric acid spray At 20-55 °C	0.3- to 0.5-$\log_{10}$ reduction	[47]
Lean beef	1% lactic acid 1% acetic acid 1.5% fumaric dip	0.78-$\log_{10}$ reduction 0.63-$\log_{10}$ reduction 1.96-$\log_{10}$ reduction	[48]

5.2 Phase 2 Findings

Phase 2 explored the efficacy of plasma activated water (PAW) against various pathogenic and spoilage bacterial species through various treatment methods. Beef and lamb samples of various cuts were procured from slaughterhouses in NSW, Australia and were collected prior to undergoing any decontamination treatment. Once received, beef and lamb cuts were further cut into 20x20x10mm samples and frozen until required. Samples were defrosted and allowed to come to room temperature before treatment.

The method of PAW generation greatly influences the concentration of reactive species present in the resulting solution. It was therefore expected that treatment of attached cells with PAW of higher reactive species concentration would improve it efficacy. In one study, PAW was generated using a reduced volume of MilliQ® water prior to discharge to produce PAWA, a solution containing 9% and 28% higher concentrations of nitrite and nitrates, respectively (refer to **Table 8**). **Fig. 27** indicates almost no change in bacterial reduction when treated with PAWA compared to PAW30. Similarly, the use of PAW60 was also explored as it also contains a higher concentration of reactive species than PAW30; however, **Fig. 28** shows a decrease in PAW's efficacy against both *E. coli* O157 and *S.* Typhimurium inoculated onto beef samples.

Beef samples were inoculated with approximately $1.1x10^8$ CFU/cm^2 *E. coli* O157 or 4.3×10^7 CFU/cm^2 *L. monocytogenes* and subjected to water wash and PAW wash treatment for 10 min as illustrated in **Fig. 7**. After treatment, beef sample was removed from wash water and bacterial cells remaining on beef surface after washing was analysed (see **Fig. 32**). The remaining treatment solution was immediately sampled (reported as time 0 min in **Fig. 33**) and continuously sampled for up to 35 min as reported below as 'time after treatment'. The initial bacterial population in treatment solution (reported as time -10min in **Fig. 33**) was estimated to be 6.95-$\log_{10}$ CFU for *E. coli* and 5.29-$\log_{10}$ CFU for *L. monocytogenes.*

Table 7. Bacterial log reduction CFU/ml after a 10-min PAW water bath treatment.

	Raw beef		Raw lamb	
	Topside	Rump	Leg	Shoulder
Salmonella	0.53 ± 0.07	0.21 ± 0.06	0.33 ± 0.05	0.24 ± 0.04
E.coli	0.54 ± 0.05	0.27 ± 0.04	0.28 ± 0.04	0.23 ± 0.14
Listeria	0.44 ± 0.09	0.94 ± 0.07	1.36 ± 0.04	1.5 ± 0.05

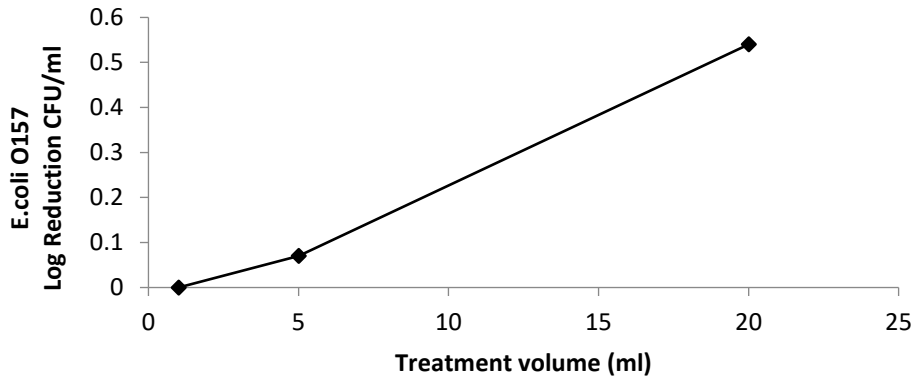

Figure 26. Inactivation rate of E. coli O157 when subjected to PAW water bath treatment of varying treatment volumes (1, 5, 20ml).

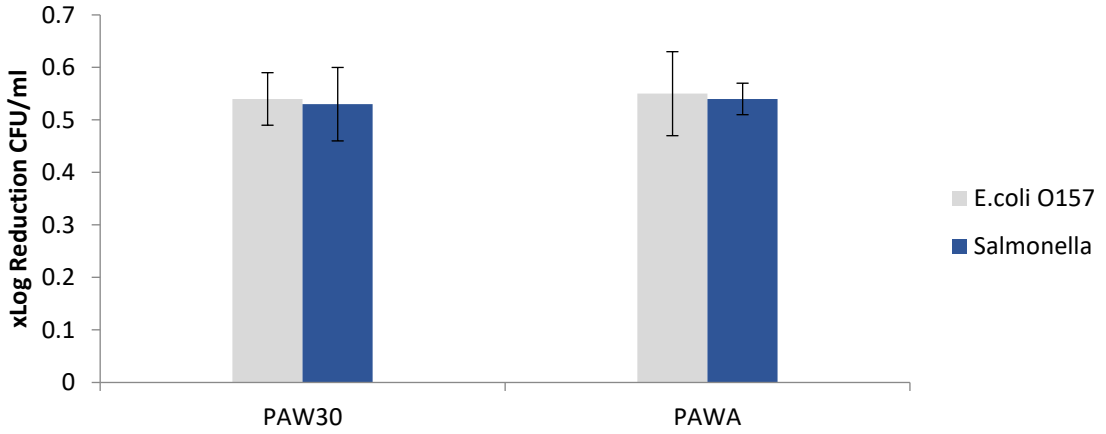

Figure 27. Comparison of the antimicrobial ability of PAWA, a solution containing higher concentrations of reactive species, against PAW30 containing lower concentrations of reactive species. Log reductions are reflective of PAW water bath treatment only.

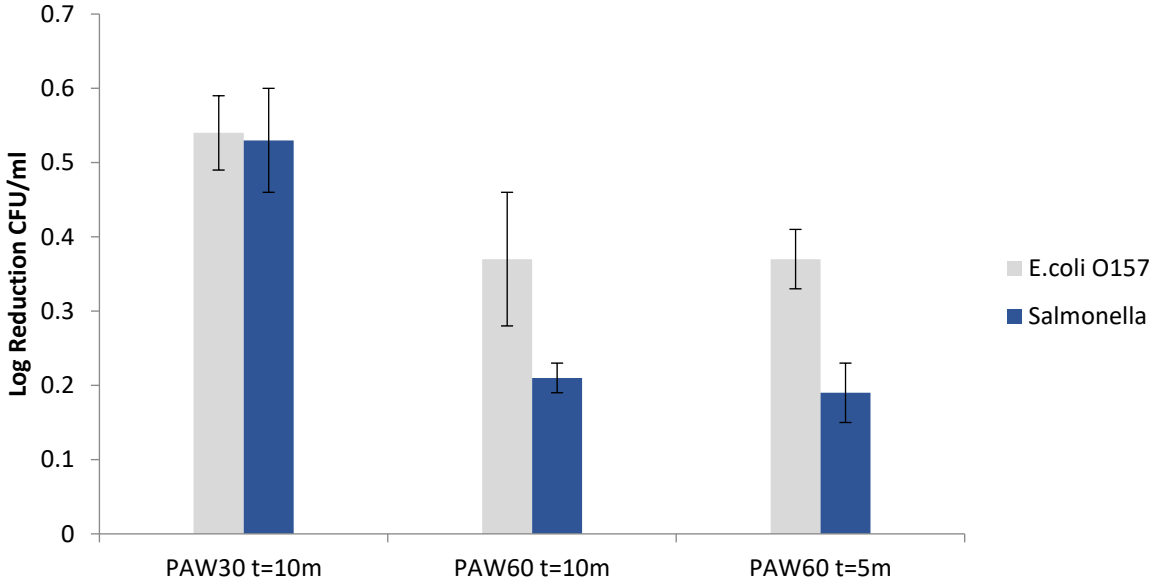

Figure 28. Comparison of the antimicrobial ability of PAW60, a solution containing higher concentrations of reactive species, against PAW30 containing lower concentrations of reactive species. Log_{10} reductions are reflective of a PAW 5- and 10-min water bath treatment only.

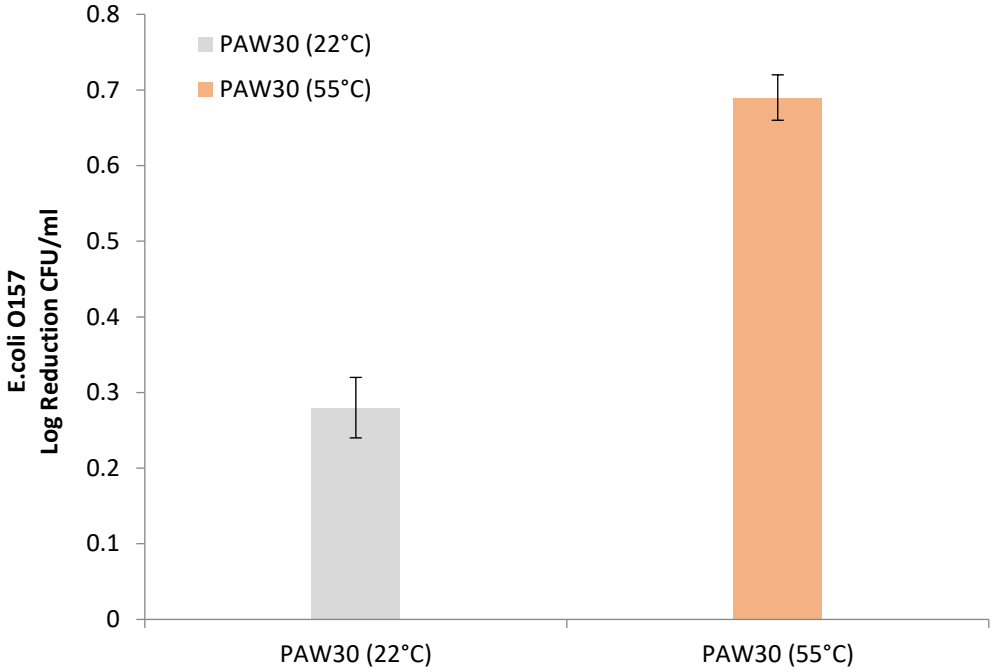

Figure 29. Comparison of the antimicrobial ability of warm PAW30 application against PAW30 applied at room temperature. Warm PAW30 was applied at a temperature of approximately 55 °C and room temperature PAW30 was applied at approximately 22 °C. Log reductions are reflective of PAW water bath treatment only.

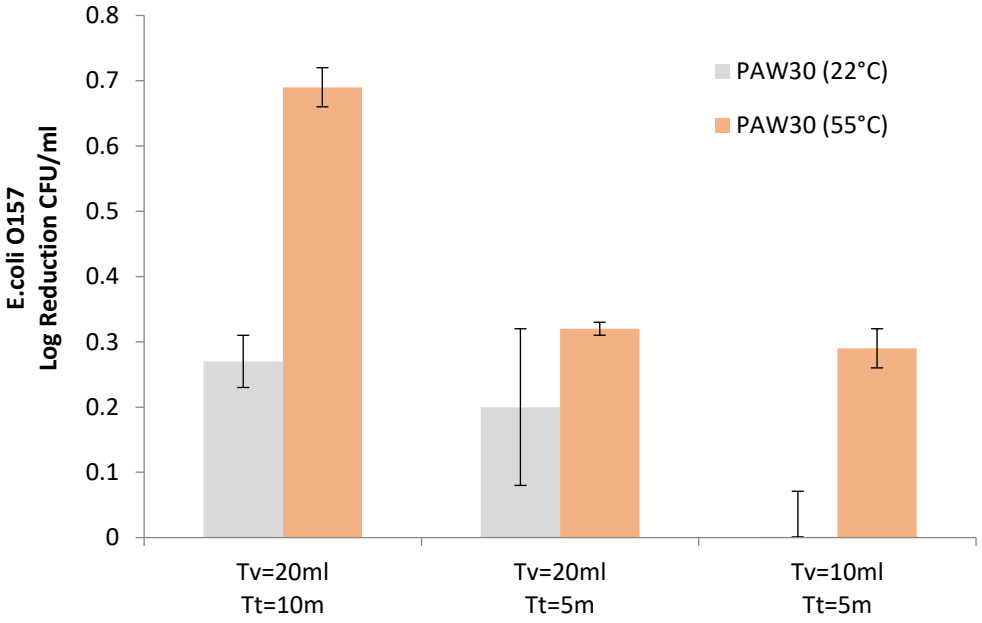

Figure 30. Comparison of the antimicrobial ability of warm PAW30 of varying treatment volumes (Tv =10, 20ml) and times (Tt = 5, 10min against PAW30 applied at room temperature at the same treatment volume and time. Warm PAW30 was applied at a temperature of approximately 55 °C and room temperature PAW30 was applied at approximately 22 °C. Log reductions are reflective of PAW water bath treatment only.

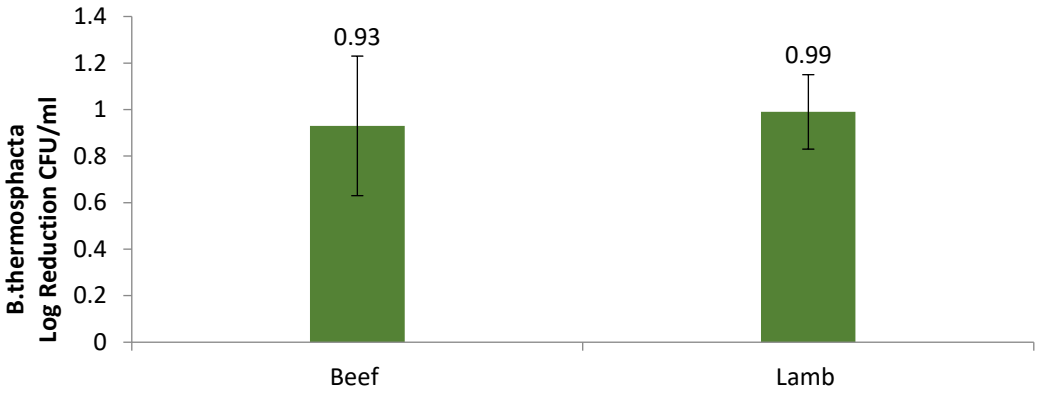

Figure 31. Reduction of B. thermosphacta inoculated onto beef and lamb samples with a 10-min PAW30 water bath treatment.

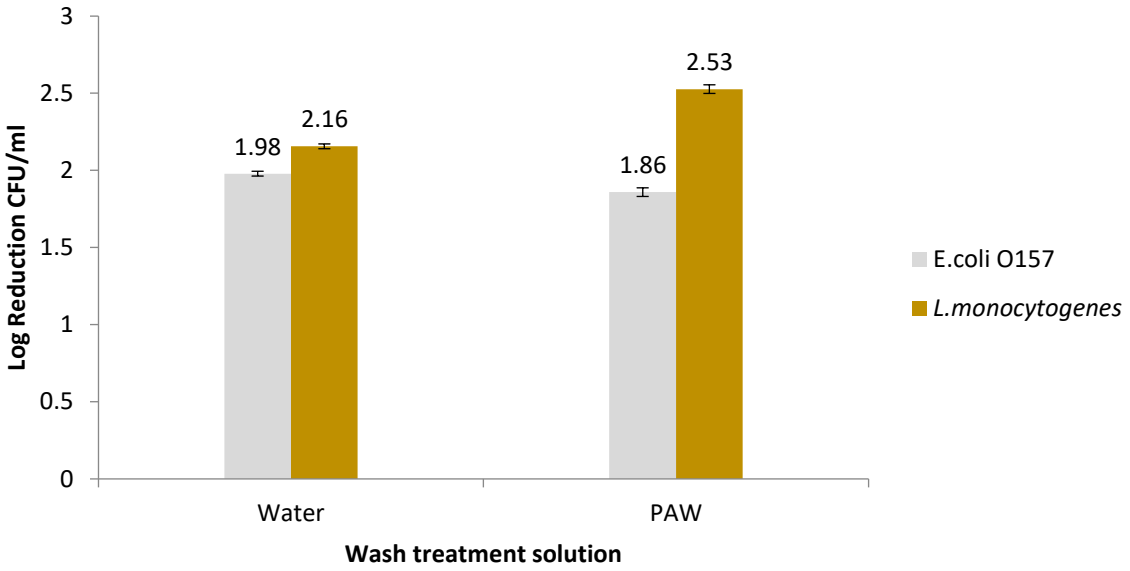

Figure 32. Reduction of E. coli and L. monocytogenes through water and PAW wash treatment.

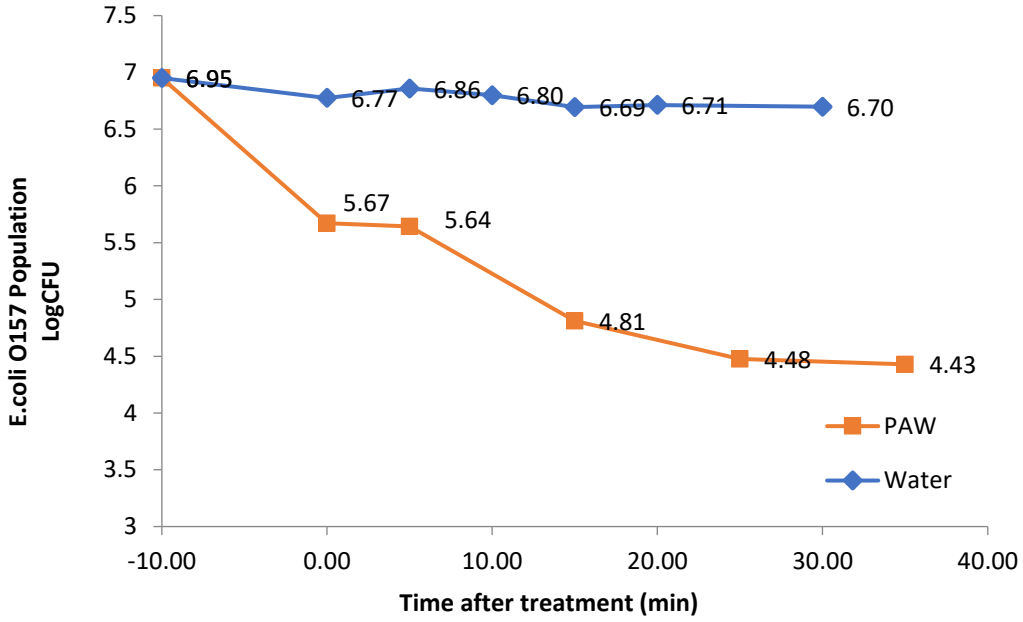

Figure 33. Bacterial population in treatment water for up to 35 min after either water or warm PAW30 treatment. Initial population in treatment water after removal of beef samples inoculated with approximately 2.2x10^{8} E. coli O157 CFU/ml.

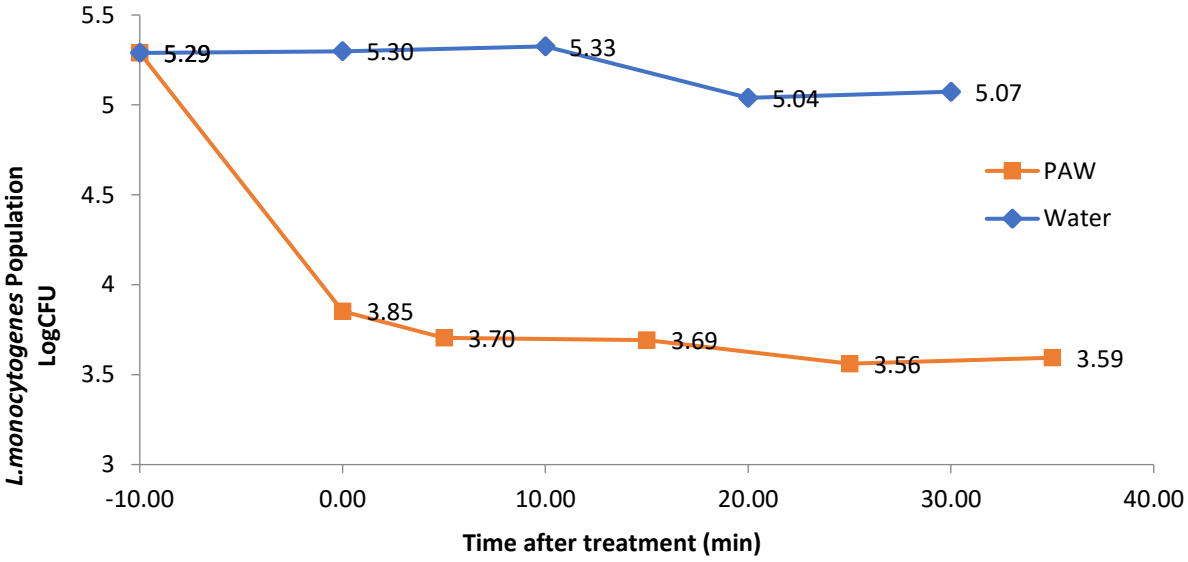

Figure 34. Bacterial population in treatment water for up to 35 min after either water or warm PAW30 treatment. Initial population in treatment water after removal of beef samples inoculated with approximately 8.5 x 10^{7} L. monocytogenes CFU/ml.

Table **8**. Estimated overall log_{10} reduction CFU/ml of PAW against *S.* Typhimurium, *E. coli* O157 and *L. monocytogenes* as a combined effect of water bath and wash water PAW treatment.

	BEEF		LAMB	
	Topside	Rump	Leg	Shoulder
Salmonella	2.66	2.34	2.46	2.37
E. coli	2.67	2.40	2.41	2.36
Listeria	2.57	3.07	3.49	3.63
B. thermosphacta	3.06		3.12	

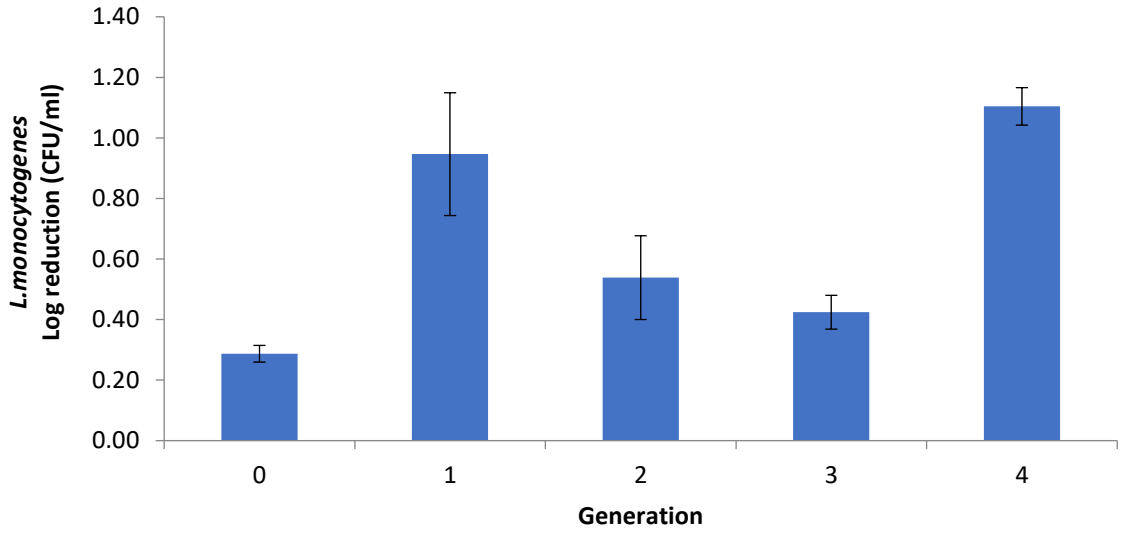

Figure 35. Experimental results of the bacterial resistance tests with L. monocytogenes treated with PAW30 for 180 s.

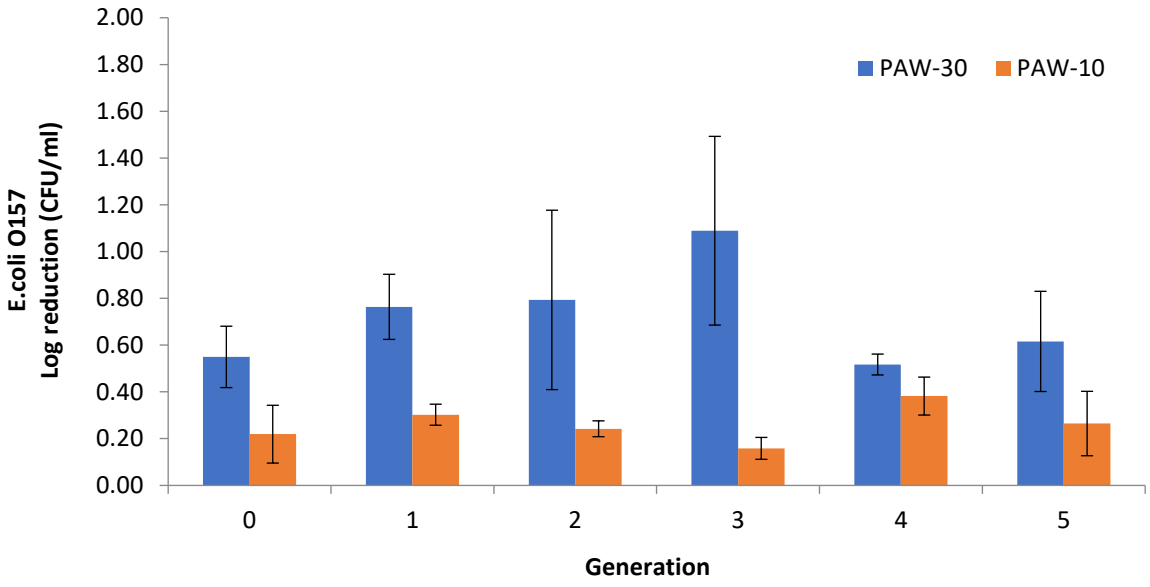

Figure 36. Experimental results of the bacterial resistance tests with E. coli treated with PAW10 and PAW30 for 390 s.

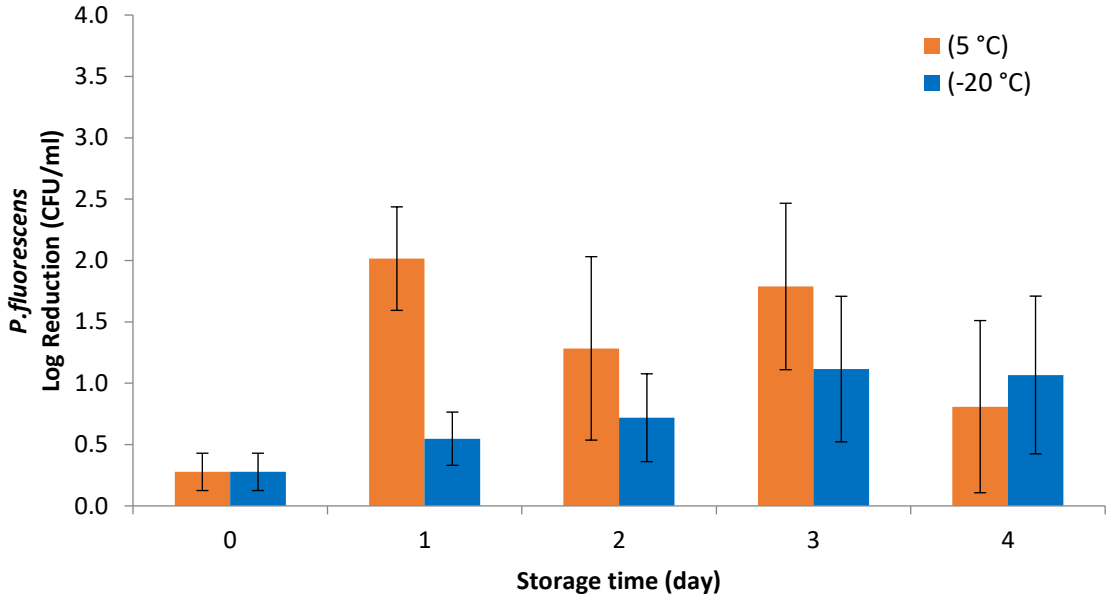

Figure 37. Bacterial reduction of P. fluorescens with PAW30 frozen for up to 4 days.

5.3 Phase 3 Findings

Table 9 provides results for nitrite and nitrate levels that occur with different PAW generation methods at two different discharge frequencies 1,000 and 2,000 Hz. Here, different PAW solutions were generated by changing the orientation of the ground electrode, copper in and copper out, as well as conductivity of water prior to plasma generation.

Table 9. Concentrations of nitrites and nitrates of PAW formed in both "Copper Out" and "Copper In" reactor with 0S.m^{-1}, 0.02S.m^{-1} water and 0.2S.m^{-1} water for 10 minutes at 1000Hz and 2000Hz.

Concentrations (μM)	NO_2^-		NO_3^-	
Discharge Frequency (Hz)	1000	2000	1000	2000
"Copper Out" & 0S.m^{-1} water	369.29 ± 24.59	770.77 ± 33.00	234.20 ± 23.05	414.27 ± 48.64
"Copper Out" & 0.02 S.m^{-1} water	462.48 ± 73.11	921.97 ± 18.63	301.92 ± 27.34	829.66 ± 107.82
"Copper Out" & 0.2 S.m^{-1} water	613.84 ± 48.46	1146.21 ± 1050.90	443.77 ± 57.05	1050.90 ± 78.11
"Copper In" & 0 S.m^{-1} water	411.62 ± 5.81	849.86 ± 51.63	80.54 ± 12.21	255.41 ± 13.25
"Copper In" & 0.02 S.m^{-1} water	718.98 ± 86.15	1186.53 ± 73.16	283.44 ± 10.85	631.58 ± 71.65
"Copper In" & 0.2 S.m^{-1} water	884.91 ± 93.91	1412.01 ± 44.42	433.52 ± 38.11	980.82 ± 38.04

Fig. 38 illustrates the concentration of nitrite, nitrate, hydrogen peroxide and total NOx species in different PAW solutions. Different PAW solutions were generated by changing plasma discharge frequency, solution conductivity and ground electrode orientation. Additionally, power, temperature, oxidation-reduction potential (ORP), and pH values are presented for each PAW solution.

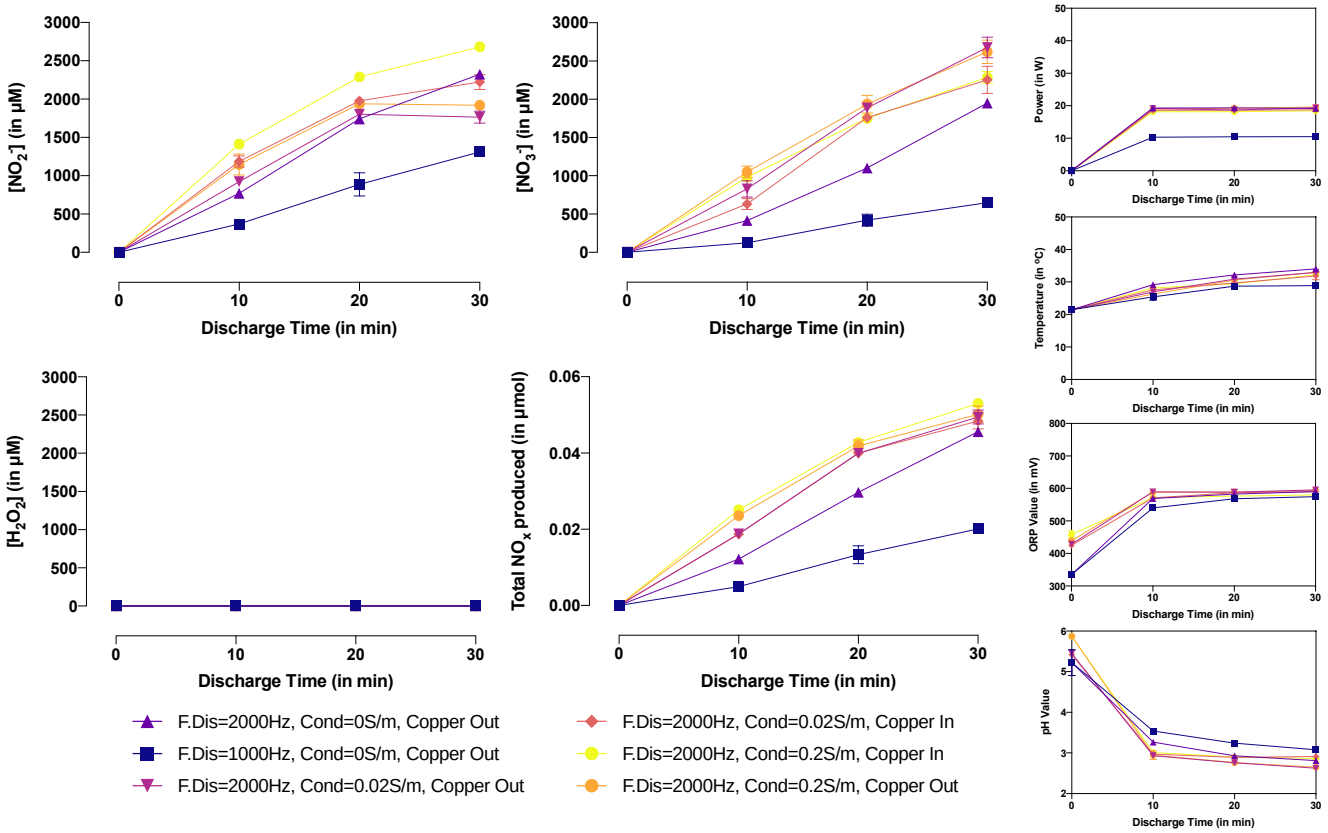

Figure 38. Physicochemical properties of PAW generated in both "Copper Out" and "Copper In" reactor with MilliQ® water, 0.02S.m^{-1} water and 0.2S.m^{-1} water for 10, 20 and 30 minutes at 1000Hz and 2000Hz of discharge frequency.

In this study, the discharge frequency was varied from 1000 Hz to 2000 Hz and in both instances reactive nitrogen species (RNS) dominated compared to reactive oxygen species (ROS). NO_2^- concentrations of the solutions generated with MilliQ® water for 10 min at 2000 Hz in both "Copper Out" and "Copper In" reactors were 770 µM and 849.86 µM, respectively, which were significantly higher ($p<0.05$) than concentrations at 1000 Hz measured at 369.29 µM and 411.62 µM, respectively. Similarly, the NO_3^- concentrations of PAW produced in both "Copper Out" and "Copper In" reactors, with MilliQ® water for 10 min at 2000 Hz, were 414.27 µM and 255.41 µM, respectively, which were also significantly greater ($p<0.05$) than concentrations at 1000Hz that yielded 124.20 µM and 80.54 µM, respectively.

Fig. 39 illustrates the total energy yield of RNOS in different PAW solutions generated by the pin discharge above the water surface at various discharge frequencies and initial conductivities. The energy yield was determined based on the NO_2^-, NO_3^- and H_2O_2 productions in PAW, which was expressed in grams, with the discharge power (kWh) at 10, 20 and 30 min of discharge time. The total energy yield by PAW was then calculated adding up the individual energy yields of the long-lived species.

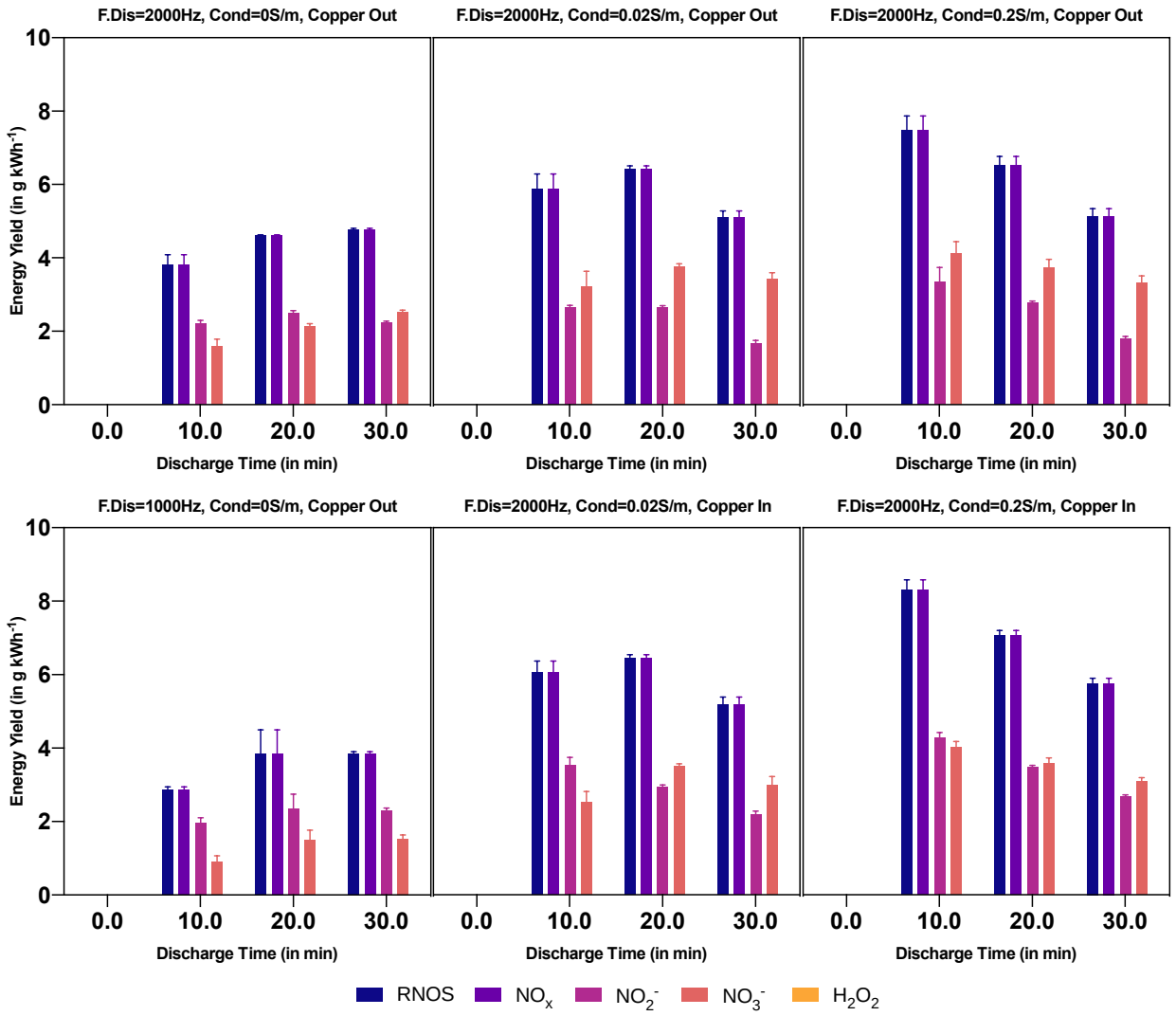

Figure 39. Calculated Energy Yield of PAW generated in both "Copper Out" and "Copper In" reactor with MilliQ® water, 0.02S.m^{-1} water and 0.2S.m^{-1} water for 10, 20 and 30 minutes at 1000Hz and 2000Hz of discharge frequency.

Table 10 provides the calculated treatment time required to achieve a 2- and 4-log$_{10}$ reduction against *E. coli* and *S.* Typhimurium using different PAW solutions. PAW solutions were generated by changing plasma discharge frequency, solution conductivity and ground electrode orientation.

Table 10. Treatment time required (in s) for 2-$\log_{10}$ reduction (99%) and 4-$\log_{10}$ reduction (99.99%) in *Escherichia coli* serovar 0157:H7 and *Salmonella enterica serovar* Typhimurium populations using Weibull model. Data reported as means.

Microorganism	*Escherichia coli* serovar 0157:H7		*Salmonella enterica* serovar Typhimurium	
Time Required to Achieve (s)	2 Log Reduction (t_{2d})	4 Log Reduction (t_{4d})	2 Log Reduction (t_{2d})	4 Log Reduction (t_{4d})
Discharge Frequency = 1000Hz & "Copper Out"				
0S.m^{-1} Water	885.99	1311.21	597.86	1107.99
Discharge Frequency = 2000Hz & "Copper Out"				
0S.m^{-1} Water	309.55	504.17	152.75	266.44
0.02S.m^{-1} Water	262.92	417.75	141.57	238.80
0.2S.m^{-1} Water	258.81	414.09	127.87	232.22
Discharge Frequency = 2000Hz & "Copper In"				
0.02S.m^{-1} Water	336.50	452.64	143.64	258.51
0.2S.m^{-1} Water	184.25	288.80	110.26	179.37

Four PAW solutions were chosen for quality attribute analysis and their generation method including orientation of ground electrode (copper in/copper out), discharge frequency, water conductivity and discharge time are summarised in **Table 11** along with their respective antimicrobial activity.

Table 11. Summary of PAW solutions used for quality attribute analysis.

PAW solution name	Orientation of ground electrode	Discharge frequency (Hz)	Water conductivity (Sm^{-1})	Discharge time (min)	*Treatment time required to achieve a 4-$\log_{10}$ reduction (99.99%) (s)*	
					Escherichia coli serovar 0157:H7	*Salmonella enterica* serovar Typhimurium
PAW(1)	Copper out	1,000	0	30	1311.21	1107.99
PAW(2)	Copper out	2,000	0	30	504.17	266.44
PAW(3)	Copper in	2,000	0.02	30	452.64	258.51
PAW(4)	Copper in	2,000	0.2	30	288.80	179.37

Table 12 provides the approximate composition of beef samples before and after treatment with water, PAW(3) and PAW(4) at different treatment volumes of 0.14 ml and 0.57 ml PAW/g beef sample. Iron, Selenium and Zinc are measured as mg/K beef sample and protein is presented as % Nitrogen.

Table 12. Nutritional and chemical composition of beef including Iron (Fe), Selenium (Se) and Zinc (Zn), Nitrogen (%) and pH treated with PAW(3) and PAW(4).

	Untreated	Water	PAW(3)		PAW(4)	
			0.14ml/g beef	0.57ml/g beef	0.14ml/g beef	0.57ml/g beef
Fe mg/Kg sample	73.86 ± 12.46	53.79 ± 14.38	73.36 ± 3.68	88.32 ± 9.37	54.82 ± 2.94	61.48 ± 1.86
Se mg/Kg sample	1.02 ± 0.16	1.03 ± 0.05	1.07 ± 0.01	1.09 ± 0.16	1.36 ± 0.22	1.340.06
Zn mg/Kg sample	103.54 ± 20.33	111.50 ± 8.22	102.89 ± 7.54	165.43 ± 19.41	72.78 ± 4.15	85.831.37
%N	13.44 ± 0.30	13.23 ± 0.95	14.09 ± 0.11	12.40 ± 0.02	13.93 ± 0.23	12.990.13
Myoglobin mg/g sample	3.46 ± 0.087	6.37 ± 0.674	6.53 ± 2.037	3.78 ± 0.082	5.11 ± 0.144	4.32 ± 0.349

Values are the mean ± standard deviations of at least three replications with at least 3 samples.

The difference in Vitamin B6 levels before and after treatment with PAW(2), PAW(3) and PAW(4) are presented in **Table 13** below. Vitamin B6 is given as mg Pyridoxine/100g sample.

Table 13. Vitamin B6 in beef before and after PAW treatment measured in mg Pyridoxine/100g sample.

	Vitamin B6 in beef (mg Pyridoxine/ 100g sample)	
	Pre-treatment	Post treatment
PAW(2)	0.28 ± 0.003	0.28 ± 0.0776
PAW(3)	0.15 ± 0.008	0.08 ± 0.028
PAW(4)	0.21 ± 0.031	0.23 ± 0.001

Values are the mean ± standard deviations of at least three replications with at least 3 samples.

Table 14 provides pH values for raw beef samples treated with water, 2% lactic acid and plasma activated solutions (PAW(1),(2),(3) and (4) at two different treatment volumes of 0.14 ml/g beef sample and 0.57 ml/g beef sample.

Table 14. pH values of raw beef after treatment.

	pH of beef sample at treatment volumes	
	0.14ml/g sample	0.57ml/g sample
Untreated	5.15 ± *0.0001*	
Water	5.16 ± *0.0003*	5.15 ± *0.0003*
Plasma Activated Water		
PAW(1)	5.14 ± *0.0299*	5.16 ± *0.0055*
PAW(2)	5.14 ± *0.0082*	5.14 ± *0.0256*
PAW(3)	5.15 ± *0.0098*	5.14 ± *0.0266*
PAW(4)	5.15 ± *0.0175*	5.16 ± *0.0190*

Lipid oxidation of raw beef samples before and after treatment with water, 2% lactic acid, PAW(2), PAW(3) and PAW(4) was determined through the measurement of TBARS values with results illustrated in **Fig. 40**(a). The effect of treatment volume on lipid oxidation was also explored and illustrated in **Fig. 40(**b).

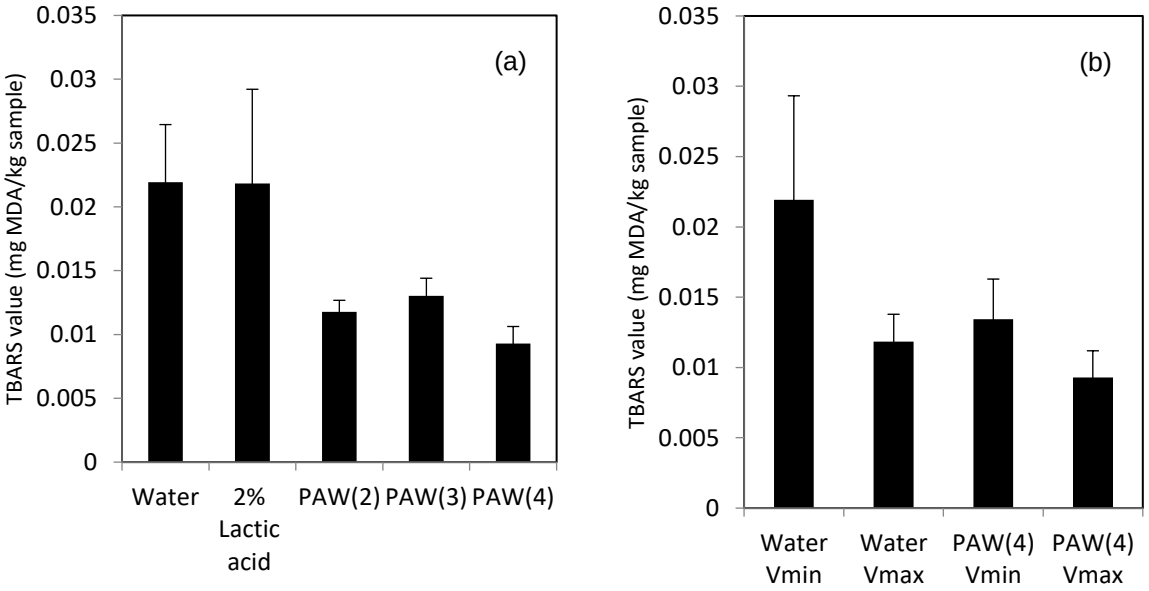

Figure 40. (a) TBARS value of unsealed beef samples (a) with treatment solutions water, 2% lactic acid, PAW(2),(3) and (4). (b) between treatment volumes of water and PAW(4) of Vmin=0.14ml/g sample and Vmax=0.57ml/g sample.

Fig. 41 illustrates changes in the relative proportions of metmyoglobin (MetMb), oxymyoglobin (OxyMb) and deoxymyoglobin (DeoMB) in raw beef samples treated with 2% lactic acid and PAW solutions (1),(2),(3) and (4).

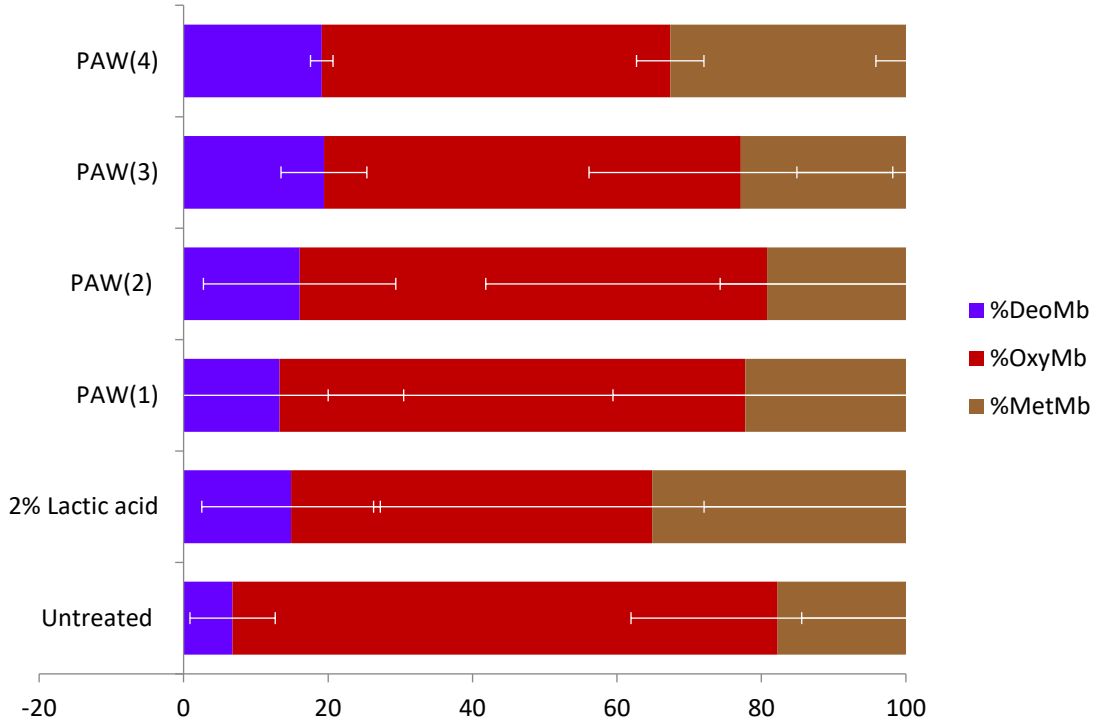

Figure 41. Proportion of metmyoglobin (%MetMb), oxymyoglobin (%OxyMb), and deoxymyoglobin (%DeoMb) in beef after treatment.

Changes to the surface colour of raw beef was measured using the L*, a* b* colour-coordinate value system. The difference in coordinate values between control and water, lactic acid, PAW(1), PAW(2), PAW(3) and PAW(4) was determined by the following equations:

- ΔL* (L* sample minus L* standard) = difference in lightness and darkness (+ = lighter, – = darker)
- Δa* (a* sample minus a* standard) = difference in red and green (+ = redder, – = greener)
- Δb* (b* sample minus b* standard) = difference in yellow and blue (+ = yellower, – = bluer)

Table 15. Difference in mean colour-coordinate values of unsealed beef samples treated with, water, 2% lactic acid,PAW(1), PAW(2), PAW(3) and PAW(4)compared to untreated control.

	Water	2% Lactic acid	PAW(1)		PAW(2)		PAW(3)		PAW(4)	
			0.14ml/g beef	0.57ml/g beef	0.14ml/g beef	0.57ml/g beef	0.14ml/g beef	0.57ml/g beef	0.14ml/g beef	0.57ml/g beef
L*	0.48 ± 3.256	-0.19 ± 2.998	-5.06 ± 1.750	-2.87 ± 2.941	-1.97 ± 0.302	-2.00 ± 1.375	-0.46 ± 1.956	0.74 ± 3.927	-2.25 ± 0.456	-0.35 ± 1.761
a*	0.35 ± 2.874	-2.73 ± 3.390	-7.52 ± 0.997	-4.23 ± 1.899	-1.74 ± 0.244	-3.71 ± 0.953	-2.30 ± 1.664	-2.36 ± 1.097	-2.61 ± 0.995	-4.12 ± 0.651
b*	-0.18 ± 2.236	-0.70 ± 1.636	-3.29 ± 0.267	-1.91 ± 1.035	0.20 ± 0.051	-0.45 ± 0.771	0.02 ± 1.714	-0.21± 0.360	-0.25 ± 0.454	0.16 ± 0.470

Correlation coefficients (P-Value) between L, a* and b* of treatment solutions*

	Water	2% Lactic acid	PAW(1)		PAW(2)		PAW(3)		PAW(4)	
			0.14ml/g beef	0.57ml/g beef	0.14ml/g beef	0.57ml/g beef	0.14ml/g beef	0.57ml/g beef	0.14ml/g beef	0.57ml/g beef
L*										
Water	*0.669*		*0.0124**	*0.120*	*0.223*	*0.078*	*0.419*	*0.075*	*0.177*	*0.678*
2% Lactic acid			*0.038**	*0.245*	*0.356*	*0.174*	*0.733*	*0.051*	*0.290*	*0.935*
a*										
Water	*0.027**		*0.00030***	*0.019**	*0.237*	*0.031**	*0.0493**	*0.0393**	*0.0251**	*0.0015**
2% Lactic acid			*0.041**	*0.491*	*0.635*	*0.643*	*0.779*	*0.800*	*0.936*	*0.346*
b*										
Water	*0.549*		*0.032**	*0.215*	*0.781*	*0.839*	*0.847*	*0.970*	*0.939*	*0.718*
2% Lactic acid			*0.025**	*0.265*	*0.379*	*0.810*	*0.425*	*0.490*	*0.526*	*0.234*

The statistical difference between treatment solution is expressed as *P < 0.05, **P < 0.01, ***P < 0.001 and **** P < 0.0001

Table 16 provides water holding capacity of raw beef samples treated with water, PAW solutions (1), (2), (3) and (4) at two different treatment volumes of 0.14 ml/g beef sample and 0.57 ml/g beef sample.

Table 16. Water holding capacity and textural analysis of PAW treated beef.

	WHC%	Warner-Bratzler Shear force (kg) with treatment volume			
		0.14ml/g beef	±	0.57ml/g beef	±
untreated		4.76[a]	1.728		
water	34.49 ± 3.74[a]	4.18[a]	1.825	3.42[a]	0.631
PAW(1)	49.90 ± 2.16[b]	2.74[b]	0.680	4.88[a]	1.698
PAW(2)	46.22 ± 0.97[b]	3.42[a]	0.816	3.30[a]	0.853
PAW(3)	38.33 ± 2.36[a]	3.52[a]	0.623	2.98[b]	0.938
PAW(4)	38.31 ± 3.27[a]	5.12[a]	1.063	2.56[c]	0.688

Table 17 provides the solution retention of PAW treatment on beef measured as weight gain (%) as well as textural analysis of cooked beef samples including Warner-Bratzler Shear Force (WBSF), cooking loss (%), cooking yield (%) and thermal shortening (%). Colour coordinate values were also measured and recorded using the L* a* b* system.

Table 17. Physical attributes of PAW treated cooked beef.

PAW treatment		Weight gain (%)	WBSF (kg)	Cooking loss (%)	cooking yield (%)	Thermal shortening (%)	L*	a*	b*
	Untreated		7.78±0.683[a]	38.24[a]	61.76	20.83[a]	44.94±0.787	6.99±0.175	8.49±0.410
(3)	0.14ml/g beef	1.69	8.24±1.521[a]	41.41[a]	58.59	8.33[a]	46.51±0.771	5.93±0.035	8.43±0.247
	0.57ml/g beef	0.00	9.29±3.067[a]	39.86[a]	60.14	10.00[a]	42.96±0.467	6.13±0.233	7.12±0.106
(4)	0.14ml/g beef	1.11	5.52±1.066[b]	43.64[a]	56.36	5.00[a]	45.91±0.099	9.15±0.113	7.79±0.148
	0.57ml/g beef	1.51	6.15±1.981[a]	45.11[a]	54.89	16.67[a]	48.48±0.636	8.37±0.007	8.72±0.035

Values are the mean ± standard deviations of at least three replications with at least 3 samples. Values within a column that are not followed by the same letter are significantly different (P≤0.05).

Quality properties of beef stored under vacuum packaging at 4 ± 1°C for 4 weeks were measured including drip loss, pH and colour coordinate values presented as mean averages ± standard deviation in **Table 18** and **Table 19**, respectively. Anaerobic and aerobic plate count of vacuum packaged beef was measured over 3 weeks and is illustrated in **Fig. 42**.

Table 18. Drip loss and pH values of raw beef samples treated with water, PAW(2), (3) and (4) and stored in vacuum pack at 4 ± 1 °C for four weeks.

Week	drip loss %					pH				
	Control	Water	PAW(2)	PAW(3)	PAW(4)	Control	Water	PAW(2)	PAW(3)	PAW(4)
0	2.40 ±1.50	5.24±0.71	6.50 ±2.74	6.56±3.94	5.11±0.16	5.35 ±0.06	5.22 ±0.09	5.21 ±0.03	5.27 ±0.11	5.20 ±0.03
1	5.73 ±2.01	5.91±3.03	9.23 ±1.58	10.72±4.25	7.92±1.76	5.07[a] ±0.01	5.16[a] ±0.13	5.07[a] ±0.02	5.05[b] ±0.01	5.03[b] ±0.01
2	8.76 ±0.51	6.90±1.09	9.29 ±1.75	6.36±6.56	7.98±4.04	5.06 ±0.06	5.24 ±0.22	5.05 ±0.02	5.21 ±0.11	5.06 ±0.04
3	6.80 ±0.39[a]	9.84±0.5[b]	13.49±1.99[bc]	9.20±0.45[bc]	8.57±0.09[bc]	5.10 ±0.01	5.13 ±0.18	5.12 ±0.04	5.10 ±0.09	5.17 ±0.09
4	12.05 ±1.91	9.83±1.91	10.94±2.99	7.99±0.79	11.41±0.21	5.12 ±0.03	5.26 ±0.16	5.12 ±0.01	5.31 ±0.17	5.17 ±0.08

Table 19. Mean colour coordinate values for raw beef samples treated with water, PAW(2), (3) and (4) and stored in vacuum pack at 4±1°C for four weeks.

Week		Control	±	Water	±	PAW(2)	±	PAW(3)	±	PAW(4)	±
0	L*	37.87	*0.551*	39.37	*0.801*	39.66	*0.890*	39.21	*0.846*	40.34	*1.550*
	a*	11.78	*1.652*	11.50	*0.586*	10.98	*1.244*	11.69	*1.422*	10.04	*1.233*
	b*	5.66	*1.041*	4.08	*0.822*	6.82	*0.605*	7.70	*0.926*	6.79	*0.657*
1	L*	39.72	*0.606*	39.99	*0.405*	43.29	*1.540*	41.49	*0.879*	41.94	*1.046*
	a*	13.36	*1.110*	14.34	*2.097*	14.74	*1.731*	13.70	*0.602*	13.97	*1.851*
	b*	3.02	*0.531*	3.74	*1.476*	7.15	*0.760*	5.12	*0.716*	5.80	*0.774*
2	L*	38.08	*1.522*	39.05	*1.063*	40.36	*1.796*	41.53	*1.422*	43.27	*2.069*
	a*	13.26	*1.064*	15.75	*1.368*	14.19	*1.756*	15.82	*2.398*	15.33	*1.201*
	b*	3.71	*0.479*	4.97	*0.414*	6.71	*0.664*	7.10	*0.841*	8.51	*1.049*
3	L*	39.77	*2.410*	37.57	*2.455*	38.81	*0.833*	41.50	*1.300*	39.38	*1.141*
	a*	11.81	*1.482*	10.56	*1.478*	11.75	*0.690*	12.03	*1.219*	13.07	*1.223*
	b*	3.98	*0.769*	4.70	*0.361*	6.02	*1.698*	7.07	*1.052*	6.98	*0.898*
4	L*	39.23	*1.378*	39.44	*0.536*	42.11	*4.644*	40.45	*1.500*	40.46	*1.002*
	a*	8.42	*0.692*	11.13	*1.392*	11.46	*0.541*	12.07	*1.984*	11.07	*0.871*
	b*	5.22	*0.425*	5.98	*2.221*	5.25	*0.448*	6.25	*0.408*	5.83	*0.876*

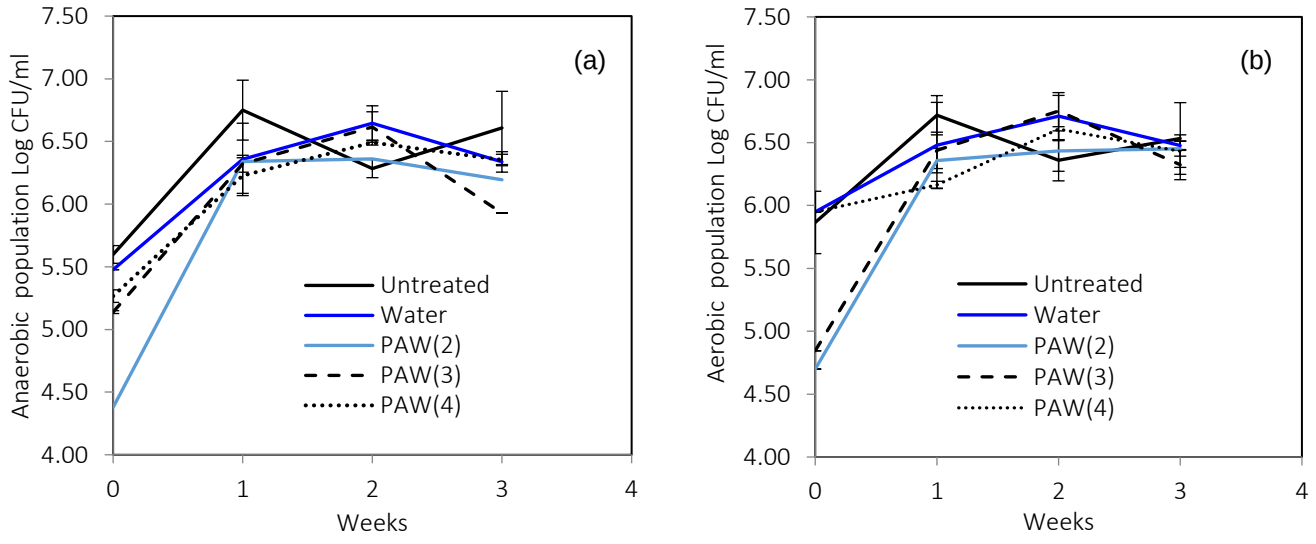

Figure 42. Anaerobic (a) and aerobic (b) plate count of vacuum-packed treated beef over 3 weeks.

Quality properties of unsealed beef stored at 4 ± 1°C for 8 days were measured including lipid oxidation, shown in **Table 20**, and colour coordinate values and pH, shown in **Fig. 43**, presented as mean averages ± standard deviation. Mesophilic aerobic plate count of treated unsealed beef over 8 days is illustrated in **Fig. 44**. Texture analysis over 8 days was determined by measuring maximum Warner-Bratzler Shear Force (WBSF) with results presented in **Table 21**.

Table 20. Lipid oxidation of beef samples treated with PAW and stored for 8 days.

	TBARS value (mg MDA/kg sample) with storage time (days)			
	Untreated	Water	PAW min	PAW max
0	0.018 ± 0.006[a]	0.016 ± 0.005 [a]	0.021 ± 0.010 [a]	0.013 ± 0.007 [a]
2	0.022 ± 0.009 [a]	0.019 ± 0.009 [a]	0.025 ± 0.007 [a]	0.028 ± 0.015 [a]
5	0.024 ± 0.004 [a]	0.032 ± 0.015 [a]	0.023 ± 0.008 [a]	0.027 ± 0.007 [a]
8	0.021 ± 0.008 [a]	0.024 ± 0.002 [a]	0.023 ± 0.009 [a]	0.024 ± 0.012 [a]

Values are the mean ± standard deviations of at least three replications with at least 3 samples. Values within a row that are not followed by the same letter are significantly different (P≤0.05).

Table 21. Texture analysis of beef samples treated with PAW (4).

	Warner-Bratzler Shear force (kg) with PAW(4)			
	Untreated	0.14ml/g sample	0.57ml/g sample	1min Dip
0	4.97 ± 2.216a	5.12 ± 1.063a	2.56± 0.688a	3.87± 1.494a
2	3.79 ± 0.49a	2.99 ± 0.313b	3.92 ± 0.543c	3.64 ± 0.359a
4	4.52 ± 0.465a	4.03 ± 0.633b	5.01 ± 1.879a	3.78 ± 0.696a
6	5.77 ± 1.601a	4.82 ± 1.125b	3.79 ± 1.464a	3.13 ± 0.541c
8	4.01 ± 1.852a	3.57 ± 1.055a	3.35 ± 0.295a	5.57 ± 2.045a

Values are the mean ± standard deviations of at least three replications with at least 3 samples. Values within a row that are not followed by the same letter are significantly different (P≤0.05).

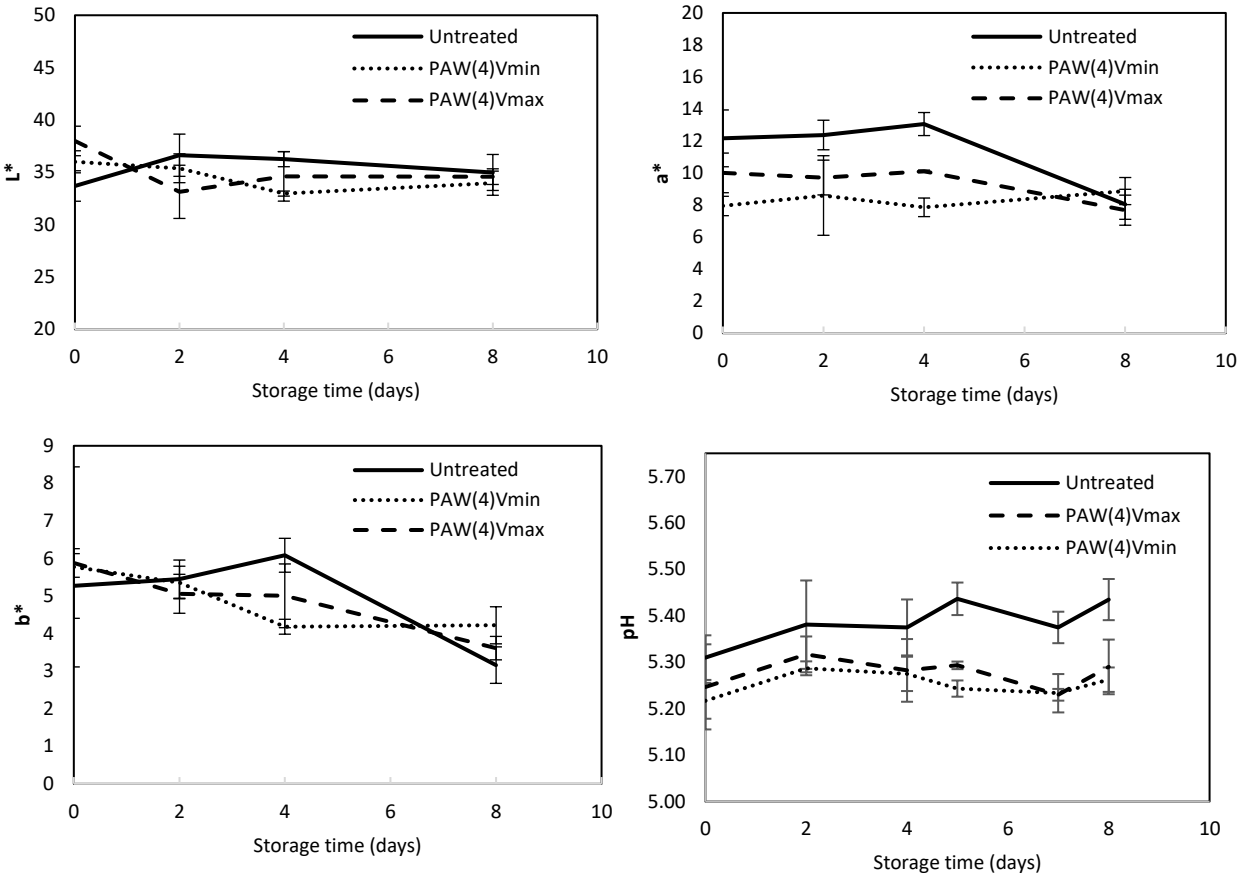

Figure 43. Shelf life analysis of beef samples treated with PAW(4) with a treatment volume of Vmin=0.14ml/g sample and Vmax=0.57ml/g sample over 8 days. Colour-cordinate values (a) L, (b) a* and (c) b* were measured along with (d) pH.*

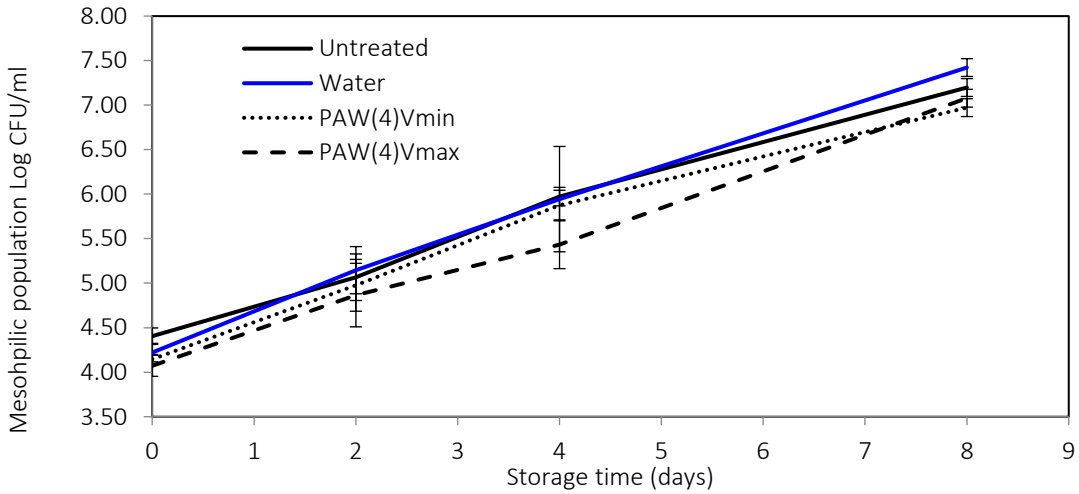

Figure 44. Total plate count of mesophilic population on beef samples treated with PAW(4) with treatment volume of 0.14 mlPAW/g sample (Vmin) and 0.57 mlPAW/g sample (Vmax) over 8 days.

5.4 Phase 4 Findings

This milestone reports on the generation of plasma-activated water (PAW) in larger liquid volumes against *Escherichia coli* (i) in the contact times from 60 to 960 s via the pin-to-liquid discharge reactor and the plasma-bubbles reactor with the liquid volume of 0.2 L; (ii) in the contact times of 10, 20 and 30 s via the hybrid plasma-bubbles discharge (HPD) reactor with 0.5, 1 and 2 L of liquid volumes; (iii) in the contact times of 20 and 30 s via the HPD reactor and ultrasonic with 1.5 L of liquid volume.

Pin-to-liquid reactor

In this study, the discharge frequencies of 1000 and 2000 Hz were chosen to ignite the plasma discharge because discharge frequency can increase the energy of each discharge, generating more frequent and energetic electrons that promote the acceleration of active species [9]. At the initial liquid conductivity of 0 $S.m^{-1}$ with the ground electrode positioned outside (GO) the pin reactor, increasing the discharge frequency from 1000 Hz to 2000 Hz increased the RONS production with a positive NO_2^- to NO_3^- ratio [**Fig. 45**(a)].

The effect of initial conductivity was investigated with NaCl added to MilliQ water in the pin reactor to increase initial conductivity to 0.02 $S.m^{-1}$ and 0.2 $S.m^{-1}$. For GO at 2000 Hz in the pin reactor, the ratio between NO_2^- and NO_3^- was shifted from favouring NO_2^-- to NO_3^- with 0.02 $S{\cdot}m^{-1}$ and 0.2 $S{\cdot}m^{-1}$, at 2678 μM and 2620 μM, respectively, while the pH reduced to the lower values at 2.6 [**Fig. 45**(a)]. ClO^- concentrations increased with 0.02 $S{\cdot}m^{-1}$ (11.5 μM) and 0.2 $S{\cdot}m^{-1}$ (47.9 μM) for the pin reactor with GO at 2000 Hz. Overall, higher ion formation generated at a higher initial conductivity promoted greater amounts of NO_x species in the solution.

Two positions of the ground electrode, GO and GI, were also investigated. By placing the ground electrode inside (GI) the pin reactor, the NO_2^- concentration was significantly greater than GO at 2000 Hz [**Fig. 45**(a)]. Under the same operating parameters, for instance at 2000 Hz and 0.02 $S{\cdot}m^{-1}$, the measured energy input by GI (4.81 $J{\cdot}pulse^{-1}$) was slightly higher than by GO (4.26 $J{\cdot}pulse^{-1}$). The increased energy may attribute to a higher formation of reactive nitrogen species (RNS) in PAW.

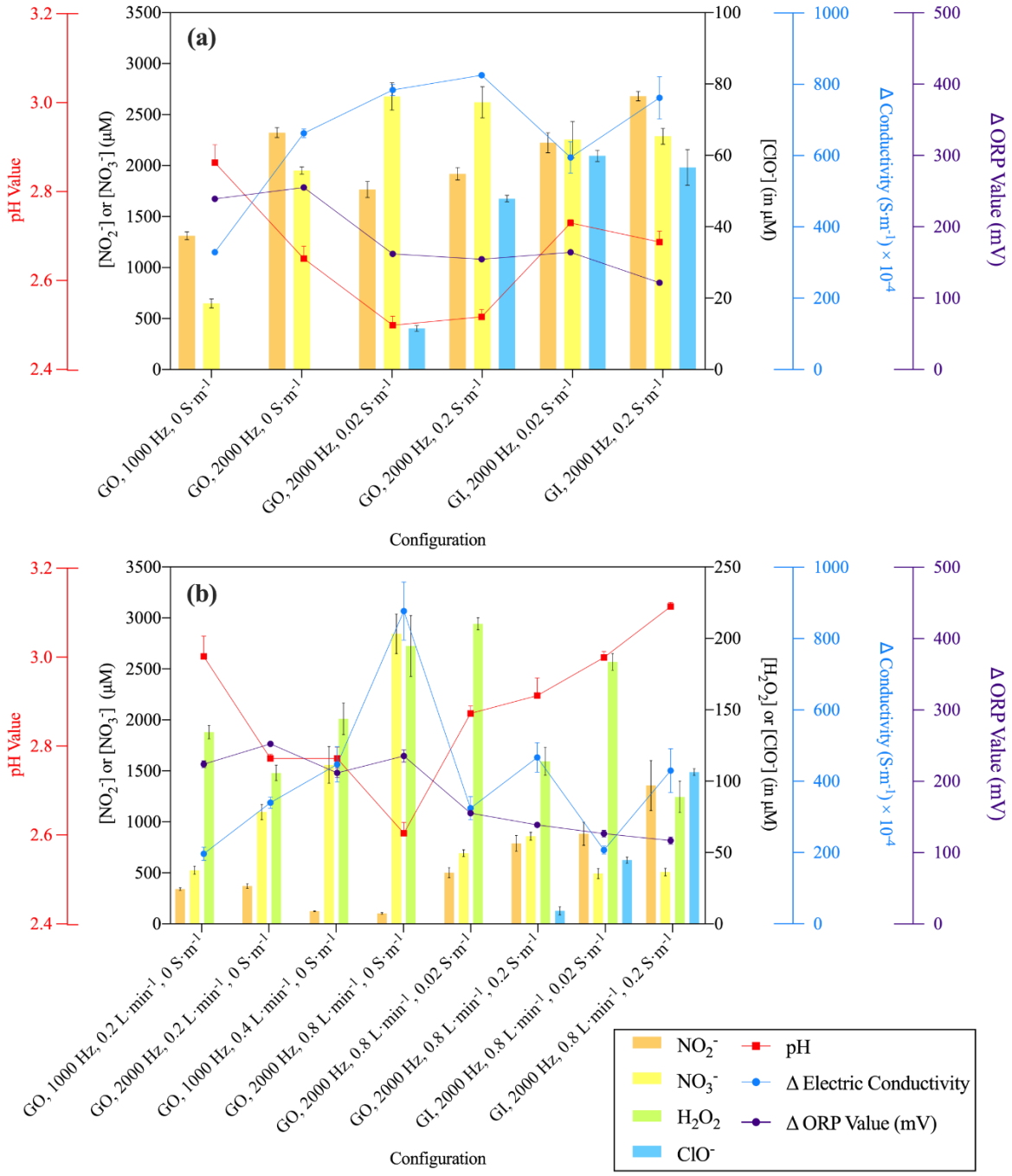

Figure 45. RONS concentrations, ClO^- concentration, pH values, changes (Δ) in solution conductivity and changes (Δ) in ORP value of PAW generated for 30 min by: (a) the pin-to-liquid reactor; (b) the plasma-bubble generator. The H_2O_2 concentration by the pin reactor was undetected. Error bars designate SD.

Plasma-bubbles reactor

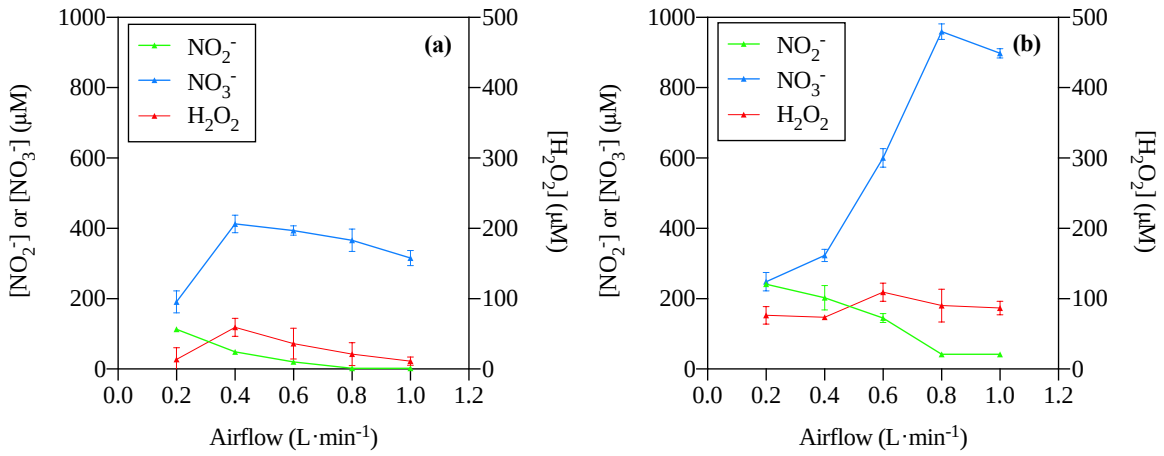

Figure 46. RNOS (NO_2^-, NO_3^- and H_2O_2) concentrations of PAW produced at 60 kHz and 2.18-4.19 kV by the air plasma-bubble generator with GO at 10 min at: (a) 1000 Hz, (b) 2000 Hz.

The effect of air flowrate was firstly investigated. The gas flow controls the gas residence time in the plasma-bubbles reactor and influences the coexistence of gaseous short-lived and long-lived species for the RONS generation. RONS concentrations generated by the plasma-bubble generator operating at 1000 Hz and 2000 Hz with an air flow ranging from 0.2 to 1 L·min^{-1} for 10-min are shown in **Fig. 46**(a)-(b). The NO_2^- concentration increased with reducing air flowrate from 1 to 0.2 L·min^{-1}, where it reached maximum values of 113 μM and 241 μM, at 1000 Hz [**Fig. 46**(a)] and 2000 Hz [**Fig. 46**(b)], respectively. Upon decreasing the flowrate, $\cdot OH$ and $\cdot NO$ species generated in the gas-phase plasma have more time to recombine before reaching the liquid phase and favour a high NO_2^- concentration in the liquid [49]. At 1000 Hz, the NO_3^- concentration significantly ($p<0.05$) increased from 0.2 to 0.4 L·min^{-1}, where it reached a maximum value of 413 μM, and then significantly ($p<0.05$) decreased when the airflow was further increased to 1 L·min^{-1} [**Fig. 46**(a)]. Similarly, the NO_3^- concentration at 2000 Hz significantly ($p<0.05$) rose from 0.2 to 0.8 L·min^{-1} with a maximum value of 960 μM and significantly ($p<0.05$) decreased with further increase to 1 L·min^{-1} [**Fig. 46**(b)].

At 0 S.m^{-1} with GO, increasing the discharge frequency from 1000 Hz to 2000 Hz increased the RONS production with a positive NO_3^- to NO_2^- ratio by the plasma-bubble reactor [**Fig. 45**(b)]. Irrespective of the air flowrates, NO_3^- concentrations produced by the plasma-bubble generator increased with increasing discharge frequency, resulted from the decreased NO_2^- and H_2O_2. The effect of electric conductivity and ground electrode position on the RONS production by the plasma-bubble generator were also investigated. For GO and 0.02 S·m^{-1} at 2000 Hz, the NO_3^- -rich solution, at 694 μM, was favoured [**Fig. 45**(b)]. For the plasma-bubble generator with GO at 2000 Hz and 0.2 S·m^{-1}, the concentration of NO_2^- and NO_3^- , at 790 μM and 860 μM, respectively, were insignificantly ($p>0.05$) different. For GI, when the initial conductivity was increased from 0.02 S·m^{-1} and to 0.2 S.m^{-1}, the NO_2^-/NO_3^- ratio shifted towards NO_2^- [**Fig. 45**(b)]. H_2O_2 concentrations decreased with the increase of conductivity for both GO and GI [**Fig. 45**(b)]. Like the pin reactor, the NO_2^--rich solution together with the decreased H_2O_2 concentration by the plasma-bubble generator [**Fig. 45**(b)] is attributed to the competing rates of different gas phase pathways and the liquid phase processes during the discharge [50].

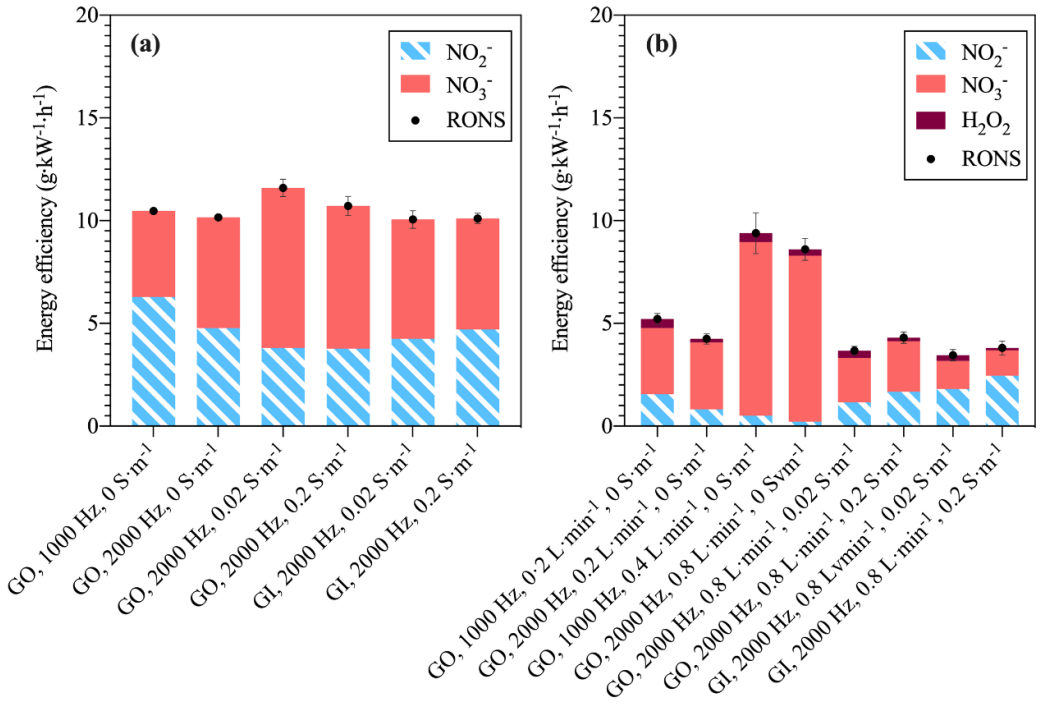

Figure 47. Energy efficiency of RONS (NO_2^-, NO_3^- and H_2O_2) productions in PAW generated for 30 min by: (a) the pin-to-liquid discharge and (b) the plasma-bubble generator. The H_2O_2 energy efficiency by the pin reactor was negligible due to the undetected H_2O_2 concentration. Error bars designate SD.

Energy efficiency of RONS by the pin-to-liquid discharge and the plasma-bubble discharge (**Fig. 47**) was calculated using the equation in Section 4.4.3, based on the average discharge power and the accumulation of the NO_2^-, NO_3^- and H_2O_2 energy efficiency.

In the pin reactor, raising the discharge frequency from 1000 to 2000 Hz reduced the NO_2^- energy-efficiency and increased the NO_3^- energy efficiency due to the enhanced charge density at 2000 Hz [**Fig. 47**(a)]. There was no significant difference ($p>0.05$) in the energy-efficiency of RONS between 1000 Hz and 2000 Hz yielding 10.5 $g{\cdot}kW^{-1}h^{-1}$ and 10.2 $g{\cdot}kW^{-1}h^{-1}$, respectively. Raising the electric conductivity from 0 $S.m^{-1}$ to 0.2 $S.m^{-1}$ at GO reduced the NO_2^- energy-efficiency and increased the NO_3^- energy-efficiency with the RONS energy-efficiency at 10.7 $g{\cdot}kW^{-1}h^{-1}$. Changing from GO to GI in the pin-to-liquid discharge at 2000 Hz with 0.2 $S{\cdot}m^{-1}$ caused an insignificant ($p>0.05$) change of the RONS energy efficiency, at 10.1 $g{\cdot}kW^{-1}h^{-1}$, although the injected energy was slightly increased from 4.68 $J{\cdot}pulse^{-1}$ to 5.24 $J{\cdot}pulse^{-1}$.

In the plasma-bubble generator, increasing the discharge frequency from 1000 Hz to 2000 Hz at 0.2 $L{\cdot}min^{-1}$ caused significant difference ($p<0.05$) in the RONS energy efficiency, which yielded 5.22 $g{\cdot}kW^{-1}{\cdot}h^{-1}$ and 4.25 $g{\cdot}kW^{-1}{\cdot}h^{-1}$, respectively [**Fig. 47**(b)]. When the airflow in the plasma bubble reactor was increased from 0.2 $L{\cdot}min^{-1}$ to the optimum values, 0.4 $L{\cdot}min^{-1}$ at 1000 Hz and 0.8 $L{\cdot}min^{-1}$ at 2000 Hz, the RONS energy efficiencies significantly ($p<0.05$) rose at 9.39 $g{\cdot}kW^{-1}{\cdot}h^{-1}$ and 8.60 $g{\cdot}kW^{-1}{\cdot}h^{-1}$, respectively. This is because of the concentrated active species being introduced into the reactor at the optimal flow rate that increased the NO_3^- concentration [**Fig. 45**(b)]. For the plasma-bubble generator with GO, an increase of the conductivity from 0 $S{\cdot}m^{-1}$ to 0.2 $S{\cdot}m^{-1}$ drastically and significantly ($p<0.05$) reduced the RONS energy efficiency at 3.67 $g{\cdot}kW^{-1}{\cdot}h^{-1}$ [**Fig. 47**(b)] due to the higher productions of NO_2^- and reduced amounts of NO_3^- [**Fig. 45**(b)]. With a further increase to 0.2 $S{\cdot}m^{-1}$ and the position of the ground electrode changed

from GO to GI, the RONS energy efficiency became statistically insignificant (p>0.05), at 3.80 g·kW^{-1}·h^{-1}, with a greater yield of NO_2^- and a lower NO_3^- yield attained.

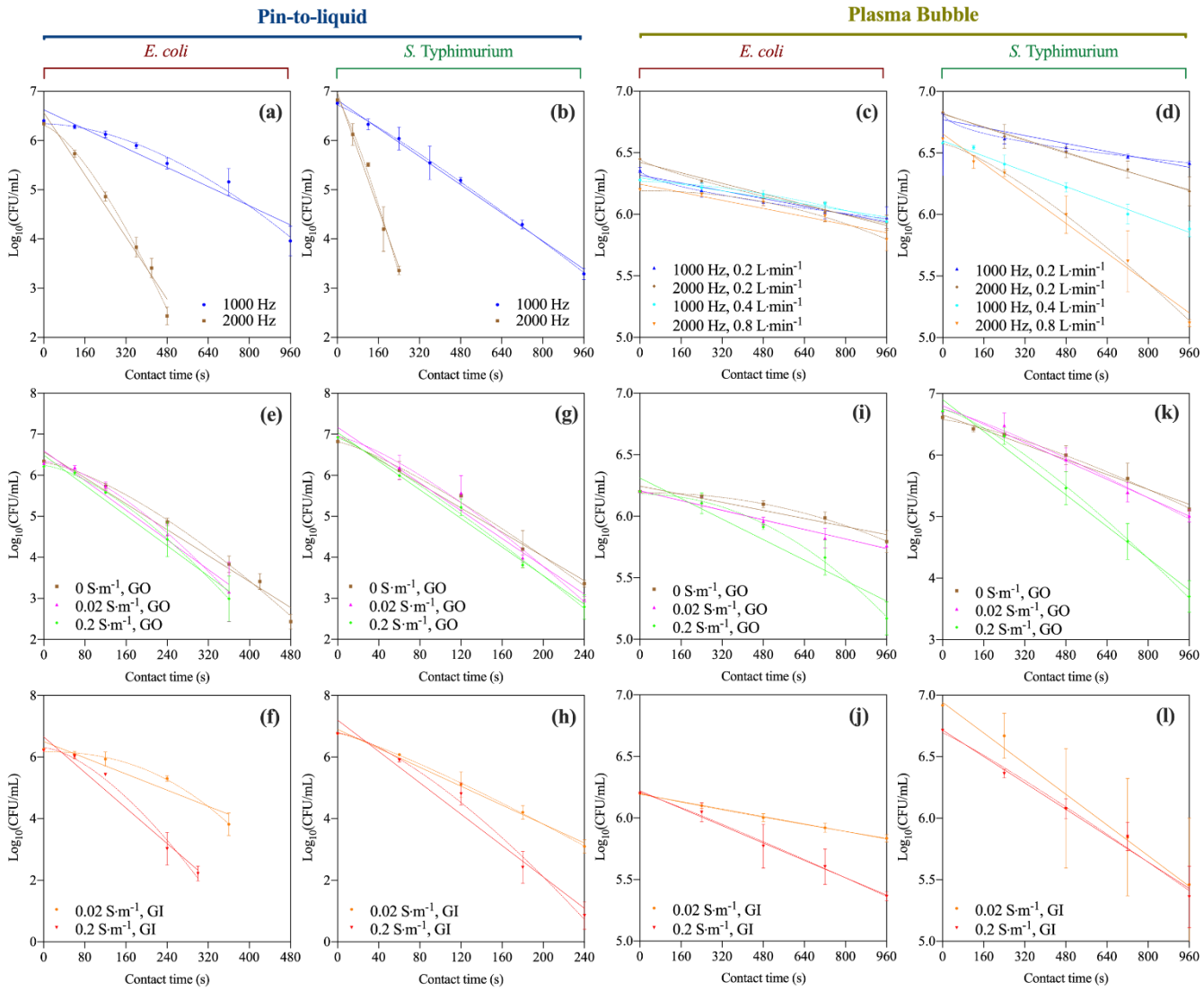

Figure 48. Bacterial inactivation by plasma-activated water generated for 30 min with various discharge schemes: (a)cE. coli by the pin-to-liquid discharge with GO & 0 S·m^{-1} water; (b) S. Typhimurium by the pin-to-liquid discharge with GO & 0 S·m^{-1} water; (c) E. coli by plasma-bubble generator with GO & 0 S·m^{-1} water; (d) S. Typhimurium by the plasma-bubble generator with GO & 0 S·m^{-1} water; (e)-(f) E. coli by the pin-to-liquid discharge at 2000 Hz; (g)-(h) S. Typhimurium by the pin-to-liquid discharge at 2000 Hz; (i)-(j) E. coli by the plasma-bubble generator at 2000 Hz; (k)-(l) S. Typhimurium by the plasma-bubble generator at 2000 Hz. The data shows a good agreement between experimental data (symbol line) and simulated data using log-linear regression model (solid line) and Weibull model (dash line). Error bars designate SD.

PAW produced by both the pin-to-liquid and bubble discharges for 30 min were employed for inactivation of *E. coli* and *S.* Typhimurium in the contact times from 60 to 960 s; the log reductions increased with treatment time (**Fig. 48**). PAW generated by both discharges with various operating configurations inactivated *S.* Typhimurium cells more rapidly than *E. coli* cells. The nature of the cell membrane has been reported to attribute to the sensitivity of Gram-negative cells towards inactivation by PAW [17].

Increasing the discharge frequency from 1000 Hz to 2000 Hz significantly (p<0.05) reduced the populations of *E. coli* and *S.* Typhimurium [**Fig. 48**(a)-(d)]. At 240 s, PAW generated at 2000 Hz by the pin-to-liquid reactor reached 1.48- and 3.46-log$_{10}$ reduction of *E. coli* and *S.* Typhimurium, respectively, which were significantly (p<0.05) higher than at

1000 Hz with 0.27- and 0.71-$\log_{10}$ reduction, respectively, as shown in **Fig. 48**(a) and **Fig. 48**(b). The NO_2^- and NO_3^- productions in PAW by the pin-to-liquid reactor increased at 2000 Hz [**Fig. 45**(a)] which maybe attributed to the observed improvement in bacterial inactivation. Higher NO_2^- and NO_3^- formations at 2000 Hz may induce more oxidative stress and bacterial damage. Similarly, at 960 s, PAW generated at 2000 Hz and 0.2 L.min^{-1} by the plasma-bubble generator reached 0.52- and 0.64-$\log_{10}$ reduction of *E. coli* and *S.* Typhimurium, respectively, which were significantly ($p<0.05$) greater than at 1000 Hz at 0.39- and 0.41-$\log_{10}$ reduction, respectively [**Fig. 48**(c) and **Fig. 48**(d)]. The increase in inactivation may be due to the increase in NO_3^- concentration by the plasma-bubble generator [**Fig. 45**(b)].

The survived populations were also decreased by the plasma-bubble generator at 1000 Hz and 2000 Hz when the airflow changed from 0.2 L·min^{-1} to the optimum value of 0.4 L·min^{-1} at 1000 Hz, and to the optimum value of 0.8 L·min^{-1} at 2000 Hz [**Fig. 48**(c) and **Fig. 48**(d)]. For *S.* Typhimurium, 0.70- and 1.50-$\log_{10}$ reductions were achieved by the plasma-bubble generator at 1000 Hz with 0.4 L·min^{-1} and at 2000 Hz with 0.8 L·min^{-1}, respectively [**Fig. 48**(d)].

In PAW generated by the pin-to-liquid discharge with GO and 0.2 S·m^{-1}, the inactivation of *E. coli* and *S.* Typhimurium at 240-s treatment reached 1.74- [**Fig. 48**(e)] and 4.14-$\log_{10}$ reductions [**Fig. 48**(g)], respectively, with an insignificant ($p>0.05$) difference for *E. coli* inactivation and a significant ($p<0.05$) difference of *S.* Typhimurium inactivation in comparison with 0 S.m^{-1}. At 240 s, the pin reactor with GI and 0.2 S·m^{-1} significantly ($p<0.05$) inactivated *E. coli* and *S.* Typhimurium with the highest values of 3.19- [**Fig. 48**(f)] and 5.90-$\log_{10}$ reduction [**Fig. 48**(h)], respectively. The NO_x production by the pin-to-liquid discharge [**Fig. 45**(a)] increased with increasing initial conductivity and the ground electrode positioned inside the reactor, improving the bacterial inactivation.

PAW generated by the plasma-bubble generator with GO and higher initial conductivity also improved the inactivation [**Fig. 48**(i)-(l)], possibly due to the increase in NO_2^-. At 0.02 S·m^{-1} and 0.2 S·m^{-1}, the plasma-bubble generator with GI [**Fig. 48**(j) and **Fig. 48**(l)] significantly ($p<0.05$) reduced bacterial inactivation compared with GO [**Fig. 48**(i) and **Fig. 48**(k)]. Inactivation studies at 960 s with GO and 0.2 S·m^{-1} were the optimum configurations for the plasma-bubble generator with 1.03- [**Fig. 48**(i)] and 3.01-$\log_{10}$ reductions [**Fig. 48**(k)] achieved for *E. coli* and *S.* Typhimurium, respectively.

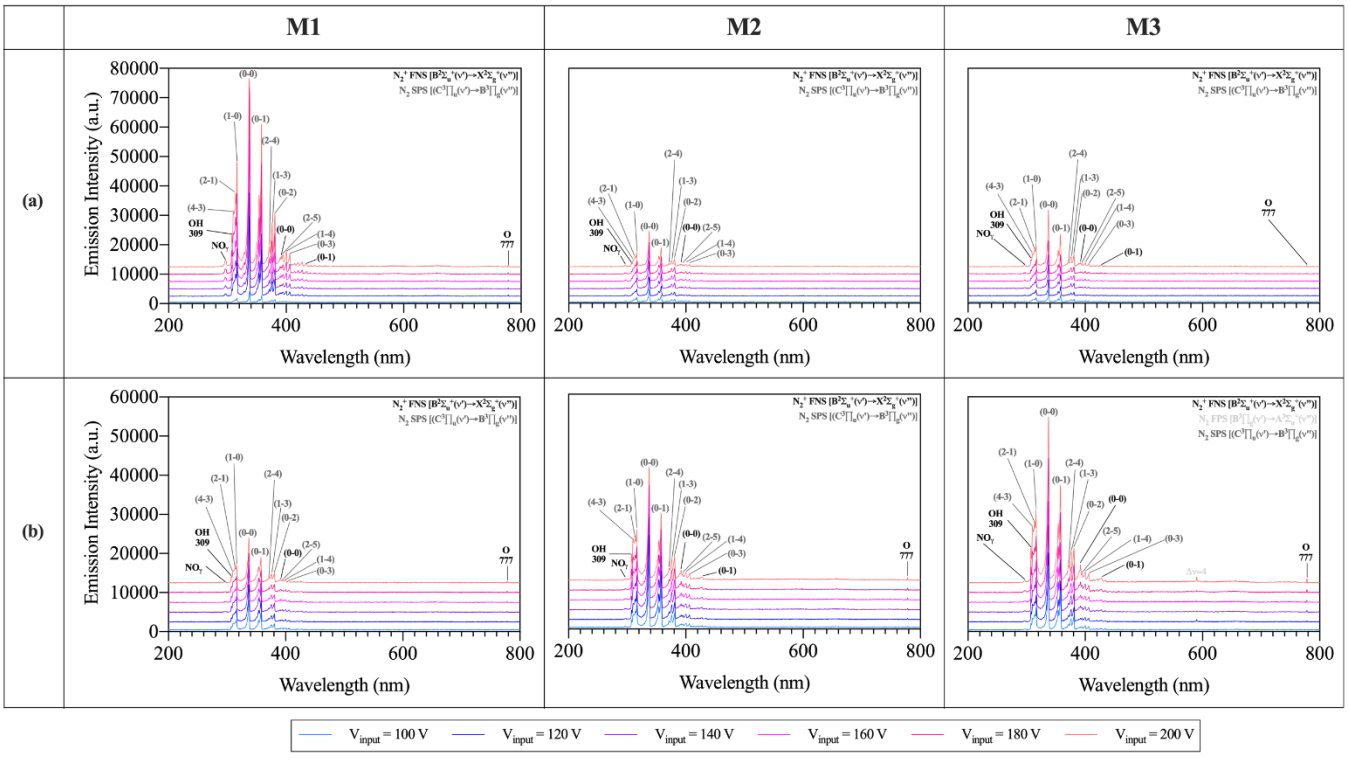

Figure 49. Optical emission spectra of (a) discharge in plasma bubbles and (b) pin-to-liquid discharge by the HPD reactor recorded at 60 kHz, 100-200 V, 50 µsec and 2500 Hz by the 0.5L reactor with a single hole (M1, 2 mm); a single hole (M2, 400 µm) and eight holes (M3, 400 µm).

During PAW generation, two different types of plasma discharges, pin-to-liquid and plasma-bubble discharges, were formed in the HPD reactors [**Fig. 11**(a)]. Strong molecular features with a peak ~280-440 nm were observed for both discharges [**Fig. 49**(a) and **Fig. 49**(b)], possibly induced by the direct collisions of energetic electrons of N_2, O_2 and H_2O molecules with air [51]. The major excited species observed in both, pin-to-liquid [**Fig. 49**(a)] and plasma-bubble discharges [**Fig. 49**(b)] across the input voltages were: N_2^+ First Negative System (FNS, 1 peak, $B^2\Sigma_u^+ \rightarrow X^2\Sigma_g^+$), N_2 Secondary Positive System (SPS, 11 peaks, $C^3\Pi_u \rightarrow B^3\Pi_g$), NO_γ (1 peak, $NO(A^2\Sigma^2) \rightarrow NO(X^2\Pi)$), OH (1 peak, $[A^2\Sigma^+(v=0)] \rightarrow [X^2\Pi^+(v=0)]$) and O bands. The N_2^+ FNS, N_2 SPS and NO_γ correspond to RNS, whereas the OH and O correspond to ROS [14]. Overall, the emission intensities in the observed OES (**Fig. 49**) demonstrates that both, reactive nitrogen species (RNS) and reactive oxygen species (ROS) were generated, with RNS formation dominating the plasma activation of water. This is further analysed in the following section via measurements of the active species concentrations.

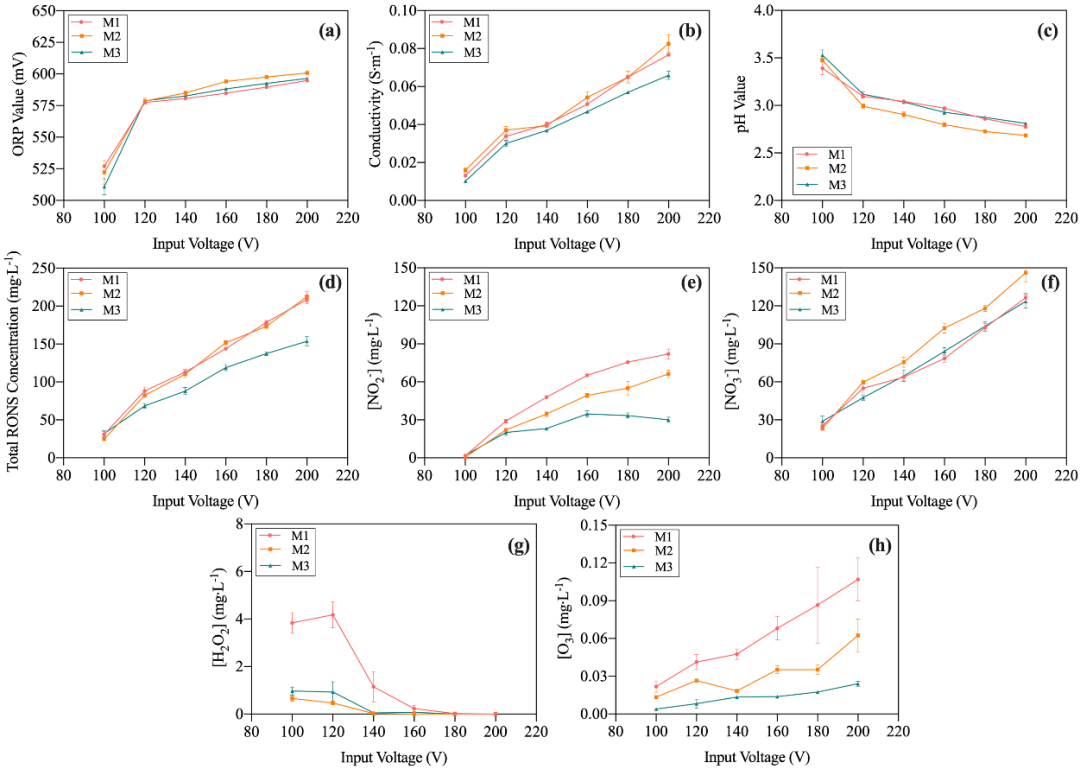

Figure 50. (a) ORP, (b) electrical conductivity, (c) pH, (d) total RONS concentration, (e) NO_2^-, (f) NO_3^-, (g) H_2O_2 and (h) dissolved O_3 of 0.5L plasma-activated water generated by a hybrid plasma-bubble discharge (HPD) reactor with a single hole (M1, 2 mm); a single hole (M2, 400 µm) and eight holes (M3, 400 µm).

The ORP of PAWs were positive in all experiments [**Fig. 50**(a)], indicating the oxidative potential of the active species in the solution, which aid microbial inactivation [13, 18]. **Fig. 50**(a) shows that the ORP increased with increasing voltage and different reactor configurations from M1 to M3. The ORP of the liquid increased from 527 to 595 mV by increasing the voltage from 100 to 200 V via the M1 reactor at 0.5 L. For comparison, the ORP of MilliQ water is ~335 mV. The electrical conductivity of PAW increased with increasing (a) input voltage (from 100 to 200 V) [**Fig. 50**(b)], indicating a higher accumulation of charged species, ions and radicals in the liquid [52]. No change in conductivity

was observed across the input voltages when the diameter of orifice was decreased from 2 mm (M1) to 0.4 mm (M2). The conductivity decreased when the number of orifices increased from 1 (M2) to 8 (M3) as seen in [**Fig. 50**(b)]. This could be attributed to a change in the concentration of active species present in PAW [14]. The pH of all generated PAW was lower than the pH of MilliQ [**Fig. 50**(c)], which is due to the acidification induced by plasma activation [53]. The pH decreased with increasing input voltage [**Fig. 50**(c)]. At 200 V, the pH of PAW slightly decreased with increasing the diameter of orifice among M1 (pH = 2.78) and M2 (pH = 2.68), while increasing the number of orifices increased the pH to 2.81.

The NO_2^- concentration increased as the input voltage increased from 100-200 V irrespective of the HPD reactors [**Fig. 50**(e)], due to higher density of active species in the plasma generated by increasing the voltage [54, 55]. Based on the RONS concentrations, NO_3^- was observed to be the dominant species in PAW in all reactors across the voltages (**Fig. 50**). The NO_3^- concentration increased when the voltage increased irrespective of the HPD reactors [**Fig. 50**(f)], attributed to the conversion of NO_2^- to NO_3^- along with the enriched gaseous O, O_2^- and O_3 generation [54]. The H_2O_2 concentration decreased as the input voltage increased, [**Fig. 50**(g)], likely due to: (a) the conversion of NO_2^- with H_2O_2 to form NO_3^-, resulting in low H_2O_2 concentration and high NO_3^- concentrations [50]; or (b) the HO_2 formation via OH radicals and H_2O_2 [56]. The dissolved O_3 concentrations across all experiments were lower than the other RONS concentrations (**Fig. 50**), due to the poor solubility of O_3 in water [29]. Increasing the input voltage increased the dissolved O_3 concentration irrespective of the HPD reactors [**Fig. 50**(h)], suggesting that excess O_3 was formed in the gas-phase plasma at higher voltages. Moreover, 200 V was chosen as the input voltage for the next study.

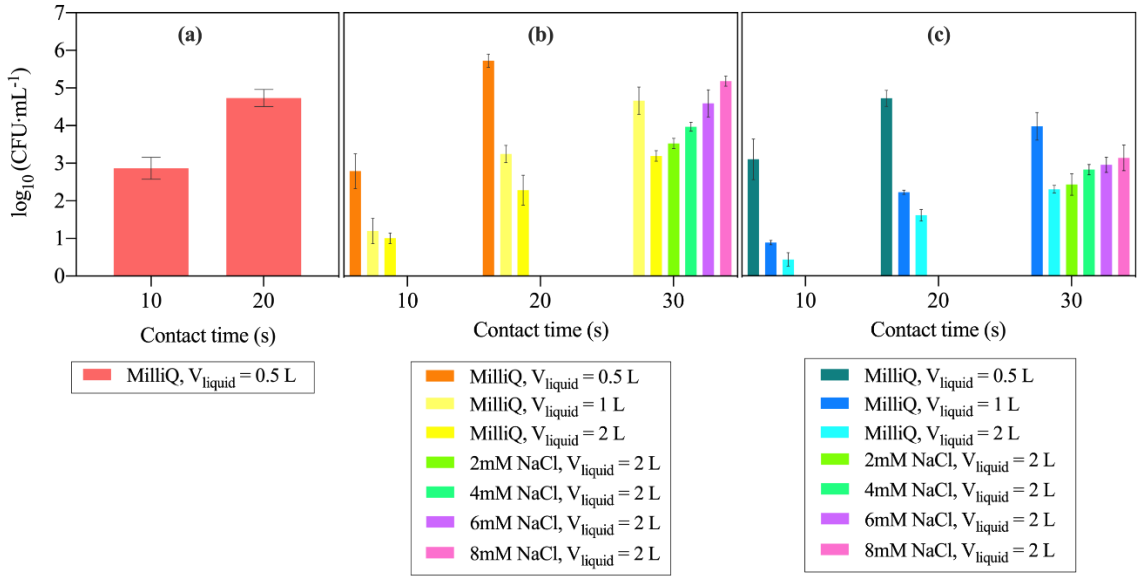

Figure 51. (a) Effect of 0.5L PAW generated by the HPD reactor with a single hole (M1, 2 mm) and MilliQ® water on E. coli for the treatment times of 10, 20 and 30 s. Effect of 0.5-2L PAWs by the reactors with (b) a single hole (M2, 400 µm) and MilliQ® water (c) eight holes (M3, 400 µm) with MilliQ® water and 2-8 mM NaCl on E. coli for 10, 20 and 30 s. For the M3 and M3 reactors with 2L MilliQ® water, the viable counts after 30-s treatment were below detection limit, <1 log_{10} (CFU/mL).

At a contact time of 10 s, the *E. coli* inactivation by PAW generated at the input voltage of 200 V remained unchanged when the orifice diameter reduced from 2 mm (M1, 2.87-log_{10} reduction) [**Fig. 51**(a)] to 400 µm (M2, 2.78-log_{10} reduction) [**Fig. 51**(b)]. A further increase in the contact time to 20 s resulted an increase in the inactivation rate when using both, the M1 [**Fig. 51**(a), 4.73-log_{10} reduction] and M2 [**Fig. 51**(b), 5.72-log_{10} reduction] reactors. This is attributed to the decline in pH, and an increase in ORP and NO_3^- concentrations with increasing time (**Fig. 51**). the ORP of the liquid increased with the reduced orifice diameter (from 2 to 0.4 mm) [**Fig. 51**(a)], likely caused by a greater ROS concentration [14]. However, the dissolved O_3 concentration decreased with the reduced orifice diameter [**Fig. 51**(h)],

indicating that (a) most of O_3 generated during the discharge immediately reacted with NO_2^- to form NO_3^- [54] or (b) the insolubility and instability of O_3 in water [57].At 30 s, more than 6-$\log_{10}$ reduction was achieved by both, the M1 and M2 reactors [**Fig. 51**(a)-(b)].

At a constant orifice diameter and airflow, an increase in the number of orifices from one (M2) to eight (M3) resulted in the *E. coli* inactivation remaining unchanged (3.10-$\log_{10}$ reduction) when the contact time was 10 s [**Fig. 51**(c)]. However, when the contact time increased to 20 s, the M3 reactor (eight orifices) resulted in a 4.72-$\log_{10}$ reduction [**Fig. 51**(c)] compared to the M2 reactor (single orifice) [**Fig. 51**(b), 5.72-$\log_{10}$ reduction]. This is attributed to the rise in pH, and a decline in the NO_2^- and NO_3^- concentrations (**Fig. 50**). The total RONS concentration reduced as the number of orifices increased from one (M2) to eight (M3) at a given orifice diameter of 400 µm [**Fig. 50**(d)], presumably caused by the decreased NO_2^-, NO_3^- and dissolved O_3 concentrations. For instance, at 200 V, the total RONS concentration generated by the M2 reactor (213 mg·L^{-1}) was higher than the M3 reactor (154 mg·L^{-1}) [**Fig. 50**(d)]. Furthermore, in the M3 reactor, voltages of 100-180 V were observed to be insufficient to maintain simultaneous discharge uniformly, which also causes a reduction in the RONS concentrations.

For both, the M2 and M3 reactors, increasing the liquid volume decreased the inactivation at the contact times of 10-30 s [**Fig. 51**(b) and **Fig. 51**(c)]. For instance, the inactivation by the 2L M2 reactor at 20 s reached 1.36-$\log_{10}$ reduction compared to the 0.5L reactor (5.72-$\log_{10}$ reduction) [**Fig. 51**(b)]. This is attributed to the high pH and low RONS concentration at the increased liquid volume (**Fig. 52**). The total RONS concentration generated by both M2 and M3 reactors also decreased to their lowest values of 74.0 mg·L^{-1} and 53.6 mg·L^{-1}, respectively, as the liquid volume increased from 0.5 L to 2 L (**Fig. 52**). This is possibly due to the decline in NO_2^-, NO_3^- and dissolved O_3 concentrations (**Fig. 52**).

Fig. 52 shows that the ORP decreased with reactor vessel volume. The ORP reduced from 600 mV to 583 mV by increasing the liquid volume from 0.5 to 2 L via the M2 reactor (**Fig. 52**). The conductivity also reduced from 0.08 S·m^{-1} to 0.02 S·m^{-1} with increasing liquid volume on the M2 and M3 reactors, likely due to lower concentrations of active species as the liquid volume increased (**Fig. 52**). The pH of PAW by the 2L M2 reactor (3.16) was higher with the 0.5L M2 reactor (**Fig. 52**), possibly due to a dilution of the active species concentrations.

Increasing salinity prior to plasma discharge increased the *E. coli* inactivation rate at 30 s contact time. For instance, in the M2 reactor, increasing the NaCl concentrations to >4 mM resulted in a greater inactivation (4-$\log_{10}$ reduction) at a contact time of 30 s [**Fig. 51**(b)] compared to the 3.19-$\log_{10}$ reduction achieved with non-saline PAW for the same contact time. This is due to the increased concentrations of reactive nitrogen species (RNS), e.g. NO_2^- and NO_3^-, and decrease in pH (**Fig. 53**). Similarly, for the M3 reactor [**Fig. 51**(c)], the increased salinity maximised the inactivation at the contact time of 30 s.

Fig. 53 shows that the ORP had a negligible impact with varying salinity. No change in ORP was observed with varying salinity for both the M2 reactor [**Fig. 53**(a)] and the M3 reactor [**Fig. 53**(b)]. The electrical conductivity of PAW increased with increasing salinity for both the M2 reactor [**Fig. 53**(a)] and the M3 reactor [**Fig. 53**(b)] due to the higher H^+ mobility in comparison to OH^- ions in salt solutions, commonly observed in saline PAW [17]. Increasing the salinity decreased the pH for both, the M2 [**Fig. 53**(a), 3.06] and M3 [**Fig. 53**(b), 3.13] reactors.

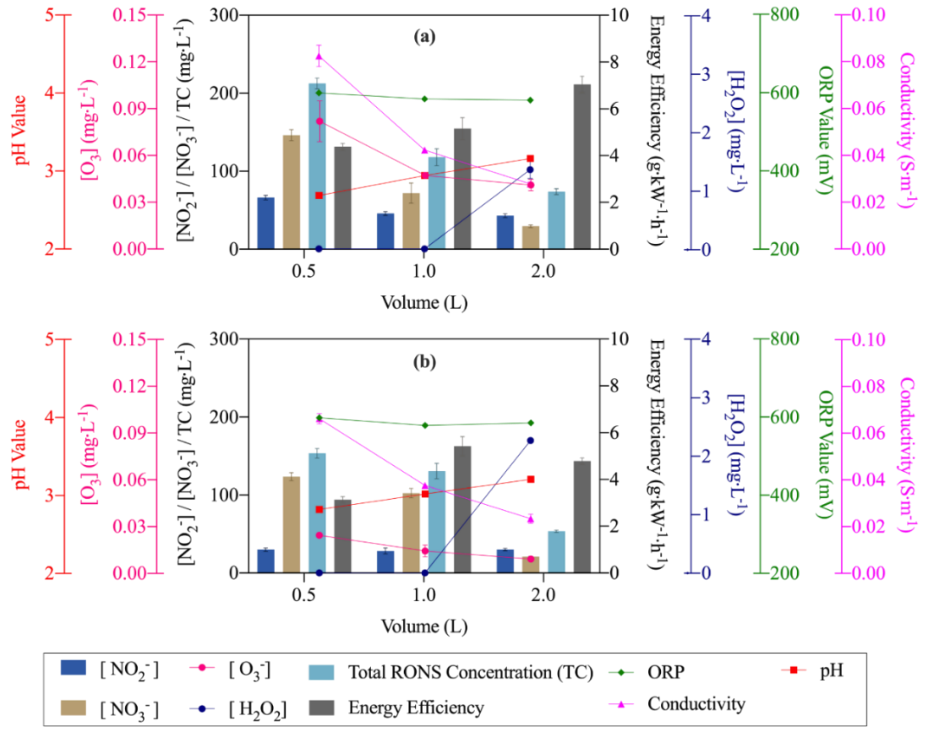

Figure 52. Physicochemical properties of PAW produced by the 0.5-2L reactors with: (a) a single hole (M2, 400 µm) and (b) eight holes (M3, 400 µm).

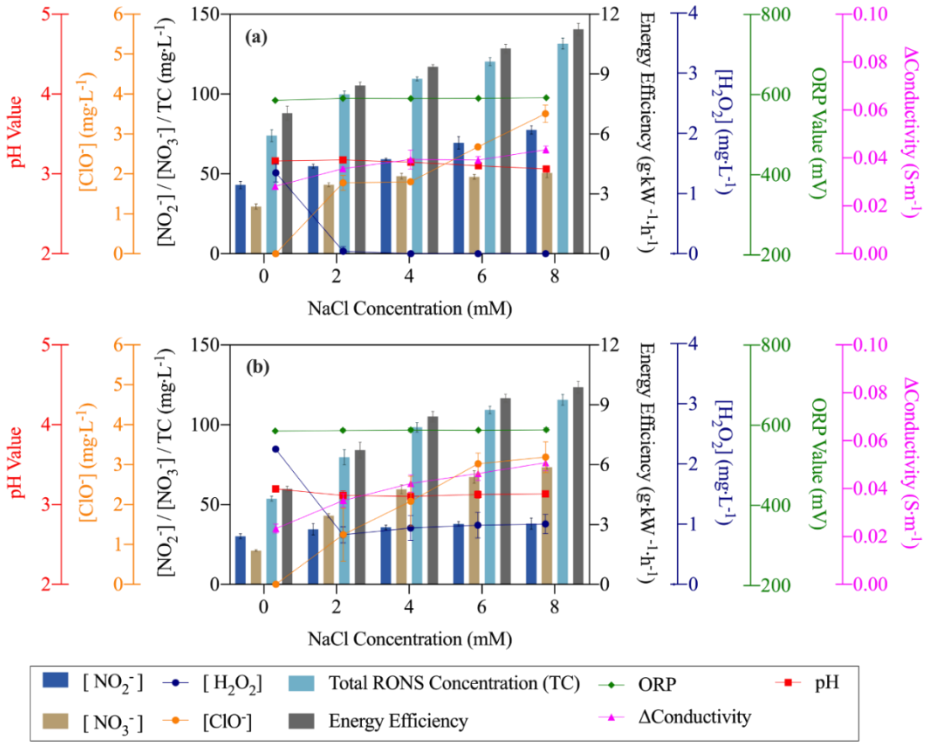

Figure 53. Physicochemical properties of PAW by altering the liquid composition at 0-8 mM NaCl, produced by the 2L reactor with: (a) a single hole (M2, 400 µm) and (b) eight holes (M3, 400 µm).

PAW destroyed the membrane integrity and confirmed the permeability changes of the cell membrane, which were observed by the TEM analysis. The control (MilliQ) had a negligible impact on the *E. coli* inactivation after 30 s contact time [**Fig. 54**(a)], revealing that the untreated *E. coli* maintained their rod-shaped structure with intact cell membranes and nuclei [58, 59]. However, upon PAW treatment, the RONS in PAW diffused into the cells [59], causing damage to the outer structure of cell membrane and the leakage of intracellular material. PAW also degraded the cytoplasmatic material of *E. coli*, and shrank the cytoplasm [**Fig. 54**(b)]; these led to cell death [59, 60].

When the DNA concentrations were measured in the control and PAW-exposed bacterial samples [**Fig. 54**(c)], the exposure of sterile MilliQ water (control) for 30 s contact time did not lead to a significant change of the free DNA concentration from the cells in the solution [**Fig. 54**(c)]; however, the free DNA concentrations of the PAW-exposed samples reached 2.68 ng·mL^{-1}. This implies that PAW exposure to bacterial samples caused cell membrane damage, a phenomenon observed in previous studies [33, 60, 61].

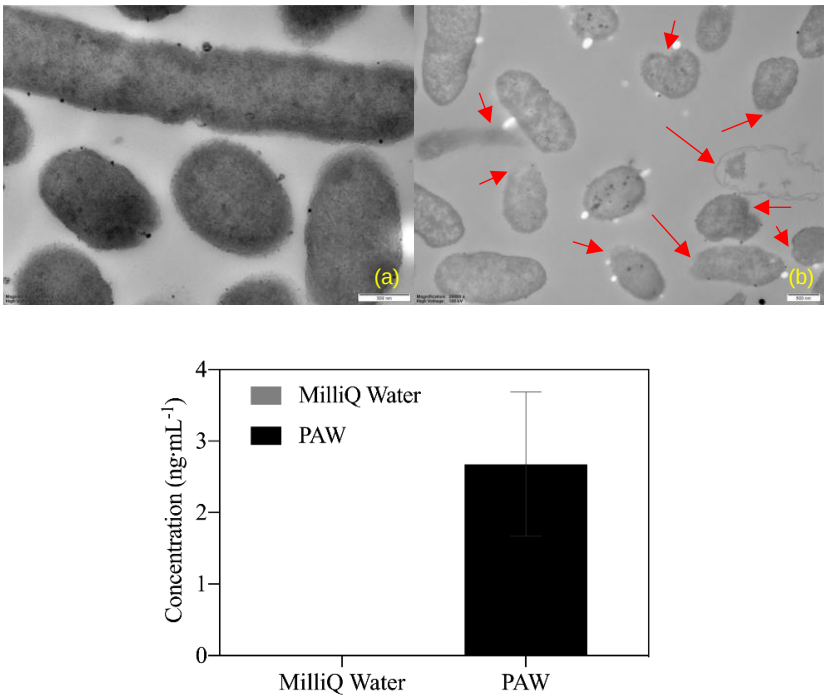

Figure 54. Transmission electron microscopy (TEM) photographs of E. coli before and after a 30s treatment with (a) MilliQ (control) and (b) plasma-activated water (PAW) with 8mM NaCl. (c) Concentrations of DNA leaking from E. coli after 30-s treatment with sterile MilliQ water and PAW (prepared with 8mM NaCl). Error bars represent the standard deviation of triplicates.

The RONS energy efficiency increased with an increase in liquid volume and salinity. The RONS energy efficiency increased to its highest value of 7.04 g·kW^{-1}·h^{-1} for the M2 reactor when the liquid volume increased to 2 L and had comparable values in the range of 4.78 to 5.42 g·kW^{-1}·h^{-1} for the M3 reactor at liquid volumes of 1-2 L (**Fig. 51**). This trend was in an agreement with previously observed results where an increase in liquid volume from 0.5 to 1 L increased the energy efficiency of double plasma jets from 0.35 to 1.81 g·kW^{-1}·h^{-1} [62]. Increasing salinity also increased the RONS energy efficiency for both, the M2 [**Fig. 52**(a)] and M3 [**Fig. 52**(b)] reactors. Among the PAW with varying salinities, PAW with 8mM NaCl in the 2L M2 reactor achieved the highest energy efficiency of 11.2 g·kW^{-1}·h^{-1} in this study [**Fig. 52**(a)].

Various RONS (NO_2^-, NO_3^-, H_2O_2, dissolved O_3 and ClO^-) at a range of concentrations were produced in the different PAWs across the HPD reactors (M1, M2, M3). The RONS energy efficiencies of HPD reactors (M1, M2, M3) with MilliQ were at the lowest (3.25-4.73 $g \cdot kW^{-1} \cdot h^{-1}$) when the liquid volume was at 0.5 L and were at the highest (4.78-11.2 $g \cdot kW^{-1} \cdot h^{-1}$) when the liquid volume was at 2 L (**Table 22**). This follows a similar trend of increasing energy efficiency that was observed by double plasma jets with RO water from a liquid volume of 0.5 L (0.35 $g \cdot kW^{-1} \cdot h^{-1}$) to 1 L (1.81 $g \cdot kW^{-1} \cdot h^{-1}$) [62]. The RONS energy efficiencies for both the M2 [11.2 $g \cdot kW^{-1} \cdot h^{-1}$, **Table 22**] and M3 [9.88 $g \cdot kW^{-1} \cdot h^{-1}$, **Table 22**] reactors at 2 L were maximised with the addition of NaCl (8 mM), consuming 61-68% less energy than 0.5 L MilliQ to produce the same concentrations of RONS in the solution.

Table 22. Summary of RONS energy efficiency and E. coli inactivation by different HPD reactors (M2, M3) generated at 200 V with various liquid volumes and salinities.

HPD reactor			Liquid		RONS energy efficiency ($g \cdot kW^{-1} \cdot h^{-1}$)	E. coli inactivation [-log_{10} reduction (% removal)]	
Name	Number of orifices	Diameter (µm)	Volume (L)	Salinity (mM NaCl)		Contact time (20 s)	Contact time (30 s)
M1	1	2000	0.5	0	4.34 ± 0.06	4.73 ± 0.13 (99%)	>6 (99%)
M2	1	400	0.5	0	4.37 ± 0.08	5.72 ± 0.09 (99%)	>6 (99%)
	1	400	1	0	5.15 ± 0.25	3.25 ± 0.17 (99%)	4.67 ± 0.21 (99%)
	1	400	2	0	7.04 ± 0.20	2.29 ± 0.21 (99%)	3.19 ± 0.08 (99%)
	1	400	2	8	11.2 ± 0.15	n.m.	5.18 ± 0.07 (99%)
M3	8	400	0.5	0	3.13 ± 0.07	4.72 ± 0.11 (99%)	>6 (99%)
	8	400	1	0	5.42 ± 0.23	2.22 ± 0.03 (99%)	3.98 ± 0.21 (99%)
	8	400	2	0	4.78 ± 0.07	1.61 ± 0.13 (98%)	2.30 ± 0.05 (99%)
	8	400	2	8	9.88 ± 0.16	n.m.	3.14 ± 0.19 (99%)

n.m.: not measured

0mM NaCl: MilliQ without the addition of NaCl

Fig. 55(a) shows the cavitation bubbles generated by ultrasound at the low ultrasonic frequency of 25 kHz and the low input ultrasonic power of 50 W during PAW generation. The power to generate ultrasound in this study is at least 10 times less than the reported values [63, 64]. **Fig. 55**(b) shows that the total RONS concentration increased from 144 $mg \cdot L^{-1}$ to 157 $mg \cdot L^{-1}$ during the PAW generation with ultrasound.

Fig. 56 shows the *E. coli* and *S.* Typhimurium inactivation of PAW by the HPD reactors with or without ultrasound. At the contact time of 20 s, PAW generated by both reactor configurations inactivated *S.* Typhimurium below the detection limit with more than 6.79-log_{10} reduction [**Fig. 56**(a)]. Interestingly, at 20s contact time, there was no significant difference between the *E. coli* inactivation by the HPD reactor with ultrasound (3.64-log_{10} reduction) and without ultrasound (3.98-log_{10} reduction) [**Fig. 56**(b)]. At 30s contact time, the *E. coli* inactivation by both reactor configurations achieved more than 6.82-log_{10} reduction [**Fig. 56**(b)].

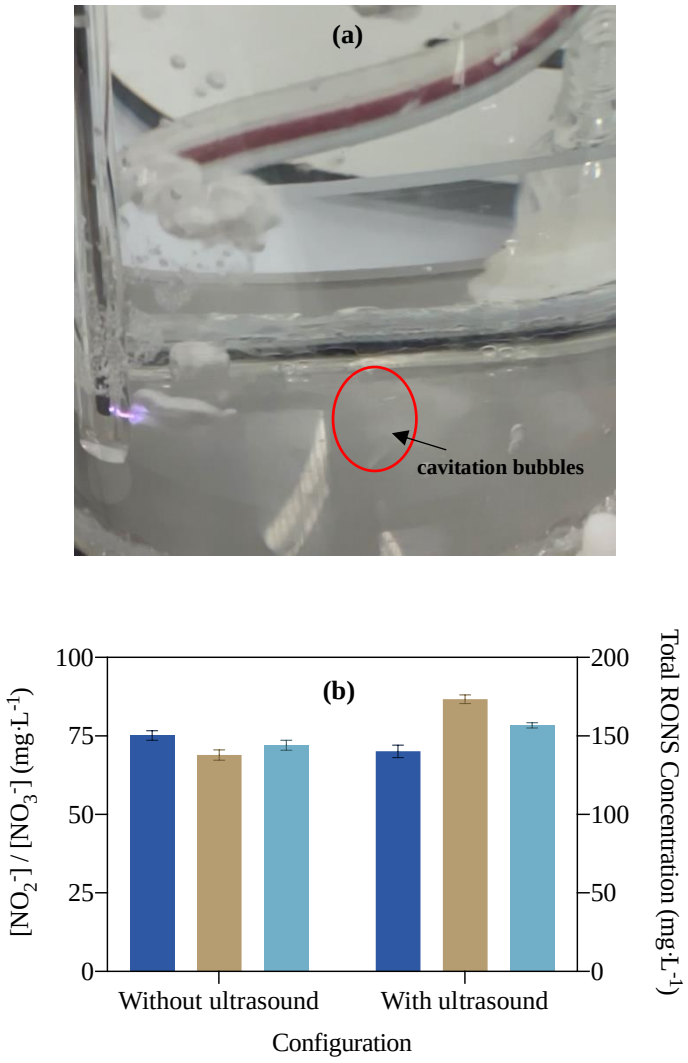

Figure 55. (a) Photograph of cavitation bubbles generated by ultrasound. (b) RONS concentrations of PAW generated via the HPD reactor without and with ultrasound.

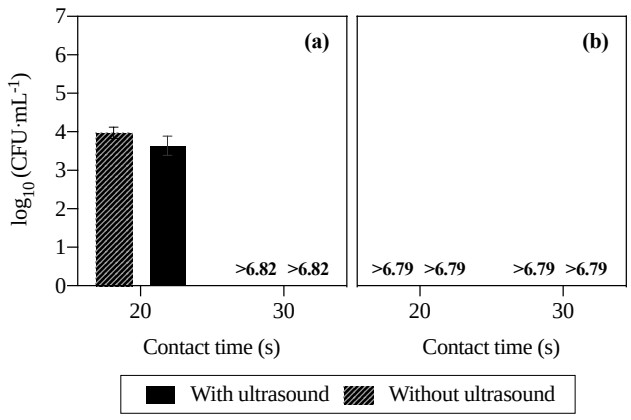

Figure 56. (a) E. coli and (b) S. Typhimurium inactivation in 20 and 30 s by PAW generated via the HPD reactor without and with ultrasound.

Phase 4 also reported on (i) the simulation of the electric field distribution in the hybrid plasma discharge (HPD) reactor to generate plasma-activated water, (ii) the antimicrobial efficacy of PAW against *S.* Typhimurium adhered to beef surfaces via two meat washing methods, spraying and immersion, at the contact times of 15, 30 and 60 s and the storage times of beef at 0, 1 and 7 days, (iii) the quality of beef and (iv) the economic analysis to project the costs of implementing this PAW technology for small and medium scale enterprise producers.

Two simultaneous plasma discharges, one from the high-voltage (HV) electrode to the liquid and the other one from the ground electrode, were generated via the HPD reactor connected to one power source. This was successfully demonstrated in **Fig. 57**, showing the simultaneous formation of regions of high electric field intensity around both the HV electrode and the ground electrode. In this study, plasma-activated water was produced with the pH, electrical conductivity, NO_2^-, NO_3^- and H_2O_2 of 3.11, 0.153 S·m^{-1}, 78.1 mg·L^{-1}, 21.2 mg·L^{-1} and 0.735 mg·L^{-1}, respectively. NO_2^- was observed to be the dominant species in PAW via the HPD reactor for the discharge time of 30 min.

Two meat washing methods were explored, including spraying and immersion, with PAW and water. For both PAW/water spraying and immersion, the inactivation against *S.* Typhimurium on beef increased when the contact time was increased from 15 to 60 s as shown in **Fig. 58**(a). Similar trends of inactivation were also observed when the PAW-treated and water-treated beef samples was stored at 4 °C for 1 day and 7 days as shown in **Fig. 58**(b)-(c). The meat washing method via spraying with the contact time of 30 s was selected for the study of meat quality in Section 4.5, based on the specific trends that are observed in **Fig. 58** as follows:

- Irrespective to the storage time of meat, meat washing method and liquid type, there was no significance difference between the inactivation at 30s and 60s.
- Irrespective to the storage time of meat and meat washing method, the PAW's inactivation efficiencies were significantly higher than water at the contact times of 30s and 60s.
- Irrespective to the storage time of meat, contact time and liquid type, there was no difference between spraying and immersion.

In terms of surface colour, PAW (T3) had no significant impact on lightness (L^*) irrespective to the meat storage time as shown in **Table 24**. However, PAW (T3) did show a significant reduction in redness (a^*) and yellowness (b^*) after the treated beef sample was stored 4 °C for 1 day as shown in **Table 24**. This can be supported by the photographs of PAW-treated beef samples (T3) as shown in **Fig. 59** and the oxymyoglobin (OxyMb) in **Fig. 60**. Introducing water washing right after the first PAW washing increased a^* with no significant difference in b^* compared to the untreated and water-treated beef samples at the meat storage time of 1 day as shown in **Table 24**, which can be supported by the photographs of T4 in **Fig. 59**. After 7 days the meat storage time, the metmyoglobin (MetMb) significantly increased for all beef samples (T1, T2, T3, T4) as shown in **Fig. 60**, compared to the storage time of 1 day.

In addition, PAW had no significant impact on the pH of the beef during the beef storage time of 1 day and 7 days as shown in **Fig. 61**. Irrespective to the beer storage time, PAW did not significantly change the water holding capacity of beef as shown in **Fig. 62**. Compared to untreated meat samples (T1), treating the beef samples with water and PAW increased the beef weight as shown in **Fig. 63**. There was no significance difference between the weight gain of PAW-treated and water-treated samples. Irrespective to the meat storage time, PAW had no significant impact on TBARS value as shown in **Fig. 64**. **Fig. 65** shows that the additional water spraying after the first PAW spraying had no significant impact on the *S.* Typhimurium inactivation compared to the PAW treatment alone.

Overall, compared to untreated and water-treated beef samples, the spraying method with PAW improved the bacterial inactivation efficiency and maintained the lightness, pH, water holding capacity and TBARS value of beef. The PAW spraying, however, reduced the redness and yellowness, which can be easily mitigated by introducing the second spraying with water 25 °C for 60 s right after the PAW spraying. Furthermore, the approximate total capital cost related

to the implemention of the PAW technology for the small and medium scale enterprise producers were estimated to be AU$ 362,767 and AU$ 1,252,051, respectively, as shown in **Table 25**.

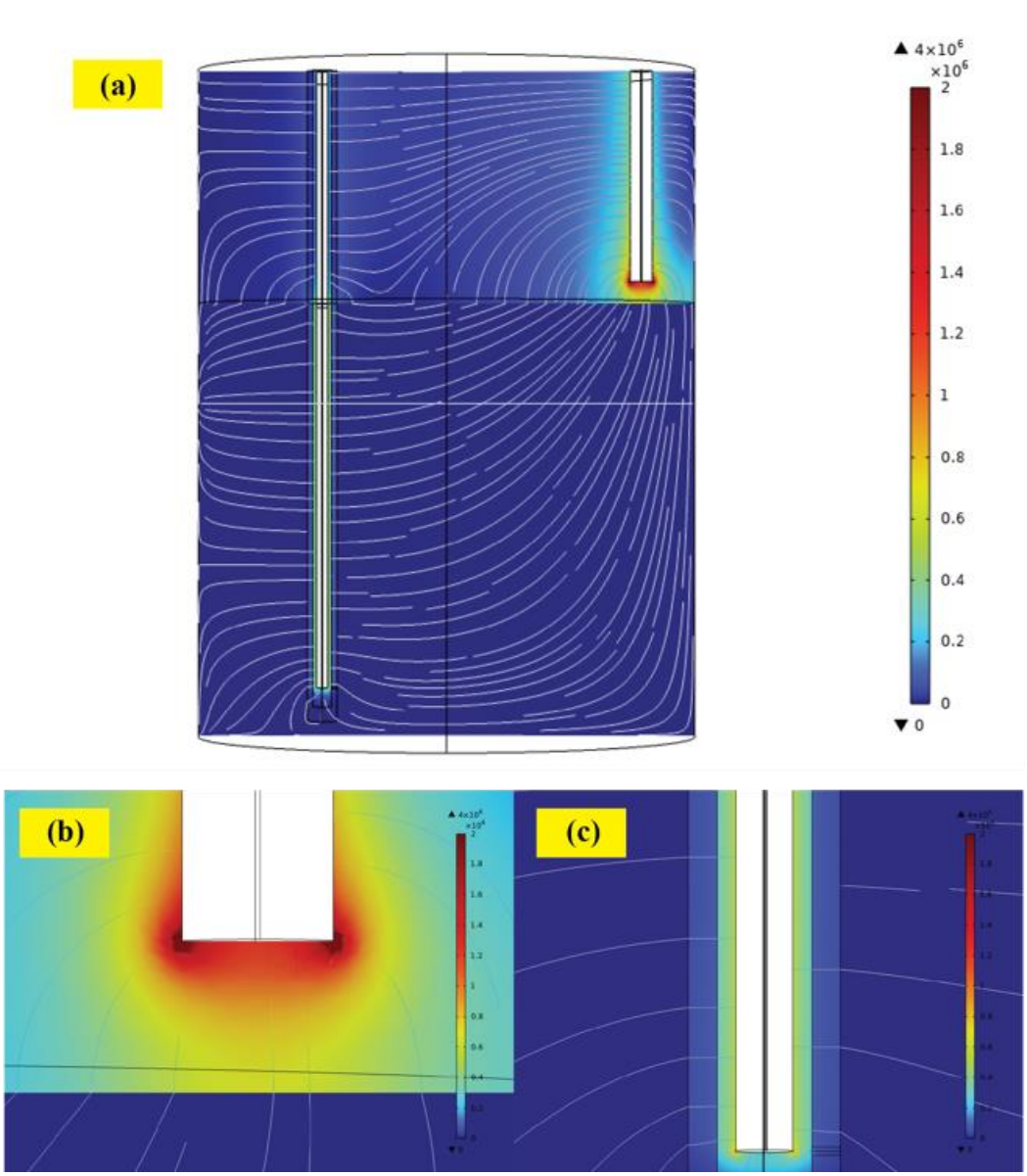

Figure 57. COMSOL results of the electric field strength distribution for (a) the HPD reactor, (b) the high-voltage electrode of HPD reactor and (c) the ground electrode of HPD reactor with a single orifice and the initial liquid conductivity of 0.0691 S·m^{-1}.

Table 23. Physiochemical properties of PAW.

pH	Electrical Conductivity (S·m^{-1})	NO_2^- (mg·L^{-1})	NO_3^- (mg·L^{-1})	H_2O_2 (mg·L^{-1})
3.11 ± 0.03	0.153 ± 0.001	78.1 ± 1.80	21.2 ± 0.6	0.735 ± 0.636

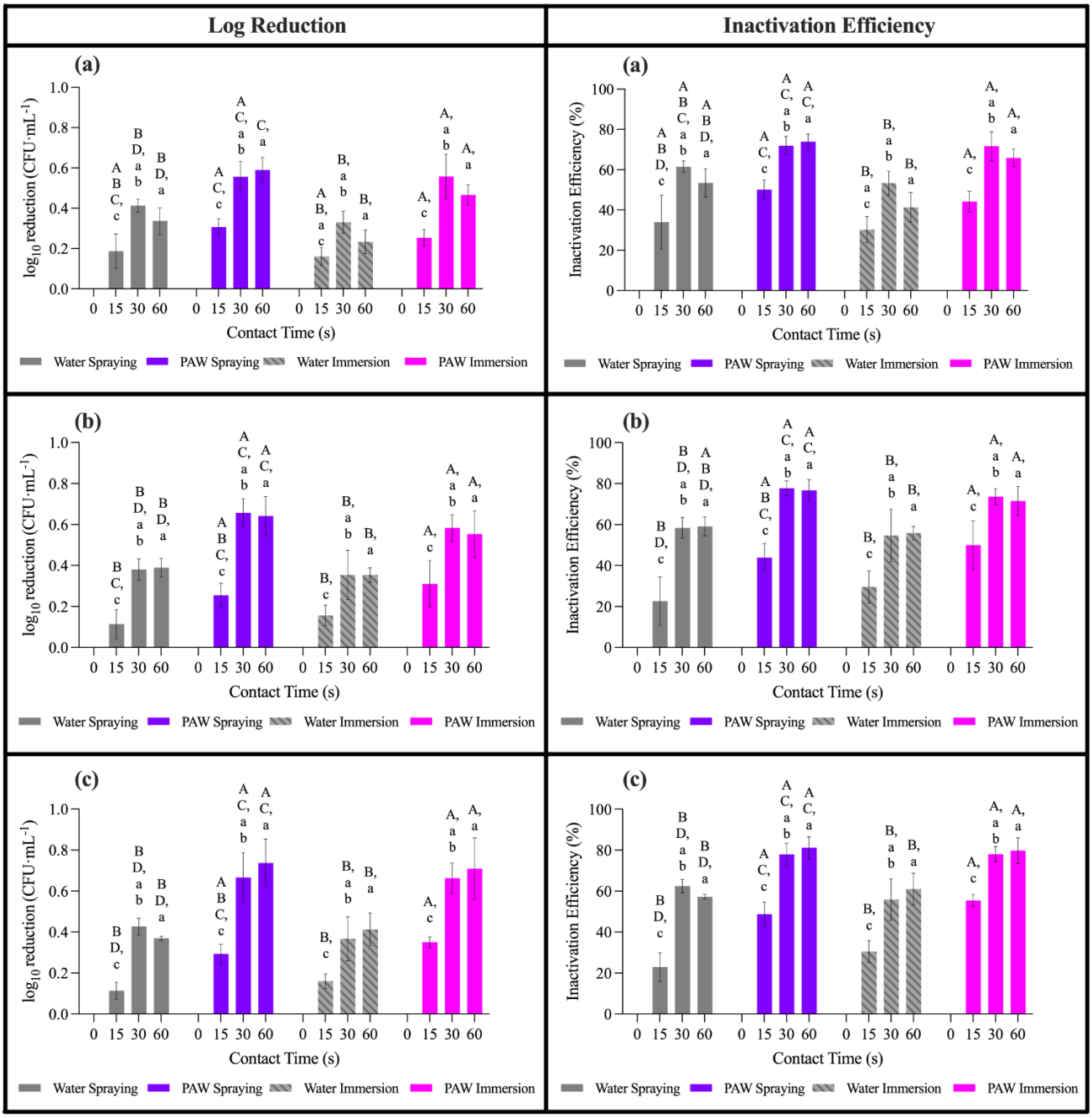

Figure 58. Log_{10} reduction (left side) and Inactivation efficiency (right side) of S. Typhimurium *on beef by PAW and water using the two meat washing methods, mist spraying and immersion, with the contact times of 0, 15, 30 and 60 s and the beef storage times of (a) 0 day, (b) 1 day and (c) 7 days at 4 °C. Different uppercase letters (A, B, C, D) indicate statistically significant difference (P<0.05) among the meat washing conditions with PAW and water within the same contact time while different lowercase letters (a, b, c) indicate statistically significant difference (P<0.05) among the contact times within the same meat washing conditions.*

Table 24. Beef surface colour coordinate values (L^*, a^*, b^*, C, h^*, ΔE) with various treatment conditions at the contact time of 30 s and the beef storage times of 1 day and 7 days at 4 °C. Different lowercase letters (a, b, c) indicate statistically significant difference (P<0.05) among the washing conditions within the same colour coordinate value and storage time.

Treatment No.	Storage Time	1 day						7 days					
	Meat Washing Method	L^*	a^*	b^*	C	h^*	ΔE	L^*	a^*	b^*	C	h^*	ΔE
T1	Untreated beef	49.8 ± 9.3^{a}	21.1 ± 0.4^{a}	11.6 ± 0.3^{a}	24.1 ± 0.5^{a}	1.64 ± 0.02^{a}	-	47.0 ± 9.2^{a}	19.2 ± 1.7^{a}	10.5 ± 0.08^{a}	21.9 ± 1.9^{a}	1.64 ± 0.06^{a}	-
T2	Water spraying at 55 °C for 30 s	48.6 ± 7.8^{a}	21.7± 0.1^{ab}	12.0 ± 0.2^{ab}	24.8 ± 0.1^{ab}	1.63 ± 0.03^{a}	2.37 ± 0.99^{b}	50.4 ± 12.0^{a}	15.4 ± 2.8^{ab}	9.4 ± 0.8^{a}	18.1 ± 2.8^{ab}	1.38 ± 0.2^{a}	5.67 ± 1.96^{a}
T3	PAW spraying at 55 °C for 30 s	48.4 ± 11.2^{ab}	11.3 ± 0.3^{c}	9.19 ± 0.47^{c}	14.5 ± 0.5^{abc}	0.95 ± 0.05^{a}	10.7 ± 0.8^{a}	46.9 ± 9.96^{a}	13.3 ± 0.2^{b}	9.21 ± 0.22^{a}	16.2 ± 0.1^{b}	1.21 ± 0.06^{a}	6.15 ± 1.97^{a}
T4	PAW spraying at 55 °C for 30 s + water spraying at 25 °C for 60 s	50.5 ± 9.7^{ac}	18.2 ± 0.4^{d}	11.1 ± 0.4^{abc}	21.3 ± 0.5^{abd}	1.44 ± 0.03^{a}	3.45 ± 0.3^{b}	40.7 ± 12.10^{a}	12.2 ± 1.6^{b}	9.07 ± 0.64^{a}	15.3 ± 1.1^{b}	1.10 ± 0.24^{a}	10.5 ± 1.88^{a}

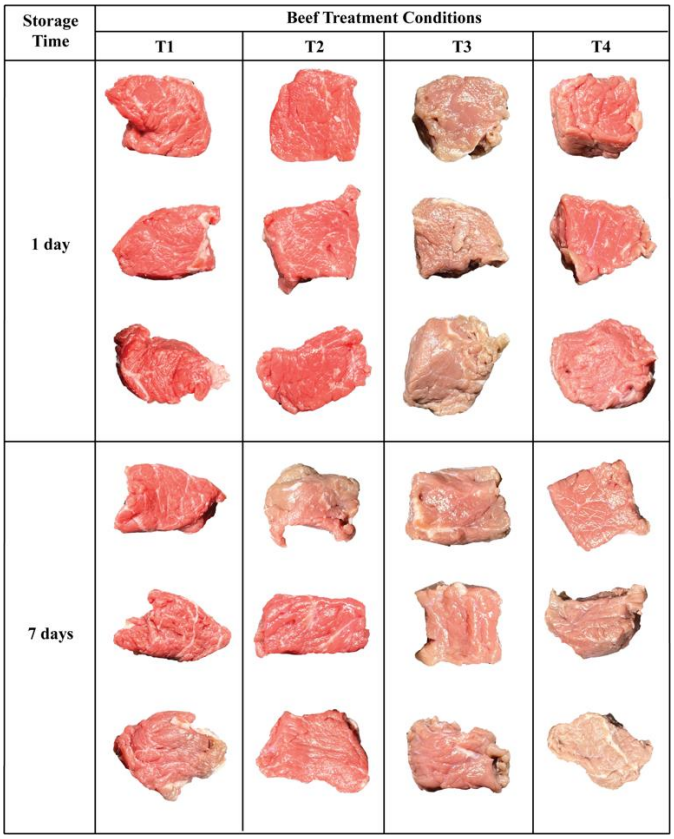

Figure 59. Photographs of untreated beef (T1, control) and beef surface samples treated with the water spraying method at 55 °C for 30 s (T2), the PAW spraying method at 55 °C for 30 s (T3) and the PAW spraying method at 55 °C for 30 s followed by the water spraying method at 25 °C for 60 s (T4) at the beef storage times of 1 day and 7 days at 4 °C.

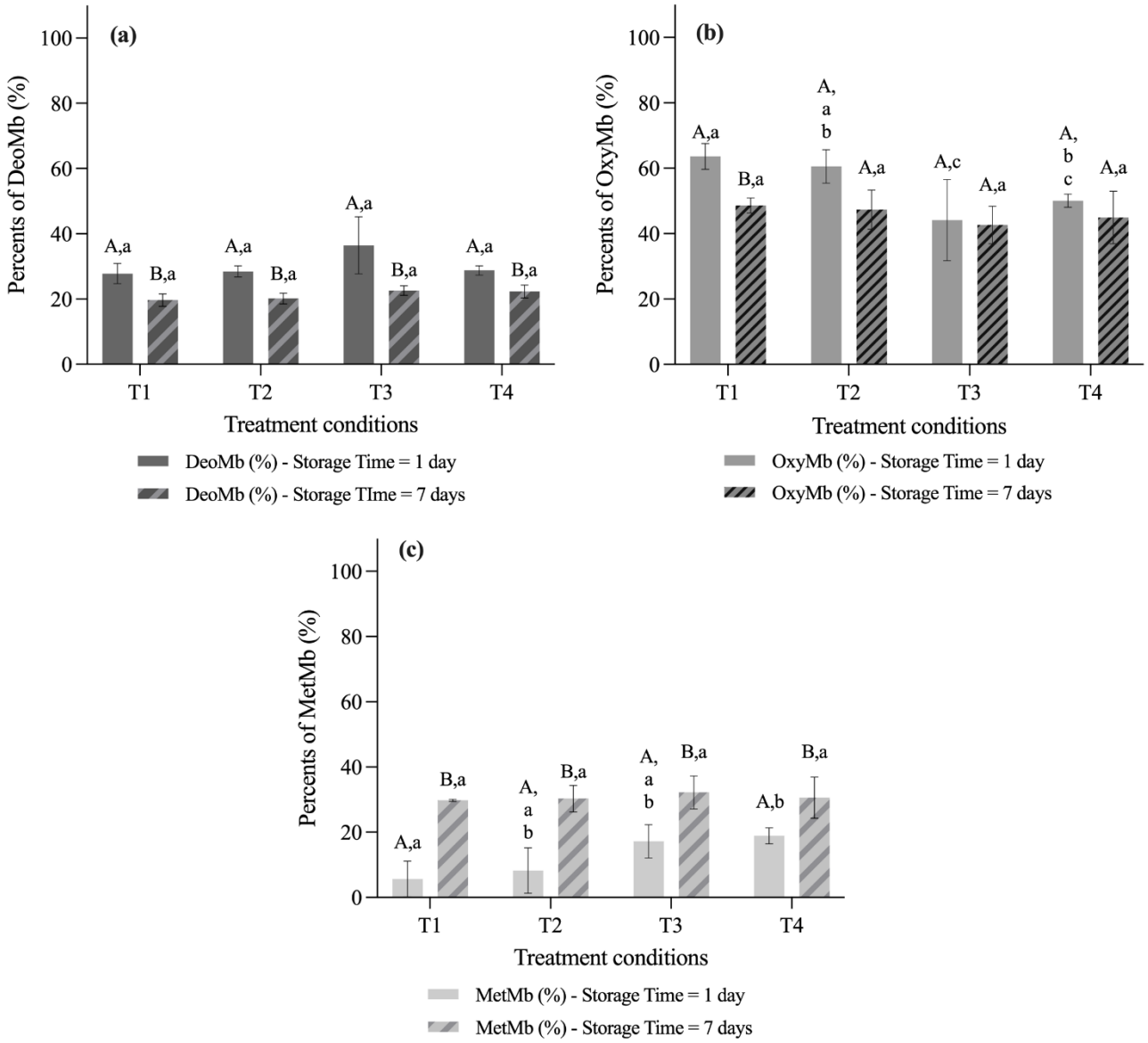

Figure 60. (a) Deoxymyoglobin (%DeoMb), (b) oxymyoglobin (%OxyMb), and (c) metmyoglobin (%MetMb) of untreated beef (T1, control) and beef samples treated with the water spraying method at 55 °C for 30 s (T2), the PAW spraying method at 55 °C for 30 s (T3) and the PAW spraying method at 55 °C for 30 s followed by the water spraying method at 25 °C for 60 s (T4) at the beef storage times of 1 day and 7 days at 4 °C. Different upperrcase letters (A, B) indicate statistically significant difference (P<0.05) among the beef storage times within the same meat washing condition. Different lowercase letters (a, b, c) indicate statistically significant difference (P<0.05) among the meat washing conditions with PAW and water within the same beef storage time.

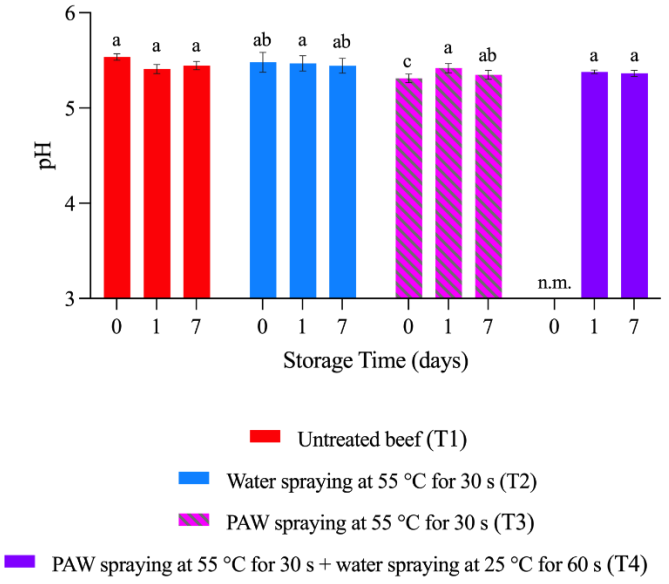

Figure 61. pH of untreated beef (T1, control) and beef samples treated with the water spraying method at 55 °C for 30 s (T2), the PAW spraying method at 55 °C for 30 s (T3) and the PAW spraying method at 55 °C for 30 s followed by the water spraying method at 25 °C for 60 s (T4) at the beef storage times of 1 day and 7 days at 4 °C. Different lowercase letters (a, b, c) indicate statistically significant difference (P<0.05) among the meat washing conditions with PAW and water within the same beef storage time. n.m. represents "not measured".

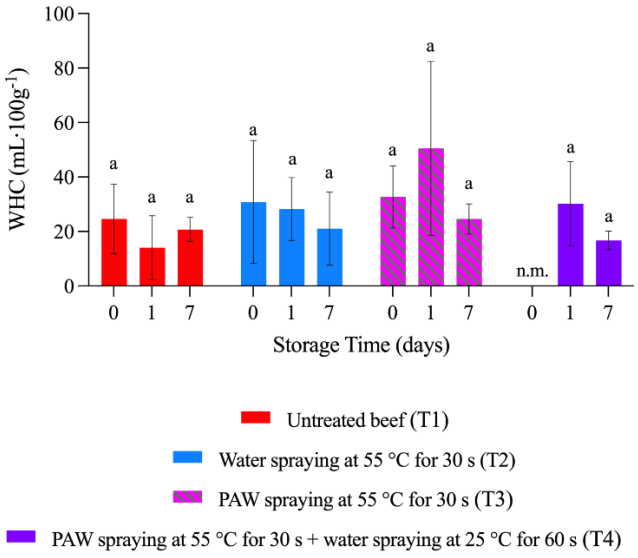

Figure 62. Water holding capacities of untreated beef (T1, control) and beef samples treated with the water spraying method at 55 °C for 30 s (T2), the PAW spraying method at 55 °C for 30 s (T3) and the PAW spraying method at 55 °C for 30 s followed by the water spraying method at 25 °C for 60 s (T4) at the beef storage times of 1 day and 7 days at 4 °C. Different lowercase letters (a, b, c) indicate statistically significant difference (P<0.05) among the meat washing conditions with PAW and water within the same beef storage time. n.m. represents "not measured".

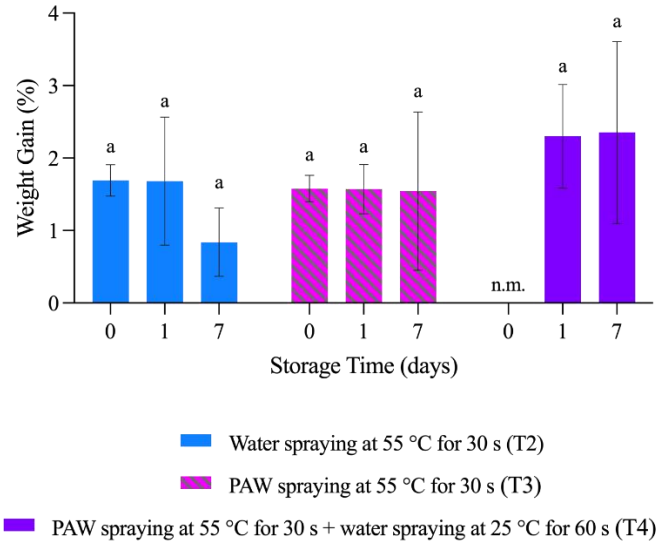

Figure 63. Weight gains of beef samples treated with the water spraying method at 55 °C for 30 s (T2), the PAW spraying method at 55 °C for 30 s (T3) and the PAW spraying method at 55 °C for 30 s followed by the water spraying method at 25 °C for 60 s (T4) at the beef storage times of 1 day and 7 days at 4 °C. Different lowercase letters (a, b, c) indicate statistically significant difference (P<0.05) among the meat washing conditions with PAW and water within the same beef storage time. n.m. represents "not measured".

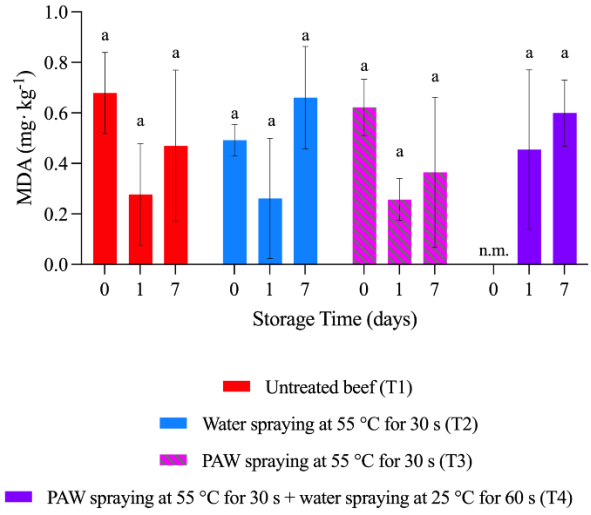

Figure 64. TBARS values (in mg MDA·kg^{-1}) of untreated beef (T1, control) and beef samples treated with the water spraying method at 55 °C for 30 s (T2), the PAW spraying method at 55 °C for 30 s (T3) and the PAW spraying method at 55 °C for 30 s followed by the water spraying method at 25 °C for 60 s (T4) at the beef storage times of 1 day and 7 days at 4 °C. Different lowercase letters (a, b, c) indicate statistically significant difference (P<0.05) among the meat washing conditions with PAW and water within the same beef storage time. n.m. represents "not measured".

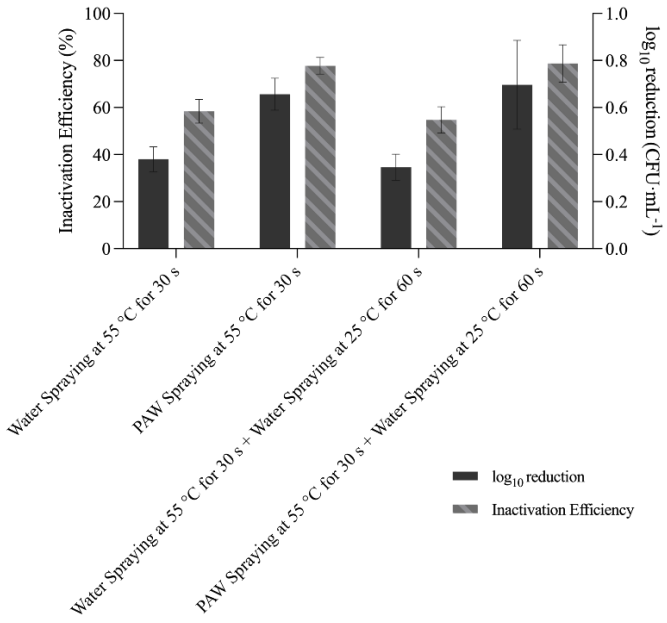

Figure 65. Log_{10} reduction (right side) and Inactivation efficiency (left side) of beef surface samples treated with the water spraying method at 55 °C for 30 s, the PAW spraying method at 55 °C for 30 s, the water spraying method at 55 °C for 30 s followed by the water spraying method at 25 °C for 60 s and the PAW spraying method at 55 °C for 30 s followed by the water spraying method at 25 °C for 60 s at the beef storage times of 1 day at 4 °C.

Table 25. Economic Analysis.

Scale of enterprise producers	Small	Medium
Hot standard carcass (t/year)	68	536
Use of town water for carcass washing (L/d)	115	905
Water saving from the use of PAW to achieve the same bacterial inactivation (obtained from Section 5.5)	40.4	40.4
PAW needed for carcass washing daily (L)	616	4857
Estimated capital cost (AU$)	345,493	1,192,429
Maintenance cost (AU$) – 5% of estimated capital cost	17,275	59,621
Total estimated capital cost (AU$)	362,767	1,252,051

6.0 Discussion

6.1 Phase 1 Discussion

The presence of reactive oxygen species (ROS) and reactive nitrogen species (RNS) in water after plasma treatment has been well established in literature with particular focus on longer lived species nitrite (NO_2^-), nitrate (NO_3^-) and hydrogen peroxide (H_2O_2) which are known to be involved in the antibacterial activity of PAW. In order to optimise the antimicrobial properties of PAW it is important to first understand the variables affecting reactive species concentration. Variables investigated in this study include plasma discharge time, initial water volume, availability of working gas and agitation.

Fig. 17 and **Table 1** show an increase in RNS concentration with discharge time (*t*) in minutes for PAW generated in both open (PAW-O) and closed (PAW-C) systems. With respect to PAW-O, NO_2^- and NO_3^- were observed to increase from 0 to 158 µM and 164 µM respectively, within *t*=30. In contrast, concentrations in PAW-C were far greater, with measured levels approximately double than that achieved in an open system. It is theorized that containment of the charged gaseous molecules generated during plasma discharge in a closed system promotes its reaction with the water sample thereby increasing the formation of NO_2^- and NO_3^-. The reverse is observed for H_2O_2 in PAW-C whereby the limitation of working gas (air) is shown to decrease the formation of H_2O_2.

It was presumed through previous works that the increase in sample volume would result in the dilution of reactive species generated [65]. The experimental results illustrated in **Fig. 18** show this to be true for NO_2^- and NO_3^- with its effect on H_2O_2 concentrations being almost negligible.

The introduction of agitation during the generation of PAW in both an open (PAW-O) and closed (PAW-C) system resulted in either a decline in long-lived reactive species or had little effect on their concentrations (**Table 2**). Continuous agitation of water samples during plasma treatment by means of either magnetic stirrers or circulatory pump systems has recently been applied by Bafoil et al. [66] and Lukes et al. [67] for activated water generated indirectly with agitation by Archimedes screws. It is of the belief that agitation facilitates the dissolving of reactive gaseous species into water and encourages the formation of longer-lived reactive species. Its significance in the promotion of longer lived RNS and ROS may be further realized in the treatment of bulk liquids, whereby interaction times between the water sample and activated gaseous species at the gas/liquid interface play a more crucial role.

Inconsistencies in reactive species concentrations were observed between PAW produced in small glass beaker with dimensions 50x70mm (water surface area of 19.6 cm^2) and PAW of the same water volume and treatment time, produced in a larger container with dimensions 70x80 mm (water surface area of 38.5 cm^2). Concentration of NO_2^- in PAW (50ml water, *t*=10) almost doubled to 871µM from 503µM when produced in a container with a larger water surface area. Likewise, concentration of NO_3^- increased to 820 µM from initial measurement of 524 µM in PAW produced in smaller container. These findings, although unanticipated, do show the importance of the reactions that occur at the gas/liquid-interface for the formation of RNS and ROS in PAW.

Fig. 20 and **Fig. 21** illustrates reactive species in PAW-10 measured over 30 days at varying storage conditions including sealed at room temperature and sealed under refrigeration (approximately 2°C). Nitrate levels increased steadily over the 30 days at both room temperature and under refrigeration while nitrite levels rapidly decreased within the first 10 days of storage. This trend was seen in both PAW-C and PAW-O (**Table 2**). It has been well established in literature that strong oxidizing agents such as the reactive species found in PAW including ozone, can rapidly oxidize nitrite into nitrates [68, 69] which could explain these findings. Traylor et al [70] reported a similar trend between the two reactive species although storage was measured for up to 7 days only.

Levels of nitrate and hydrogen peroxide in PAW stored at room temperature and at 2°C had little effect over the storage period which was comparable to a previous study by Shen et al [71]. They reported a greater retention of nitrite at a lower storage temperature which was not seen in this study. Storage temperature of PAW will be explored further in phase 2 with the formation and application of plasma-activated ice.

Table 4 and **Table 5** show the effects of storage conditions on the concentration of reactive species in PAW. Most notably is the rapid decrease in nitrite when stored unsealed at room temperature with levels as low as 6.6µm after 5 days when compared to 171µm nitrite when stored sealed. Similarly, nitrite levels decreased to 14µm from 212µm after just 24hrs when subjected to agitation via a magnetic stirrer. These findings are likely attributed to the increase in reactions occurring at the gas-liquid interface when exposed to air and more so when surface area of PAW is increased through agitation.

These findings provide insight into the retention of PAW's antimicrobial ability over time as well as showing the capability of PAW to revert back to its original state. Future studies will look at the introduction of organic matter to determine its effect on reactive species concentrations.

The antimicrobial activity of PAW against known pathogenic and spoilage organisms were examined over a range of treatment times (**Fig. 23**) and discharge times (**Fig. 24**). 50 µl of *E. coli*, *S.* Typhimurium, *L. Lactis* and *P. fluorescens* suspensions were treated with 5ml PAW-C (*t*=10, 30) for 30, 180 and 390 s before colony forming units were counted. Exposure to PAW-C (containing approximately 871±110 µM NO_2^-, 820±116 µM NO_3^-) decreased microbial populations by 0.67-$\log_{10}$ (*E. coli* O157:H7); 2.24-$\log_{10}$ (*S.* Typhimurium); 1.32-$\log_{10}$ (*L. lactis*) and 1.37-$\log_{10}$ (*P. fluorescens*). The reduction in bacterial population caused by PAW treatment can be attributed to the presence of reactive long-lived species. Their role in PAW's antimicrobial properties have been well documented by Naitali et al. [72] with their research suggesting a synergistic relation between species NO_2^-, NO_3^- and H_2O_2 as well as shorter-lived reactive species. This connection between reactive species concentration and bacterial reduction is illustrated in **Fig. 24**, whereby PAW produced with a higher plasma discharge time, hence higher concentrations of reactive species, yielded greater log reductions in all bacterial species. This trend is seen within various works [72-75].

Similar $\log_{10}$ reductions are seen with current post-slaughter decontamination methods such as organic acid washes (**Table 6**) however these reductions are greatly determined by delivery pressure, temperature, concentration as well as exposure time. Currently in industry, H_2O_2 is used as a common disinfectant at concentrations of up to 5% (1.6 M) however favourable bacterial reductions have been reported in PAW with H_2O_2 concentration as low as 10 µM [72, 75]. Maximum concentrations of H_2O_2 achieved in PAW-O and PAW-C were 70 µM and 42 µM at *t*=30 and *t*=20 respectively.

The use of nitrites and nitrates in fresh meat in Australia is not currently permitted under FSANZ legislation; however, levels of up to 125 ppm (2,716.8 µM) and 500 ppm (8,063.88 µM) are permitted in cured meats. Maximum nitrite and nitrate levels seen in PAW-O, PAW-C as reported in this study are far below the aforementioned levels permitted on cured meats. It is the aim of this study to tailor these reactive species in PAW for maximum efficacy against microorganisms detrimental to the meat industry.

The antimicrobial properties of PAW against adhered cells are illustrated in **Fig. 25** which show a 1.2-$\log_{10}$ reduction in *E. coli* population adhered to silicon wafers when treated with PAW-C (containing approximately 871±110 µM NO_2^-, 820±116 µM NO_3^-). As discussed above, challenges were faced during the attachment of cells onto beef fat spin coated surfaces however a clear trend has already been observed in **Fig. 23**, **Fig. 24**, and **Fig. 25** that supports the disinfecting effects of PAW. These findings will be used to further explore the antimicrobial activity of PAW against species adhered directly onto fresh meat.

6.2 Phase 2 Discussion

The control of microbial growth of adhered cells on fresh meats proves far more challenging than work completed on planktonic cells as described previously in Phase 1. The complexity of a raw meat matrix greatly influences the adhesion between cells and surface due to their respective physiochemical characteristics, specialized cell surface structures including the secretion of extracellular bridging materials as well as the potential for biofilm formation. Studies describe the kinetics of bacterial attachment to meat surfaces as being not specific to bacterial strains but also highly dependent on meat tissue type which can see attachments occurring within only 20 min of contact. Consequently, this contributes to the difficulties of cell destruction through antimicrobial treatments [76, 77]. In this study, PAW treatment of such adhered cells was investigated. **Table 7** shows the reduction of pathogenic strains *S.* Typhimurium, *E. coli* O157 and *L. monocytogenes* after a 10-min PAW water bath. Results show a maximum $\log_{10}$ reduction of 0.53 ± 0.07 for *S.* Typhimurium and 0.54 ± 0.05 for *E. coli* O157 inoculated on Beef topside samples while maximum $\log_{10}$ reduction of *L. monocytogenes* was seen on lamb shoulder samples with a 1.5 ± 0.05 $\log_{10}$ reduction.

Kamgang-Youbi reported a similar reduction in the inactivation rate of adherent cells when compared to planktonic [75] due to the complexity of attachment structures as discussed above.

To optimize PAW treatment and combat difficulties faced with adherent cells, various methods of PAW treatment and generation was explored. **Fig. 26** illustrates the increase in *E. coli* O157 cell inactivation with treatment volume with a maximum reduction seen using 20ml PAW30. Although increasing PAW30 treatment volume and time was seen to improve its antimicrobial effect, it is well beyond volume/time treatments seen in industry with most washes ranging from a few seconds to a few minutes with volumes from 200 ml to 1 L for a whole carcass as oppose to the small sample size used in this study [78].

PAW was shown to be most effective when applied as a warm treatment at temperatures of approximately 55°C. For this study, PAW30 was generated and placed in a 55°C water bath for at least 60 minutes. Once the temperature was reached, reactive species were recorded (**Table 7**) and solution used to treat Lamb leg samples following procedure outlined in **Fig. 6**. Log reduction through this treatment more than doubled when compared to the same treatment using PAW30 at room temperature. This was also compared to treatment with peptone water at 55°C as a control, which showed no reduction, thereby confirming these significant improvements in PAW efficacy is reliant on the changes in PAW's physicochemical properties as temperature increases rather than cell death caused by high temperatures. To further optimize this treatment, warm PAW was used to treat *E. coli* O157 at varying volumes and treatment times. As shown in **Fig. 30**, decreasing treatment time of warm PAW from 10min to 5min decreased its antimicrobial effect by half from a 0.7- to a 0.32-$\log_{10}$ reduction but still had a better antimicrobial effect than samples treated for 10 minutes with room temperature PAW30. Further to this, decreasing the treatment volume of warm PAW had very little change to its overall antimicrobial activity but still outperformed treatment of room temperature PAW which was applied at a larger volume and longer treatment time. From these results it can be concluded that treatment with warm PAW greatly increases its antimicrobial effect on adhered cells.

PAW has been shown to be effective against common meat spoilage microorganisms as well as against the pathogenic species already mentioned. *B. thermosphacta* is of particular concern within the meat industry, it has the ability to grow under aerobic and anaerobic conditions and are known to tolerate high salt environments, low pH and can grow under refrigeration. In an oxygen limited environment, they have the ability to produce lactic acid, ethanol, formate and acetate thereby leading to foul odours and deterioration of a product [79]. In an oxygen rich environment, *B. thermosphacta* produces 2-methylbutyric acid, acetoin and acetic, isobutyric and isovaleric acids [80, 81]. This has made them the dominant spoilage species under modified atmosphere and vacuum packaging. **Fig. 31** demonstrates the significant antimicrobial effect PAW30 has against *B. thermosphacta* inoculated on beef and lamb with a 0.9- and 1- $\log_{10}$ reduction respectively, with the potential of doubling efficacy when treated with warm PAW.

The eventual integration of PAW into wash water treatments already established within the industry is desired. Washing systems are capable of reducing aerobic bacteria, coliforms and E. coli on carcasses by up to 1- $\log_{10}$ reduction simply through dislodging and without any decontamination ability [82]. This was confirmed in washing treatments performed on beef samples inoculated with either *E. coli* or *L. monocytogenes* (**Fig. 32**), which saw an average $\log_{10}$ reduction of 1.92 and 2.35 with both water and PAW wash water treatments, respectively. It can then be expected that integrated PAW wash water systems will exhibit the same ability to remove bacterial cells in addition to having a disinfecting effect. As a result of this, the overall efficacy of PAW against *E. coli* O157, *S.* Typhimurium, *L. monocytogenes* and *B. thermosphacta* was estimated and presented in **Table 8**.

In comparison to wash water treatments, chemical washes have the ability of achieving greater bacterial reduction as well as exhibiting continued bactericidal effects however recent trends towards 'cleaner' processing and away from the use of harsh chemicals, has seen the rise of many novel technologies. Traditional antimicrobial interventions used either solely or in combination, have limitations in terms of their efficacy and effects on quality parameters. This was demonstrated by Elder et al. [83] when looking into the prevalence of shiga toxin producing *E. coli* on beef carcasses before and after antimicrobial interventions including steam pasteurization, hot water washes, organic acid washes or

a combination of these treatments. They found that of the 30 lots of carcasses sampled, 17% of samples were still positive for the bacterium thereby demonstrating the need for improvements in the efficiency of antimicrobial intervention.

As already demonstrated, PAW produces favourable reductions in both pathogenic and spoilage microorganisms with the added benefits of improved sustainability as well as displaying continued antimicrobial effects. To demonstrate this, beef samples inoculated with approximately 1.1x108 CFU/cm2 *E. coli* O157 were subjected to a washing process of either 20ml sterile water or 20ml warm PAW30. After 10 min, samples were removed from treatment water and analysed. The treatment water was continuously sampled to determine continued bactericidal effects. Upon analysis both water wash and PAW wash reduced bacterial count on meat surface by approximately 2-$\log_{10}$ however continued sampling of the treatment PAW (**Fig. 33**), shows a continued bactericidal effect reaching as high as a 4-$\log_{10}$ reduction in *E. coli* O157. Similar results were shown for the destruction of *L. monocytogenes* species (**Fig. 34**) with continued PAW effects resulting in an overall 4.3-$\log_{10}$ reduction. The continued bactericidal effects displayed by PAW can greatly reduce the risk of contamination that is currently seen within the industry with the redistribution of bacterial cells during simple water wash treatments [84].

The potential for bacterial species to form resistance to decontamination treatments has been of great concern in many industries. Resistance studies were achieved using *E. coli* O157 and *L. monocytogenes* as gram negative and gram-positive models. Each strain was subjected to the same PAW30 treatment and incubated for 24-48 h at 37 °C. Surviving colonies of each species were isolated, inoculated into peptone water, incubated for 24-48 h at 37 °C and treated with PAW, this was repeated over several generations with results shown in **Fig. 35** and **Fig. 36**. **Fig. 36** also shows log reduction of *E. coli* when treated with a less severe PAW treatment (PAW10) for up to 5 generations. Both *L. monocytogenes* and *E. coli* showed an increase in PAW efficacy after the first generation with bacterial reductions then staying fairly consistent with initial treatment. A similar trend is seen when bacterial strains are treated with a weaker treatment of PAW10. No reduction in PAW's efficacy was seen even with continued treatments over several generations and therefore induced resistance to PAW treatment is unlikely.

Combining PAW with freezing was explored in this report whereby PAW30 solutions were generated and subsequently frozen for up to 4 days and sampled daily. PAW was thawed and allowed to reach room temperature before application as a treatment method. 50 µl of a planktonic *P. fluorescens solution* was added to 5ml thawed PAW. A tenfold serial dilution was performed after 390 s with results shown in **Fig. 37.** Unlike reported studies [71] storing PAW at frozen temperatures was not shown to have a greater retention of efficacy when compared to storage at refrigerated temperatures. This proves beneficial in industry application as additional energy is not required to maintain PAW at below freezing temperatures. Furthermore, it was shown that storage of PAW at either refrigerated or frozen temperatures for over 24 h produced an increase in its overall antimicrobial effect. It is theorized that as plasma activated species are generated above the water surface in an enclosed system, they will continue to diffuse and react with the water long after the discharge is removed and may then explain why reactive species increase with storage time. It is also suggested that when exposing PAW to below freezing temperatures, the diffusion rate of reactive species into the water may be slowed and therefore its subsequent antimicrobial effect will not be as high when compared to refrigerated samples. Although the chemistry behind this trend is still unclear, these results do indicate an added benefit to the use of PAW within the industry.

6.3 Phase 3 Discussion

The discharge of non-thermal plasma is typically driven by the voltage power source and the discharge frequency is believed to be one of the most influential parameters to govern plasma characteristics [85]. This is due to the strong dependence of power coupling and plasma sheath characteristics on frequency [9].

Prior to plasma excitation with atmospheric air (mainly O_2 and N_2), the formation of nitric oxide NO is a first step in forming NO_x ($x = 2,3$) species. NO and N species in the gaseous state are formed via the rate-limiting reaction between N_2 and O[13]. NO are also formed via the reaction of O_2 with N, and the reaction between N_2 and OH (formed from the electron-impact dissociation of water vapor in atmospheric air) [10, 86]. The NO_x formations then occur via the oxidation reactions of the primary species NO, shown in pathways (1) – (6) [86, 87]. It was reported that gaseous NO_x underwent the following pathways (7) – (9) when being transferred into water during the discharge [87]. Gaseous NO and NO_2 species dissolve into water to generate NO_2^-, NO_3^- and H^+ by involving oxidising species such as O, O_2, O_3, and OOH [87, 88]. The ionic pathways (10) – (13) were also believed to be undertaken during the conversion of NO_2^- ions to NO_3^- [87].

$$\mathrm{NO + O \rightarrow NO_2} \quad (1)$$
$$\mathrm{NO + O_2 \rightarrow NO_2 + O} \quad (2)$$
$$\mathrm{2NO + O_2 \rightarrow 2NO_2} \quad (3)$$
$$\mathrm{NO + O_3 \rightarrow NO_2 + O_2} \quad (4)$$
$$\mathrm{NO_2 + O + M \rightarrow NO_3 + M} \quad (5)$$
$$\mathrm{NO_2 + O_3 \rightarrow NO_3 + O_2} \quad (6)$$
$$\mathrm{2NO_{2aq} + H_2O \rightarrow NO_2^- + NO_3^- + 2H^+} \quad (7)$$
$$\mathrm{4NO_{2aq} + O_{2aq} + 2H_2O \rightarrow 4NO_3^- + 4H^+} \quad (8)$$
$$\mathrm{NO_{2aq} + OH_{aq} \rightarrow NO_3^- + H^+} \quad (9)$$
$$\mathrm{NO_2^- + O_{3aq} \rightarrow NO_3^- + O_{2aq}} \quad (10)$$
$$\mathrm{NO_2^- + H_2O_2 \rightarrow NO_3^- + H_2O} \quad (11)$$
$$\mathrm{3NO_2^- + 3H^+ \rightarrow 2NO_{2aq} + NO_3^- + H_2O + H^+} \quad (12)$$
$$\mathrm{NO_2^- + NO_{3aq} \rightarrow NO_3^- + NO_{2aq}} \quad (13)$$

Since discharge frequency is directly related to the energy input to the electric field, increasing the frequency improved the energy of discharge, generating more frequent and energetic electrons that promote and accelerate the formation active species [24, 89]. Increasing the frequency also increased the supply and energy of chemically active species and high-energy electrons due to the bombardment between high-energy electrons and ambient particles [10, 86]. It is reported that more energetic electron bombardments with water particles at higher discharge frequency can generate more NO_2^-, NO_3^- and H_2O_2 species [89]. The plasma discharge at 2000Hz was also observed to be more intense than at 1000Hz. The intensity of the discharge was enhanced at higher discharge frequency, leading to a higher yield of the reactive species. The experimental results show that Reaction (1) is highly involved during the plasma discharge in the gas phase because a greater intensity of the discharge resulted in a higher NO_2^- concentration in the solution. These results are in agreement with the study conducted by Pavlovich, M.J., et al [86, 90].

Additionally, nitrite concentrations were predominantly higher than nitrates in both “Copper Out” and “Copper In” reactors with MilliQ® water and discharge frequencies at 1000 Hz and 2000 Hz. This may be because of the competition between the rates of oxidation pathways in the gas phase and the dissolution and diffusion rates of nitrogen oxides into water that take part to induce a change in the production and the ratio of nitrites and nitrates in the solution [89]. Tachibana, K., J.-S. Oh, and T. Nakamura suggested that the dissociative ionisation of nitrous acid HNO_2 in water, in Reaction (15), is distincly attributed to the NO_2^--rich solution [87]. Similarly, it was also reported that HNO_2 with $pK_a = 3.3$ is unstable under acidic environments, which quickly decays into acidified nitrites, nitrogen dioxide and nitrous acid intermediates, as shown in Reaction (16) [23, 87]. This route was believed to trigger the dispropotion between nitrites and nitrates in the PAW [91], and hence, PAW was enriched with nitrates as the dominant species.

$$\mathrm{NO_{2aq} + NO_{aq} + H_2O_{aq} \rightarrow 2HNO_{2aq}} \quad (14)$$
$$\mathrm{HNO_2 \rightarrow NO_2^- + 2H^+} \quad (15)$$
$$\mathrm{2HNO_2 \rightarrow NO^* + NO_2^* + H_2O} \quad (16)$$

In terms of the physical properties of PAW, results show that raising discharge frequency increased the power consumption, the water acidity, the conductivity and the oxidation-reduction potential. At a greater discharge frequency, the increased power also increased the energy consumption.

The experiments indicated that there was a significant difference ($p<0.05$) between "Copper Out" and "Copper In" in the formation of NO_2^-. By placing the grounded electrode inside the reactor, the NO_2^- concentration was significantly greater than the "Copper Out" reactor at 1000 Hz and 2000 Hz of discharge frequency. In terms of the NO_3^- formation in the solution for "Copper Out and "Copper In" reactors, there is an insignificant difference at 1000 Hz and a significant difference at 2000 Hz. Although different values obtained by changing the position of grounded electrode cannot be fully explained, it may be concluded that the dielectric barrier the "Copper Out" reactor changes the discharge intensity during plasma ignition affecting the production of NO_2^-. Water added in both reactors acts as liquid electrodes, which can be regarded as a resistance connecting in series with the discharge circuit [92]. Adding a dielectric layer increases the dielectric constant and the resistance in the system. However, the discharge becomes less intense, which was observed during the experiments. The diminished discharge intensity suggested that the localised electric field was weakened with reduced electron density during the activation of electrons in the ionisation, excitation and dissociations by electron impact. Having lower plasma density decreased the number of active ions during the plasma ignition, likely reducing the production of nitrite in the solution as shown on the experimental data.

The effect of conductivity was also investigated. Before the discharge on each configuration, sodium chloride was added into MilliQ® water to increase the conductivity of the initial solution from 0.02 $S.m^{-1}$ to 0.2 $S.m^{-1}$, mimicking the conductivities of tap water and juice, respectively. Table 9 summarises the concentrations of nitrites and nitrates in water of conductivities of 0 $S.m^{-1}$, 0.02 $S.m^{-1}$ and 0.2 $S.m^{-1}$ after 10 min of discharge time. It was found that increasing initial conductivity of the solution did not increase the power consumption but caused significant ($p<0.05$) and greater concentrations of nitrites and nitrates at 1000 Hz and 2000 Hz of discharge frequency. It was concluded that the initial conductivity of the solution plays an important role that can influence the reaction kinetics of the plasma discharge [93, 94]. The improvement in the physicochemical properties of PAW with an increase in conductivity demonstrates the potential integration of PAW generators into established water systems at plant sites without the need to source ultra-pure water.

Six discharge conditions (shown below) were selected for further antimicrobial and physicochemical analysis at 30 min:

1. Discharge Frequency = 1000Hz, Conductivity = 0$S.m^{-1}$, "Copper Out"
2. Discharge Frequency =2000Hz, Conductivity = 0$S.m^{-1}$, "Copper Out"
3. Discharge Frequency =2000Hz, Conductivity = 0.02$S.m^{-1}$, "Copper Out"
4. Discharge Frequency =2000Hz, Conductivity = 0.2$S.m^{-1}$, "Copper Out"
5. Discharge Frequency =2000Hz, Conductivity = 0.02$S.m^{-1}$, "Copper In"
6. Discharge Frequency =2000Hz, Conductivity = 0.2$S.m^{-1}$, "Copper In"

As the discharge time increased with the increasing frequency in 0 $S.m^{-1}$ water, the nitrites were significantly greater than the nitrates ($p<0.05$). However, this was not the case when expanding the activation time with higher initial conductivities at 2000Hz. At 30 min, the proportion of nitrites and nitrates in the solution shifted and significantly ($p<0.05$) favoured greater production of nitrates than nitrites. It has been reported that the oxidation pathways, shown in Reaction (4) and (10), might be responsible for leading nitrates to be predominant in the solution [87]. Alternatively, Reaction (12) was suspected to have occurred, causing the disproportion of NO_x while converting nitrites to nitric oxides and nitrates under acidic environments [95, 96]. This can be confirmed by the reduction in pH, along with the increase of electrical conductivity over greater activation time [95].

Energy yield of each condition, which needs to be considered for reactor performance and optimisation, was calculated and demonstrated in **Fig. 39**. Energy yield was expressed as the amount of RNOS produced in grams per power consumption in kWh. Increasing the discharge frequency to 2000 Hz showed a higher energy yield compared to 1000 Hz. Similarly, a greater yield was observed at greater initial conductivity for both "Copper Out" and "Copper In" reactors.

Higher frequency increased the inactivation efficiency of *E. coli* 0157:H7 and *S.* Typhimurium due to the higher yield of NO_x species, which was higher at 2000Hz than at 1000Hz. NO_2^- and NO_3^- under acidic conditions were believed to play a major role in the antimicrobial characteristic of PAW, inactivating bacterial cells by causing oxidative stress on the cell membrane, overcoming the tensile strength of the cytoplasmic membrane and consequently triggering the destruction of the cell membrane, including rupture to the intracellular constituents of the cell [97-99].

At 30 min of discharge time, there was a significant increase ($p<0.05$) of total NO_x production from 0 $S.m^{-1}$ to 0.02 $S.m^{-1}$. However, the total NO_x production from 0.02 $S.m^{-1}$ to 0.2 $S.m^{-1}$ did not increase significantly ($p>0.05$). Moreover, the insignificant difference between 0.2 $S.m^{-1}$ and 0.02 $S.m^{-1}$ for *E.coli* 0157:H7 inactivation at 360 s may be due to the shape and the size of the bacteria and the nature of cell membrane used during treatment [97]. On the other hand, the log_{10} reductions of *E. coli* 0157:H7 at 240 s achieved by PAW generated with 0.02 and 0.2 $S.m^{-1}$ at 2000 Hz in the "Copper In" reactor were 0.95 and 3.19, respectively, which were significant ($p<0.05$). After 300s, PAW generated from 0.2 $S.m^{-1}$ water at 2000 Hz in the "Copper In" reactor achieved a 4-log_{10} reduction. At 240 s, the log_{10} reductions of *S.* Typhimurium achieved by PAW generated with 0.02 and 0.2$S.m^{-1}$ water at 2000Hz in the "Copper In" reactor were 3.67 and 5.90, respectively, which were also significant ($p<0.05$).

Log-linear regression and Weibull Models were used to fit the experimental results. Overall, the Weibull model was able to fit well all experimental data with $R^2 = 0.99$, shown in Appendix 9.1, indicating that there was a non-linear relationship between PAW inactivation and treatment time. A similar non-linear trend has been observed by other authors [90, 100]. Therefore, the Weibull model was used to predict the time required (t_{xd}) to achieve 2-log_{10} reduction (x=2) and 4-log_{10} reduction (x=4) for each discharge configuration (see **Table 10**), using the equation below:

$$t_{xd} = \delta - (x)^{\frac{1}{p}}$$

The times to achieve 4-log_{10} reduction of *E. coli* 0157:H7 and *S.* Typhimurium, with PAW solution generated with 0.2$S.m^{-1}$ water at 2000 Hz of discharge frequency in the "Copper In" reactor with atmospheric air, were 288.80 s and 179.37 s, respectively.

Table 11 outlines the PAW solutions chosen for quality attribute studies. PAW(1) and PAW(4) are representative of a low and extreme treatment which corresponds to RONS content and ORP value. PAW(2) and PAW(3) represent mild treatments but with a retention in efficacy against *E. coli* and *S.* Typhimurium as discussed above. PAW(3) was also chosen to replicate industry application with initial water conductivity comparable to that of tap water.

In this study, fresh cut beef samples were treated with PAW(3) and PAW(4). Two treatment volumes, 0.14 ml and 0.57 ml/g sample were chosen through consultation with ProAnd Associates Australia Pty Ltd. Beef was analysed for iron, selenium, zinc and protein content (represented as % Nitrogen). No significant changes in iron and selenium content was determined for all PAW treated samples, however, a significant increase ($P<0.05$) in zinc content for beef treated with 0.14ml PAW(3)/g sample was observed when compared to untreated samples. There was also no significant difference in nitrogen content for beef treated with PAW(4), however, there was a significant decrease in nitrogen content for beef treated with the 0.57ml PAW(3)/g sample.

To investigate the effect of PAW on vitamin content in beef, pyridoxine (PN), a vitamer of vitamin B6, was determined through HPLC analysis. PN content, before and after PAW treatment, is shown in **Table 13**. Animal tissue is an important source of B6 and their abundance and high bioavailability make them an especially rich source when compared to fruits and vegetable. B6 vitamers is generally unstable, it is partially lost during cooking and it may be

susceptible to degradation during storage. From this study, PAW showed little effect on the PN content of beef samples with only PAW (3) showing any significant decline in vitamin content from 0.15 mg PN/100g sample to 0.08 mg PN/g sample after treatment.

The pH value of beef is an important indicator of beef freshness and is generally within the range of 5.30 -5.70. pH above 5.7 negatively impacts on the acceptable eating quality as well as enabling the growth of spoilage and pathogenic microorganisms, which in turn reduces the shelf life of the product. pH also influences the water holding capacity (WHC) of beef with a high WHC leading to low drip loss and cook loss, making it highly desirable. The isoelectric point (IEP) of major proteins in beef is approximately 5.5 and any shifts from the IEP can lead to swelling or shrinkage of myofibrils. pH values of beef treated with PAW(1), PAW(2) PAW(3) and PAW(4) are provided in **Table 14**, showing not be significantly different compared to untreated beef.

Other important indicators of beef freshness are the extent of lipid oxidation and the formation of malondialdehyde (MDA), a product of polyunsaturated fatty acid degradation. The products of fatty acids oxidation give off-flavours and odours that are rancid. The effect of PAW treatment on lipid oxidation was measured in TBARS values, presented in mg MDA/kg sample and based on the spectrophotometric measurement of a complex formed between thiobarbituric acid (TBA) and MDA. As PAW is an oxidative process, it is important to determine the effects of free radicals on lipids. The TBARS values for beef treated with 2% lactic acid, PAW(2), (3) and (4) are illustrated in **Fig. 40**(a). PAW reduced the extent of lipid oxidation in beef samples compared with water and lactic acid. Treatment volumes ranging from 0.14ml/g to 0.57ml/g sample decreased the extent of lipid oxidation in beef as demonstrated in **Fig. 40**(b). All samples treated with PAW resulted in TBARS values well below the rancidity threshold of 2mgMDA/kg beef.

Myoglobin is a heme pigment carrying protein which exists in different states, namely oxymyoglobin (OxyMb), metmyoglobin (MetMb) and deoxymyoglobin (DeoMb). %OxyMb, %MetMb and %DeoMB where measured in beef treated with PAW (1), (2), (3) and (4). Myoglobin is readily oxidised into OxyMb when in contact with oxygen and is responsible for the desirable red appearance of meat that is expected by consumers. There were no significant differences observed in %OxyMb between PAW treated beef and untreated control. The surface colour of raw beef plays a major role in consumer acceptability. **Table 15** shows the differences in colour coordinate values, lightness (ΔL*), redness (Δa*), and yellowness (Δb*), for treatment with water, 2% lactic acid, PAW(1), (2), (3) and (4) against untreated control. **Table 15** shows the effects of water, PAW and lactic acid on colour coordinate values. Beef treated with PAW (2), (3) and (4) showed no significant difference in lightness (L*). Treatment of beef with PAW(1), (2), (3) and (4) resulted in a significant reduction in redness(b*) when compared to water, however, was not significantly different to the impact on beef redness (b*) using lactic acid, a common disinfectant in the meat industry.

Like colour, the textural profile of beef also plays a role in consumer acceptability. The water holding capacity (WHC) of beef affects not only consumer quality attributes such as tenderness, texture and drip loss, but also plays a major role in production yield and the overall economic value of meat. WHC relates to the ability of meat to hold its own or added water with the application of a force. WHC % of beef treated with PAW(1), (2), (3) and (4) is listed in **Table 16**. There is a significant increase in beef WHC when treated with PAW(1) and PAW(2). This can be related to increase in tenderness in beef treated with PAW(1) as shown in Warner-Bratzler Shear Force analysis, also in **Table 16**. A significant reduction in shear force was observed for beef treated with 0.57ml/g sample PAW (3) and (4) demonstrating the ability of PAW to improve beef tenderness.

The impact of PAW on beef tenderness after cooking to an internal temperature of 70 ± 1°C was studied. **Table 17** shows textural and physical quality attributes of cooked beef treated with PAW(3) and PAW(4) at volumes of either 0.14 and 0.57 ml/g sample. A significant decrease in shear force and therefore an increase in tenderness in beef treated with 0.14 ml PAW(4)/g sample, was observed. However, no significant differences were observed when using PAW(3). Overall, beef treated with PAW did not show significant changes to cooking loss, cooking yield, thermal shortening and surface colour (table 9).

In this study, beef samples were treated with water, PAW(2), PAW(3), and PAW(4) and subsequently packaged, vacuumed packed and stored at 4 ± 1 °C for 4 weeks. The shelf life of vacuum packaged meat was determined through the analysis of drip loss, pH, anaerobic and aerobic mesophilic plate count as well as changes in colour. There was no significant difference in drip loss between treatments during the first 2 weeks. A significant increase in drip loss for PAW treated samples was observed at week 3, compared to untreated control, but was not shown to be significantly different to water treatment. To extend the shelf life of unsealed beef, an effective pH well below 5.7 should be maintained for a long period of time. pH of samples decreased initially in the first week and began to steadily increase throughout the next 3 weeks but did not exceed 5.31. There was a significant decrease in pH observed in beef treated with PAW(3) and PAW(4) in the first week compared to other treatments. During the first 3 weeks, there was no significant changes in colour between PAW treated and untreated beef. At week 4, PAW treatment increased the lightness (L*) and redness (b*), suggesting a good retention in colour during storage. Initial population of anaerobic and aerobic mesophilic plate count was significantly lower in PAW treated samples, as expected (**Fig. 42**). Throughout 3 weeks, PAW(2), (3) and (4) performed greater at controlling anaerobic population when compared to water. At the end of storage, final bacterial population was lower in PAW treated samples than control. A similar trend was observed for aerobic mesophilic population within the first 2 weeks.

The shelf life of unsealed beef (PAW treated and stored without vacuum sealing) was determined by treating beef with 0.14 ml PAW(4)/g sample and 0.57 ml PAW(4)/g sample and stored at 4 ± 1 ºC for up to 8 days. Sampling was done at 0, 2, 4 and 8 days for analysis of colour, pH, TBARS, texture profile and total plate count. During storage beef treated with PAW(4) retained its lightness (L*) and redness (a*) better than water treatments (**Fig. 43**). Yellowness (b*) decreased over time for all treatment methods. At day 8, there were no significant differences in L*, a* or b* between samples treated with PAW(4) and samples treated with water. The pH value was expected to increase during storage due to the breakdown of proteins by microorganisms and enzymes into ammonia and amines. This is demonstrated in **Fig. 43** with the untreated sample reaching pH 5.44 at day 8 from an initial pH of 5.33. The pH of beef treated with 0.14 ml PAW(4)/g sample and 0.57 ml PAW(4)/g sample, remained below pH 5.33 during storage reaching a final pH of 5.26, 5.29 at day 8, respectively. The capability of PAW treatment to maintain a low pH in beef samples can be attributed to the reduction in bacterial species and therefore protein breakdown as demonstrated in **Fig. 44**.

TBARS value was expected to increase during storage due to the ongoing oxidation caused by available oxygen [34], as oxygen levels in packaging were not controlled. From **Table 20**, TBARS value increased after 2 days from 0.013g MDA/kg sample to 0.028 g MDA/kg sample with treatment of PAW of 0.14 ml/g sample and from 0.021 to 0.025 MDA/kg sample when treated with 0.57 ml/g sample. TBARS value remained constant over the following 6 days, which was not significantly different from untreated and water treated samples.

Shear force was measured for samples treated with PAW(4) at treatment volumes of 0.14 ml/g sample, 0.57 ml/g sample and a 1 minute dip. There was no initial difference in shear force on day 0. By days 2 and 4, shear force with 0.14 mlPAW/g sample was significantly lower compared to untreated sample. By day 6, shear force of both 0.14 ml/PAW g sample and a 1-min dip treatment were significantly lower than untreated samples.

This study shows the advantages of PAW treatment for shelf-life extension with improved tenderness, retention of low pH and without negative effects on lipid oxidation.

6.4 Phase 4 Discussion

The optimization of the lab scale PAW generation was firstly investigated in two basic configurations (the pin-to-liquid reactor and the plasma-bubbles generator). Discharges above the water surface (pin to liquid) [50] and discharge in bubbles [11] are a few of many reactor designs that cause distinct breakdown strengths in the gas phase and liquid

during plasma discharge, and consequently, influence the composition of reactive oxygen and nitrogen species (RONS) generated not only in the gaseous plasma but also in the liquid [101].

The pin-to-liquid reactor was used in previous milestones but the plasma-bubbles reactor was introduced in this report. Few studies have investigated the benefits of plasma bubbles for the water activation [11, 16], promoting the maximisation of gas-liquid contact with better mass transfer rate [57, 102]. Glow [in the dielectric barrier discharge (DBD) section] and spark (bubble formation) discharges were observed during the discharge process [**Fig. 10**(a)-(b)]. The presence of the DBD component in the reactor attributed to the NO_3^- enrichment in PAW due to the formation of O_3 as a main product in the gas phase [87], while spark discharges are responsible for NO_x generation [90]. In addition, the input power supplied during the PAW generation by both reactors was below 20 W with the discharge power of ~10 W.

PAW has the ability to inactivate bacterial cells by causing oxidative stress on the cell membrane, which leads to cell death [103]. The present results shows that an improved inactivation of both Escherichia coli and Salmonella Typhimurium was obtained by the pin-to-liquid reactor and the plasma-bubbles generator when:

1. PAW was generated at a higher discharge frequency of 2000 Hz. In principle, at higher frequencies, more energy is transferred to the gas-liquid system during plasma discharge, which subsequently leads to the generation of activated species at higher energy levels via collisions between electrons, gas particles and water molecules [9].
2. PAW was generated with a higher initial liquid conductivity of 0.2 $S{\cdot}m^{-1}$ using NaCl during plasma discharge. Conductivity is believed to play an important role in the reaction kinetics by plasma discharge [93]. Increasing the conductivity strengthens the localised electric field and creates greater electron density during the PAW generation.

Energy efficiencies at 1.00 $g{\cdot}kW^{-1}h^{-1}$ or below indicate low yields [104]. In this study, 3.45-11.6 $g{\cdot}kW^{-1}h^{-1}$ of RONS energy efficiencies were achieved by the pin-to-liquid and plasma-bubbles discharges. It is worth noting that we achieved a 5.70 times higher RONS energy efficiency with the pin-to-liquid discharge compared with the maximum value of 1.75 $g{\cdot}kW^{-1}h^{-1}$ reported in the literature [104].

As indicated in Section 5, PAW produced by the pin-to-liquid discharge reduced survived bacterial populations faster than plasma bubble at various operating configurations. Even though the pin-to-liquid discharge reactor exhibited higher energy efficiency, the plasma-bubble generator design lends itself to increased efficacy and scale-up due to the ease of employing numerous holes in the design.

In this report, a novel hybrid plasma discharge was also developed to further optimise the energy efficiency and the disinfectant ability of PAW at a higher input power (~95 W). It is of great importance to regulate the RONS composition in PAW for the industrial feasibility of an energy-efficient, low-cost and rapid disinfectant unit.

Hybrid plasma discharge, which combined two bubble reactors within one power source (one reactor connected to the positive terminal of the plasma power source and the other one connected to the negative terminal), has been utilised in the production of ammonia as a renewable energy carrier and a material for hydrogen storage [105]. This hybrid discharge was reported to be beneficial for higher production of aqueous reactive nitrogen species and energy efficiency. Hence, this inspired our research into combining the pin-to-liquid discharge and the plasma-bubble discharge, referred to as a hybrid plasma discharge (HPD) in this report.

At a higher input voltage of 200 V during plasma activation in the HPD reactor, the total RONS concentration increased. This is because a greater ionisation rate with a higher plasma density was induced at higher voltages compared to lower voltages [54, 55].

In addition, the present results show that PAW generated by all configurations (orifice diameter, orifice number, liquid volume and salinity) of HPD reactors inactivated *E. coli* with at least 2-$\log_{10}$ reduction after the contact time of 30 s. Higher inactivation was achieved when:

1. The orifice diameter of the bubble column in the HPD reactor was reduced from 2 mm to 0.4 mm. This is attributed to the increased NO_3^- concentration [**Fig. 50**(f)] by the increased generation of bubbles with a smaller diameter resulting in an increased gas-liquid interfacial area [106], and an expansion in the internal gas pressure of the bubbles [107, 108].
2. The HPD reactor had one orifice compared to eight orifices. This is likely because when the number of orifices increased to eight orifices, the NO_2^-, NO_3^- and dissolved O_3 concentrations decreased [**Fig. 50**(e)] due to a reduction in the plasma intensity; this was a result of maintaining a fixed flow rate while increasing the number of orifices [109].
3. Reducing the liquid volume.

The *E. coli* inactivation by 2L PAW via the HPD reactor was further optimised with increasing the salinity of the liquid during plasma discharge. Among the PAW with varying salinities, 8 mM NaCl PAW generated by the M2 reactor was the most efficient with 5.18-$\log_{10}$ reduction after 30 s contact time [**Fig. 51**(b)]. This is attributed to the increased NO_2^- concentrations and the reduced pH resulting from increased salinity.

With regard to the RONS energy efficiencies of the HPD reactors, the energy efficiencies at 2 L in this study were (i) ~1.5-3.4 times higher than the gliding-arc reactor at 0.2 L [110], (ii) ~2-5.6 times higher than the pin-to-liquid reactor at 0.02 mL [104], (iii) up to 1.9 times higher than the bubble DBD reactor at 0.04 L [104], (iv) at least 1.3-3.1 times higher than the single micro-bubble reactor at 0.2 L [15], (v) up to 0.7 times higher than the double micro-bubble reactors at 0.2 L [15] and (vi) up to 6.2 times higher than the double plasma jets at 0.1 L [62]. Additionally, the HPD reactors utilised in this study achieved similar or greater bacterial removal of 99% within seconds compared to the other reported studies that used PAW for bacterial removal, thereby demonstrating the dual benefits of using this technology [111]. It is worth nothing that most of reported studies used contact times of several minutes [112] and hours [99, 112, 113] to achieve at least 99% bacterial removal while the HPD reactors inactivated 99% of bacteria populations in seconds with outstanding RONS energy efficiencies.

The present results demonstrate that the HPD reactors proposed in this study consumed less energy and promoted a more sustainable process to produce RONS for fast and effective bacterial removal, which has not been demonstrated previously in other studies. Furthermore, PAWs generated by the HPD reactors can be applied for meat surface disinfection, while at the same time achieving a high inactivation rate in seconds.

Furthermore, the combination of PAW and ultrasound was developed in this study. The synergetic effect of PAW and ultrasound improved the bacterial inactivation in chicken [96], fish [63] and tomato [64]. It was reported that PAW was firstly generated, and the bacterial sample was soaked in PAW and sonicated in an ultrasonic bath for more than 10 min to achieve a significant difference of the inactivation in comparison to the PAW treatment alone [63, 64, 96]. However, this approach is inefficient and would lead to longer installation time and cost for industrial implementation. Instead of sonicating after PAW generation, we proposed and designed an ultrasonic HPD reactor (**Fig. 12**) that combines plasma and ultrasound for the RONS generation in PAW. To the best of our knowledge, there is no research available showing the cavitation effect of ultrasound during PAW generation.

As indicated in Section 5.4, ultrasound increased the total RONS concentration during the generation of PAW via the HPD reactor with more than 6-$\log_{10}$ reduction of both *E. coli* and *S.* Typhimurium inactivation after the contact time of 30 s. This suggests that the explosion of ultrasonic cavitation bubbles increased the RONS concentration [64, 96].

The high-voltage (HV) electrode and the bubble column in the HPD reactor produced plasma discharges simultaneously, one at top of the liquid surface and the other one through the fabricated hole of the ground electrode, which allows air to flow through the side of the electrode. The electric field distribution of the HPD reactor, shown in Figure 3, contributes to the ionisation rate and the high average electron energy, which sustain the plasma discharges via both the high-voltage and ground electrodes and improve the production of excited oxygen and nitrogen species. The NO_2^- species was dominant compared to other species (NO_3^- and H_2O_2) during the production of PAW due to the increased formation of singlet $^1O_2$ via pathways (17)-(25) during the interaction between plasma and NaCl solution, and (b) the oxidation reaction of NO with singlet $^1O_2$ to form ONOOH, which decompose to OH^- and NO_2^- (28 %) or into NO_2^- and H^+ (78 %) [114].

$$Cl^- + O \rightarrow ClO^- \quad (17)$$

$$Cl^- + O_3 \rightarrow ClO^- + O_2 \quad (18)$$

$$Cl^- + 2 \cdot OH \rightarrow ClO^- + H_2O \quad (19)$$

$$Cl^- + H_2O_2 \rightarrow ClO^- + H_2O \quad (20)$$

$$ClO^- + H_2O_2 \rightarrow Cl^- + H_2O + O_2 \quad (21)$$

$$\cdot OH + Cl^- \rightarrow HOCl^{\cdot -} \quad (22)$$

$$HOCl^{\cdot -} \rightarrow Cl^{\cdot} + OH^- \quad (23)$$

$$Cl^{\cdot} + Cl^- \rightarrow Cl_2^{\cdot -} \quad (24)$$

$$Cl_2^{\cdot -} + H_2O_2 \rightarrow 2Cl^- + {}^1O_2^{\cdot} + 2H^+ \quad (25)$$

All reported studies in the literature investigated the antibacterial efficiency of PAW only via the meat immersion method. However, the immersion method is only suitable for smaller cuts of meat. Findings in this study have successfully proven the use of spraying as a meat washing method, inactivating *S.* Typhimurium on beef, which has not been validated by other reported studies. **Fig. 58**(a) indicates that the PAW inactivation against *S.* Typhimurium on beef increased when the contact time was increased from 15 to 60 for the meat washing methods, spraying and immersion. Compared to water, the reactive species, NO_2^-, NO_3^- and H_2O_2, of PAW with low pH contributed higher bacterial inactivation through the damages in cell membrane and intracellular components. Irrespective to the storage time of meat and meat washing method, the PAW's inactivation efficiencies were significantly higher than water at the contact times of 30 and 60s. In this study, the bacterial inactivation via the meat immersion in PAW has successfully been demonstrated in 15-60 s compared to other literatures that demonstrated the inactivation in more than 5 min [115, 116].

Surface colour plays a major role in consumer acceptability. L^* (lightness) colour value can be linked with the fat content of meat with higher fat content reflecting more light [39]. Irrespective to the storage time of meat, the L^* colour values of all samples are in the range of 46.7-50.5 (**Table 24**) with an insignificant difference. This means that the fat contents of all samples are about the same, reflecting the same amount of light. **Table 24** also shows that PAW had a significant impact on the a^* (redness) colour values compared to untreated and water-treated samples. A

discolouration was observed on the surface of PAW-treated sample in T3 in **Fig. 59**. This phenomenon indicated that the reactive species in PAW accelerated the formation of metmyoglobin, resulting a decrease in the a^* colour value [115]. A reduction in a^* colour value makes meat less acceptable to consumers. This can be supported by a significant reduction in the oxymyoglobin (OxyMb) of beef rump by PAW (**Fig. 60**), which affects red appearance of meat. For instance, at the beef storage time of 1 day, the OxyMb decreased from 63.6 % (T1) to 44.1 % (T3) (**Fig. 60**). However, this was mitigated by introducing an additional water washing after spraying with PAW. This increased the a^* colour value from 11.3 in T3 to 18.2 in T4 at the storage time of 1 day (**Table 24**). The colour retention after PAW treatment followed by water washing and 1 day storage is observed in T4 (**Fig. 59**). After the water-treated beef samples were stored at 4 °C for 7 days, there was a change in colour an all samples, including the control samples, due the effect of oxygen as samples were not vacuum sealed. This is expected and can be linked with lipid oxidation [39]. Similarly, to the results after 1 day storage, PAW treated samples without a subsequent water washing underwent a discolouration process after 7 days of storage (T3 in **Fig. 59**); the a^* colour value in T3 reduced from 21.7, for 1 day of storage, to 15.4, for 7 days of storage (**Table 24**). After 7 days of meat storage in a container at 4 ^{o}C, all beef samples (T1, T2, T3 and T4) appeared to have browning characteristics, shown in **Fig. 59**, indicating chemical changes in myoglobin due to the oxygen content. This can be supported a reduction in the deoxymyoglobin (DeoMb) and an increase in the metmyoglobin (MetMb) with the meat storage time of 7 days, compared to the storage time of 1 day (**Fig. 60**).

PAW had no significant impact on the C colour value at the storage time of 1 day. However, there is a significant decrease between the untreated sample and the PAW-treated sample at the storage time of 7 days, from 21.9 in the control samples, to 16.2 in T3 (**Table 24**). Lower C colour value indicates that meat has a less vivid colour. h^* (hue angle) colour value indicates the colour stability and show if there is a colour development from red to yellow. **Table 24** shows that the h^* colour values are in the range of 0.95-1.64 but with no significant differences at both storage times of 1 day and 7 days. The colour difference (ΔE) values of all samples were calculated in Table 2. ΔE describes small differences between colours as detected by human eyes: 0-0.5 trace, 0.5-1.5 slight, 1.5-3 noticeable, 3.0-6.0 appreciable, 6.0-12.0 much, >12.0 very much [39]. Our results in **Table 24** shows that after 1 day storage, PAW treatment without water washing exhibited a “much” difference (10.7 in T3 in **Table 24**) compared to control, but PAW followed by water washing exhibited changes that are appreciable (3.45 in T2 in **Table 24**). it must be noted that just water washing induced a noticeable change (2.37 in T4 in **Table 24**) which is not very different to PAW followed by water washing. Table 2 also indicated that there was an insignificant difference between T2 and T4. Again, the full data after 7 days of storage will be complete for the final milestone. The pH of meat is a highly important indicator of beef freshness and is generally within the range of 5.3-5.70. pH above 5.7 negatively impacts on the acceptable eating quality as well as enabling the growth of spoilage and pathogenic microorganisms, which in turn reduces the shelf-life of the product. The pH in **Fig. 61** were in the range of 5.31-5.54. To extend the shelf-life of beef, an effective pH well below 5.7 should be maintained [35]. pH is known to influence the water holding capacity (WHC) of beef. With the isoelectric point (IEP) of major proteins in beef being approximately 5.5, any shifts from the IEF leads to swelling or shrinkage of myofibrils. The WHC relates to the ability of meat to hold its own or added water with the application of force. It affects not only consumer quality attributes such as tenderness, texture and drip loss, but also plays a major role in production yield and the overall economic value of meat. From this study, PAW has no significant impact on WHC of the untreated and water-treated beef samples as shown in **Fig. 62**, likely due to no change in the space in the myofibril compartment [34].

The extend of lipid oxidation and the formation of malondialdehyde (MDA) is an important indicator of beef freshness. MDA is a product of polyunsaturated fatty acid degradation. The products of fatty acids oxidation give off-flavours and odours that are referred to as ‘rancid’. The effect of PAW on lipid oxidation was measured in TBARS values as shown in **Fig. 64**, presented in mg MDA·kg^{-1} sample and based on the spectrophotometric measurement of a complex formed between thiobarbituric acid (TBA) and MDA. As PAW is an oxidative process, it is important to determine the effects of radical species on lipid present on the beef surface. From this study, PAW had no significant impact on lipid oxidation as shown in **Fig. 64**. Throughout the meat storage time, untreated, PAW-treated and water-treated beef samples

resulted in TBARS values well below the rancidity threshold of 2 mg MDA·kg^{-1} [35]. Moreover, the TBARS values obtained in this study were in the range of 0.256 to 0.679, which indicate that the meat is fresh [39]. These results indicates that PAW could preserve the lipid oxidation of beef.

In terms of the inactivation of *Salmonella* on beef rump, **Fig. 65** shows that there was a significant difference between the water spraying at 55 ^{o}C for 30 s (0.38-log$_{10}$ reduction or 58.4% inactivation efficiency) and the PAW spraying at 55 ^{o}C for 30 s (0.66-log$_{10}$ reduction or 77.6% inactivation efficiency) at meat storage time of 1 day. Similarly, when the additional water spraying at 25 ^{o}C for 60 s was introduced, there was a significant difference between the water spraying (0.35-log$_{10}$ reduction or 54.7% inactivation efficiency, **Fig. 65**) and PAW spraying (0.7-log$_{10}$ reduction or 78.7% inactivation efficiency, **Fig. 65**). These findings agreed to the reported PAW studies on (i) the inactivation of *E. coli* (from 0.08- to 0.49-log$_{10}$ reduction) and *S.aureus* (from 0.02 to 0.49-log$_{10}$ reduction) on chicken at the contact times of 30-60 min [96] and (ii) the inactivation of bacteria of the Fibrobacteres-Chlorobi-Bacteriodetes (FCB) group (3.1-log$_{10}$ reduction) on beef at the contact time of 24 h [117]. We demonstrated that PAW killed bacteria faster in seconds than those reported in the literature.

In terms of economic analysis, **Table 25** indicates the approximate capital costs of PAW technology for the small- and medium-scale enterprise producers. The total amounts of hot standard carcass were estimated to be 68 tons per year for the small producers and 536 tons per year for the medium producers, assuming that the annual cattle production is 200 head for the small producers and 1576 head for the medium producers [41] and the operating day and daily operation are 251 days and 9 h, respectively [44]. Assuming that 1 ton of hot standard carcass requires 10.6 kL of town water and 4% of the water is used for carcass washing [43], the amounts of town water needed for carcass washing for the small and medium producers were about 115 L and 905 L per day, respectively. If we select the meat washing with the additional water spraying of water at 25 ^{o}C for 30 seconds (from Section 5.4) for the scale-up technology, the antibacterial efficiencies of washing with both water and PAW followed by water washing were 54.7% and 78.7%, respectively. From our experiment, the total volume of PAW with the addition of water washing at 25 ^{o}C for 30 seconds (from Section 5.4) is about 303 mL. In order to achieve the same inactivation as PAW with the addition of water washing, 508 mL of water is required. This means that meat washing with PAW can save water by 40.4%. From this, the amounts of PAW needed for the small and medium producers were estimated to be 616 L and 4,857 L, respectively. The capital cost in this experiment is around A$ 34,900, including the costs of plasma reactor, plasma generator, mist spray with pump, liquid tank and heating equipment. By applying the six-tenth power rule starting from the cost of the lab-scale device, the total costs of scale-up PAW technology for the small and medium scale producers were estimated to A$ 362,767 and A$ 1,252,051, respectively (**Table 25**). In addition, the capital cost of PAW technology for the medium producers(AU$ 1,252,051, **Table 25**) is comparable with (i) the cost of hot water treatment system for a plant killing around 100 heads per hour (A$ 719,500) [118] and (ii) the cost of a cabinet with organic acids (A$ 431,700) [118]. The capital costs of of hot water and organic acid treatments were recalculated using the inflation calculator by Reserve Bank of Australia with the total change in cost of 43.9% (from 2005 to 2021) because the costs were outdated, estimated in 2005 [118]. However, the capital costs of PAW technology calculated in this study are cheaper than the total capital cost of scale-up non-thermal plasma reactor for wastewater (A$ 2,067,659) [40].

7.0 Conclusions / Recommendations

In Phase 1, favourable reductions in microbial populations were achieved with a PAW treatment of 390 s on both free-living and adhered cells. Maximum efficacy was achieved with PAW containing approximately 871 ± 110 µM NO_2^- and 820 ± 116 µM NO_3^- , generated in a closed system with a 30-min plasma discharge exposure time using a larger container thereby increasing the water surface area. This report also found that retention of reactive species could be achieved when stored under favourable conditions for up to 30 days. PAW's retention of efficacy over storage time and PAW's effect on bacterial species including the treatment of cells inoculated onto red meat.

In Phase 2, the data reported shows how optimal PAW efficacy can be achieved by varying treatment procedure rather than improving upon the concentration of reactive species within PAW. Treatment volume, contact time, temperature and wash treatment type play important roles in both the removal and destruction of pathogenic and spoilage microorganisms. As a result of the combined effects of cell removal and destruction through PAW treatment, $\log_{10}$ reductions of 2.67 can be estimated for *E. coli* O157, 2.66 for *S.* Typhimurium, 3.63 for *L. monocytogenes* and 3.12 for *B. thermosphacta*. PAW was also shown to have continued antimicrobial effects with efficacy continuing for over 30 min. The continued bactericidal properties of PAW will make it advantageous for industry applications where the control of cross contamination is of high concern.

In Phase 3, PAW was optimised with discharge type, frequency and conductivity. It was shown that a “Copper in” reactor, along with a higher frequency of 2,000Hz and conductivity of 0.2S.m^{-1}, produced PAW (PAW(4)) with a significantly higher concentration of reactive species and subsequently imparted a higher antimicrobial effect against *E. coli* and S. Typhimurium. To assess the impact of PAW on the quality attributes of beef, PAW(4) along with milder PAW solutions were used to determine their effects on minerals including iron, zinc and selenium, vitamin B6, colour, pH, lipid oxidation and texture profile analysis (TPA) of unsealed beef. The following combinations were used: 1) PAW(1) with Copper out , 1,000Hz and 0S.m^{-1}, 2) PAW(2) with Copper in, 2,000Hz and 0S.m^{-1} and 3) PAW(3) with Copper in, 2,000Hz and 0.02S.m^{-1}.

There was no significant difference observed in vitamin B6, zinc, selenium and iron level in beef treated with PAW(2) and PAW(4). Colour analysis showed that treatment with PAW(2), (3) and (4) has no significant difference in lightness (L*), and yellowness (b*) compared to beef treated with water. There was a significant reduction in redness (a*) with PAW treatment compared to water. However, this was not significantly different to the reduction in redness observed when treated with 2% lactic acid, a traditional chemical disinfectant. The limited effects on beef colour was also confirmed through haem pigment analysis showing no significant differences in %OxyMb between PAW treated and untreated beef. OxyMb is the oxygenated form of myoglobin state responsible for the red appearance of beef. Interestingly, the extent of lipid oxidation improved with PAW treatment compared to both water and lactic acid treatment. Treatment with PAW(1) and PAW(2) showed a significant increase in the water holding capacity of beef compared to untreated. Furthermore, textural analysis, measured as shear force, revealed a significant increase in beef tenderness with 0.14ml PAW(2)/g sample, 0.57ml PAW(3) and PAW(4) /g sample. Significant Improvements in beef tenderness after cooking was observed in beef treated with 0.14ml PAW(4). Besides, no negative impacts on cooking loss, cooking yield and thermal shortening were observed for beef treated with PAW(3) and PAW(4).

This study demonstrated that the shelf life of fresh meat, either unsealed or under vacuum packaging, improved with PAW treatment. Unsealed beef treated with PAW had lower aerobic microbial population after 8 days of storage when compared to untreated and water treated samples. An increase in pH during storage was also inhibited with the use of PAW treatment thereby improving eating quality. No significant effects on lipid oxidation were observed using PAW during storage. Tenderness of beef also improved over storage time when compared to untreated beef. Vacuum-packaged beef maintained the redness value (a*) better than untreated sample with no negative impacts on drip loss and pH during 4 weeks storage. Anaerobic microbial population in PAW treated beef samples was lower than untreated and water treated samples thereby improving its overall acceptability.

In Phase 4, plasma-activated water (PAW) was firstly produced at 0.2 L and optimised with discharge type, discharge frequency and initial liquid conductivity. The concentration of reactive nitrogen species (RNS) increased with increased values of the initial liquid electric conductivity for the pin-to-liquid discharge. For the plasma-bubble discharge, the NO_2^- increased, the NO_3^- decreased, with increasing liquid conductivity when the ground electrode was positioned on the outside of the reactor. PAW generated by the pin-to-liquid discharge at a frequency of 2000 Hz, initial conductivity of 0.2 S·m^{-1} and with the grounded electrode positioned inside the reactor, achieved the highest rate of inactivation of *E. coli* and *S.* Typhimurium with a 3.99 ± 0.13-$\log_{10}$ reduction at 300 s and 5.90 ± 0.24-$\log_{10}$ reduction at 240 s, respectively, with an RONS energy-efficiency of 10.1 ± 0.1 g·kW^{-1}·h^{-1}. In contrast, a RONS energy-efficiency of 3.80 ± 0.20 g·kW^{-1}·h^{-1} was achieved by the plasma-bubble generator at 2000 Hz, 0.2 S·m^{-1} and with the ground electrode

positioned outside the reactor. This set of conditions reached inactivation levels of 1.03 ± 0.08- and 3.01 ± 0.14-log_{10} reduction for *E. coli* and *S*. Typhimurium, respectively, at 960 s.

This study also scaled up the production of PAW from 0.2 L (via the pin-to-liquid discharge) to 2 L [via the novel hybrid plasma-bubbles discharge (HPD) reactor] while achieving more than 5-log_{10} reduction in 30 seconds of contact time, which can be implemented for the washing and decontamination of carcasses on processing lines in abattoirs. The effect of input voltage (from 100 to 200 V), orifice size (from 400 to 200 µm), number of orifices (from one to eight orifices), liquid volume (from 0.5 to 2 L) and liquid composition (from 0 to 8mM NaCl) on the physicochemical properties of PAW and its microbial inactivation efficiency were investigated. The specific conclusions are as follows:

- Input voltage, orifice size, number of orifices, liquid volume and salinity acidified the water during plasma discharge and changed the electrical conductivity and the ORP of PAW.
- Increasing input voltage, reducing orifice diameter, increasing liquid volume and increasing salinity increased the total RONS concentration; however, increasing the number of orifices decreased the total RONS concentration.
- The RONS energy efficiencies of HPD reactors (M1, M2, M3) with 0.5L MilliQ were at the lowest (3.25-4.73 $g \cdot kW^{-1} \cdot h^{-1}$) and the highest (4.78-11.2 $g \cdot kW^{-1} \cdot h^{-1}$) with 2L MilliQ.
- 5.18-log_{10} reduction of *E. coli* inactivation was achieved in the contact time of 30 s by PAW with 8mM NaCl via the 2L M2 reactor.

The HPD reactors in this study demonstrated the dual benefits of high bacterial removal (99%) within seconds and exceptional RONS energy efficiencies compared to literature studies, which take several minutes or hours to achieve same level of bacterial inactivation. This study also demonstrated that ultrasound increased the production of reactive and nitrogen species (RONS) during the generation of PAW, from 144 to 157 $mg \cdot L^{-1}$. At the contact of 20 s, the HPD reactors with and without ultrasound achieved more than 6.79-log_{10} reduction of *S.* Typhimurium inactivation. The *E. coli* inactivation at 20 s by the HPD reactors with and without ultrasound were 3.64 and 3.98-log_{10} reduction, respectively.

Furthermore, a simulation of the electric-field distribution in the hybrid plasma discharge (HPD) reactor was demonstrated. In a short contact time, spraying and immersion methods with PAW produced about the same antimicrobial efficacy of PAW against *S.* Typhimurium adhered to beef surface. Irrespective to the application method, increasing the contact time from 15 s to 30 s improved the antimicrobial efficiacy. In terms of beef quality, PAW preserved the lightness, pH, water holding capacity and TBARS value of beef. Although PAW reduced the redness of the beef, this was successfully mitigated by introducing the water spraying at 25 ^{o}C for 60 s right after the PAW spraying at 55 ^{o}C for 30 s. The PAW spraying at 55 ^{o}C for 30 s followed by the water washing at 25 ^{o}C for 60 s achieved the inactivation of 0.7-log_{10} reduction or 78.7% inactivation efficiency. The total capital costs of scale-up PAW technology were estimated to be A$ 362,767 for the small scale enterprise producers and and A$ 1,252,051 for the medium scale enterprise producers. The findings of this study provide the tools for larger scale designs that can be implemented in actual meat processing facilities.

For future work, the production of PAW at a commercial scale and the effect of PAW technology on carcasses in commercial facilities would be needed for the commercialisation of this technology. As PAW contains many reactive species, future work should also verify whether there is no formation of any toxic substances that could affect the meat safety.

8.0 Bibliography

[1] M. Kirk, L. Ford, K. Glass, G. Hall, Foodborne illness, Australia, circa 2000 and circa 2010, Emerg Infect Dis 20(11) (2014) 1857-64. https://doi.org/10.3201/eid2011.131315.
[2] P. Mafart, O. Couvert, S. Gaillard, I. Leguerinel, On calculating sterility in thermal preservation methods: application of the Weibull frequency distribution model, International Journal of Food Microbiology 72(1-2) (2002) 107-113. https://doi.org/10.1016/s0168-1605(01)00624-9.
[3] M. Peleg, M.B. Cole, Reinterpretation of microbial survival curves, Crit Rev Food Sci Nutr 38(5) (1998) 353-80. https://doi.org/10.1080/10408699891274246.
[4] M. van Boekel, On the use of the Weibull model to describe thermal inactivation of microbial vegetative cells, International Journal of Food Microbiology 74(1-2) (2002) 139-159. https://doi.org/10.1016/s0168-1605(01)00742-5.
[5] A.H. Geeraerd, V.P. Valdramidis, J.F. Van Impe, GInaFiT, a freeware tool to assess non-log-linear microbial survivor curves, Int J Food Microbiol 102(1) (2005) 95-105. https://doi.org/10.1016/j.ijfoodmicro.2004.11.038.
[6] P.M. Girard, A. Arbabian, M. Fleury, G. Bauville, V. Puech, M. Dutreix, J.S. Sousa, Synergistic Effect of H2O2 and NO2 in Cell Death Induced by Cold Atmospheric He Plasma, Sci Rep 6 (2016) 29098. https://doi.org/10.1038/srep29098.
[7] S. Park, W. Choe, S.Y. Moon, J.J. Shi, Electron Information in Single- and Dual-Frequency Capacitive Discharges at Atmospheric Pressure, Sci Rep 8(1) (2018) 7516. https://doi.org/10.1038/s41598-018-25892-w.
[8] A. Zeb, F. Ullah, A Simple Spectrophotometric Method for the Determination of Thiobarbituric Acid Reactive Substances in Fried Fast Foods, J Anal Methods Chem 2016 (2016) 9412767. https://doi.org/10.1155/2016/9412767.
[9] S. Tang, N. Lu, J. Li, Y. Wu, Removal of bisphenol A in water using an integrated granular activated carbon preconcentration and dielectric barrier discharge degradation treatment, Thin Solid Films 521 (2012) 257-260. https://doi.org/10.1016/j.tsf.2011.10.201.
[10] R. Zhang, C. Zhang, X. Cheng, L. Wang, Y. Wu, Z. Guan, Kinetics of decolorization of azo dye by bipolar pulsed barrier discharge in a three-phase discharge plasma reactor, J Hazard Mater 142(1-2) (2007) 105-10. https://doi.org/10.1016/j.jhazmat.2006.07.071.
[11] A. Mai-Prochnow, D. Alam, R. Zhou, T. Zhang, K. Ostrikov, P.J. Cullen, Microbial decontamination of chicken using atmospheric plasma bubbles, Plasma Processes and Polymers 18(1) (2020). https://doi.org/10.1002/ppap.202000052.
[12] B. Sun, M. Sato, J. Sid Clements, Optical study of active species produced by a pulsed streamer corona discharge in water, Journal of Electrostatics 39(3) (1997) 189-202. https://doi.org/10.1016/s0304-3886(97)00002-8.
[13] X. Su, Y. Tian, H. Zhou, Y. Li, Z. Zhang, B. Jiang, B. Yang, J. Zhang, J. Fang, Inactivation Efficacy of Nonthermal Plasma-Activated Solutions against Newcastle Disease Virus, Appl Environ Microbiol 84(9) (2018). https://doi.org/10.1128/AEM.02836-17.
[14] V. Rathore, S.K. Nema, Optimization of process parameters to generate plasma activated water and study of physicochemical properties of plasma activated solutions at optimum condition, Journal of Applied Physics 129(8) (2021). https://doi.org/10.1063/5.0033848.
[15] R. Zhou, T. Zhang, R. Zhou, S. Wang, D. Mei, A. Mai-Prochnow, J. Weerasinghe, Z. Fang, K. Ostrikov, P. Cullen, Sustainable plasma-catalytic bubbles for hydrogen peroxide synthesis, Green Chemistry (2021). https://doi.org/10.1039/d1gc00198a.
[16] R. Zhou, R. Zhou, D. Alam, T. Zhang, W. Li, Y. Xia, A. Mai-Prochnow, H. An, E.C. Lovell, H. Masood, R. Amal, K. Ostrikov, P.J. Cullen, Plasmacatalytic bubbles using CeO2 for organic pollutant degradation, Chemical Engineering Journal 403 (2021). https://doi.org/10.1016/j.cej.2020.126413.
[17] Y.M. Zhao, A. Patange, D.W. Sun, B. Tiwari, Plasma-activated water: Physicochemical properties, microbial inactivation mechanisms, factors influencing antimicrobial effectiveness, and applications in the food industry, Compr Rev Food Sci Food Saf 19(6) (2020) 3951-3979. https://doi.org/https://doi.org/10.1111/1541-4337.12644.
[18] T. Royintarat, P. Seesuriyachan, D. Boonyawan, E.H. Choi, W. Wattanutchariya, Mechanism and optimization of non-thermal plasma-activated water for bacterial inactivation by underwater plasma jet and delivery of reactive species underwater by cylindrical DBD plasma, Current Applied Physics 19(9) (2019) 1006-1014. https://doi.org/10.1016/j.cap.2019.05.020.
[19] G.E. Conway, A. Casey, V. Milosavljevic, Y. Liu, O. Howe, P.J. Cullen, J.F. Curtin, Non-thermal atmospheric plasma induces ROS-independent cell death in U373MG glioma cells and augments the cytotoxicity of temozolomide, Br J Cancer 114(4) (2016) 435-43. https://doi.org/10.1038/bjc.2016.12.
[20] S.A. Sajib, M. Billah, S. Mahmud, M. Miah, F. Hossain, F.B. Omar, N.C. Roy, K.M.F. Hoque, M.R. Talukder, A.H. Kabir, M.A. Reza, Plasma activated water: the next generation eco-friendly stimulant for enhancing plant seed

germination, vigor and increased enzyme activity, a study on black gram (Vigna mungo L.), Plasma Chemistry and Plasma Processing 40(1) (2019) 119-143. https://doi.org/10.1007/s11090-019-10028-3.
[21] M.F. Mustafa, X. Fu, Y. Liu, Y. Abbas, H. Wang, W. Lu, Volatile organic compounds (VOCs) removal in non-thermal plasma double dielectric barrier discharge reactor, J Hazard Mater 347 (2018) 317-324. https://doi.org/10.1016/j.jhazmat.2018.01.021.
[22] M. Janda, K. Hensel, P. Tóth, M.E. Hassan, Z. Machala, The Role of HNO2 in the Generation of Plasma-Activated Water by Air Transient Spark Discharge, Applied Sciences 11(15) (2021). https://doi.org/10.3390/app11157053.
[23] H. Bader, Determination of Ozone In Water By The Indigo Method: A Submitted Standard Method, Ozone: Science & Engineering 4(4) (2008) 169-176. https://doi.org/10.1080/01919518208550955.
[24] B. Tarabová, P. Lukeš, M. Janda, K. Hensel, L. Šikurová, Z. Machala, Specificity of detection methods of nitrites and ozone in aqueous solutions activated by air plasma, Plasma Processes and Polymers 15(6) (2018). https://doi.org/10.1002/ppap.201800030.
[25] Z. Machala, B. Tarabová, D. Sersenová, M. Janda, K. Hensel, Chemical and antibacterial effects of plasma activated water: correlation with gaseous and aqueous reactive oxygen and nitrogen species, plasma sources and air flow conditions, Journal of Physics D: Applied Physics 52(3) (2019). https://doi.org/10.1088/1361-6463/aae807.
[26] G. Gordon, B. Bubnis, Residual Ozone Measurement: Indigo Sensitivity Coefficient Adjustment, Ozone: Science & Engineering 24(1) (2007) 17-28. https://doi.org/10.1080/01919510208901591.
[27] V. Kondeti, C.Q. Phan, K. Wende, H. Jablonowski, U. Gangal, J.L. Granick, R.C. Hunter, P.J. Bruggeman, Long-lived and short-lived reactive species produced by a cold atmospheric pressure plasma jet for the inactivation of Pseudomonas aeruginosa and Staphylococcus aureus, Free Radic Biol Med 124 (2018) 275-287. https://doi.org/10.1016/j.freeradbiomed.2018.05.083.
[28] Y. Song, Y. Xia, Z. Bi, X. Wang, Z. Qi, L. Ji, B. Li, D. Liu, Generation of large-area and glow-like surface discharge in atmospheric pressure air, Physics of Plasmas 23(8) (2016). https://doi.org/10.1063/1.4959586.
[29] R. Zhou, R. Zhou, K. Prasad, Z. Fang, R. Speight, K. Bazaka, K. Ostrikov, Cold atmospheric plasma activated water as a prospective disinfectant: the crucial role of peroxynitrite, Green Chemistry 20(23) (2018) 5276-5284. https://doi.org/10.1039/c8gc02800a.
[30] W.D. Bigelow, J.R. Esty, The Thermal Death Point in Relation to Time of Typical Thermophilic Organisms, Journal of Infectious Diseases 27(6) (1920) 602-617. https://doi.org/10.1093/infdis/27.6.602.
[31] A. Rezaeimotlagh, M. Resch, R.P. Kuchel, J. Biazik, D. Ziuzina, P. Bourke, P.J. Cullen, F.J. Trujillo, Unveiling the synergistic effect of combining low and high frequency electric fields for microbiological safety in liquid food processing, Journal of Food Engineering 303 (2021). https://doi.org/10.1016/j.jfoodeng.2021.110588.
[32] E. Tsoukou, P. Bourke, D. Boehm, Temperature Stability and Effectiveness of Plasma-Activated Liquids over an 18 Months Period, Water 12(11) (2020). https://doi.org/10.3390/w12113021.
[33] P. Estifaee, X. Su, S.K. Yannam, S. Rogers, S.M. Thagard, Mechanism of E. coli Inactivation by Direct-in-liquid Electrical Discharge Plasma in Low Conductivity Solutions, Sci Rep 9(1) (2019) 2326. https://doi.org/10.1038/s41598-019-38838-7.
[34] R. Moutiq, N.N. Misra, A. Mendonca, K. Keener, In-package decontamination of chicken breast using cold plasma technology: Microbial, quality and storage studies, Meat Sci 159 (2020) 107942. https://doi.org/10.1016/j.meatsci.2019.107942.
[35] J. Barrales Astorga, K. Hadinoto, P. Cullen, S. Prescott, F.J. Trujillo, Effect of plasma activated water on the nutritional composition, storage quality and microbial safety of beef, Lwt 154 (2022). https://doi.org/10.1016/j.lwt.2021.112794.
[36] K. Jo, S. Lee, C. Jo, H.J. Jeon, J.H. Choe, Y.S. Choi, S. Jung, Utility of winter mushroom treated by atmospheric non-thermal plasma as an alternative for synthetic nitrite and phosphate in ground ham, Meat Sci 166 (2020) 108151. https://doi.org/10.1016/j.meatsci.2020.108151.
[37] Y. Xu, Y. Tian, R. Ma, Q. Liu, J. Zhang, Effect of plasma activated water on the postharvest quality of button mushrooms, Agaricus bisporus, Food Chem 197(Pt A) (2016) 436-44. https://doi.org/10.1016/j.foodchem.2015.10.144.
[38] H.I. Yong, M. Han, H.J. Kim, J.Y. Suh, C. Jo, Mechanism Underlying Green Discolouration of Myoglobin Induced by Atmospheric Pressure Plasma, Sci Rep 8(1) (2018) 9790. https://doi.org/10.1038/s41598-018-28096-4.
[39] E. Pogorzelska, J. Godziszewska, M. Brodowska, A. Wierzbicka, Antioxidant potential of Haematococcus pluvialis extract rich in astaxanthin on colour and oxidative stability of raw ground pork meat during refrigerated storage, Meat Sci 135 (2018) 54-61. https://doi.org/10.1016/j.meatsci.2017.09.002.
[40] L.M. Martini, G. Coller, M. Schiavon, A. Cernuto, M. Ragazzi, G. Dilecce, P. Tosi, Non-thermal plasma in waste composting facilities: From a laboratory-scale experiment to a scaled-up economic model, Journal of Cleaner Production 230 (2019) 230-240. https://doi.org/10.1016/j.jclepro.2019.04.172.

[41] Cattle and beef market study - Interim report, Australian Competition and Consumer Commision, 2016.
[42] R. Holland, D. Loveday, K. Ferguson, How much meat to expect from a beef carcass, University of Tennessee.
[43] Economic Analysis of Demineralisation, Meat & Livestock Australia, 2009.
[44] T. CONSULTANTS, V&V Integrated Waste Management, Australian Meat Processor Corporation, 2022.
[45] A.M. Laury, M.V. Alvarado, G. Nace, C.Z. Alvarado, J.C. Brooks, A. Echeverry, M.M. Brashears, Validation of a lactic acid- and citric acid-based antimicrobial product for the reduction of Escherichia coli O157: H7 and Salmonella on beef tips and whole chicken carcasses, J Food Prot 72(10) (2009) 2208-11. https://doi.org/10.4315/0362-028x-72.10.2208.
[46] K. Harris, M.F. Miller, G.H. Loneragan, M.M. Brashears, Validation of the use of organic acids and acidified sodium chlorite to reduce Escherichia coli O157 and Salmonella typhimurium in beef trim and ground beef in a simulated processing environment, J Food Prot 69(8) (2006) 1802-7. https://doi.org/10.4315/0362-028x-69.8.1802.
[47] M.C. Rojas, S.E. Martin, R.A. Wicklund, D.D. Paulson, F.A. Desantos, M.S. Brewer, Effect of High-Intensity Pulsed Electric Fields on Survival of Escherichia Coli K-12 Suspended in Meat Injection Solutions, Journal of Food Safety 27(4) (2007) 411-425. https://doi.org/10.1111/j.1745-4565.2007.00086.x.
[48] C.N. Cutter, G.R. Siragusa, Reduction of Brochothrix thermosphacta on beef surfaces following immobilization of nisin in calcium alginate gels, Lett Appl Microbiol 23(1) (1996) 9-12. https://doi.org/10.1111/j.1472-765x.1996.tb00018.x.
[49] W. Van Boxem, J. Van der Paal, Y. Gorbanev, S. Vanuytsel, E. Smits, S. Dewilde, A. Bogaerts, Anti-cancer capacity of plasma-treated PBS: effect of chemical composition on cancer cell cytotoxicity, Sci Rep 7(1) (2017) 16478. https://doi.org/10.1038/s41598-017-16758-8.
[50] P. Lu, D. Boehm, P. Cullen, P. Bourke, Controlled cytotoxicity of plasma treated water formulated by open-air hybrid mode discharge, Applied Physics Letters 110(26) (2017). https://doi.org/10.1063/1.4990525.
[51] T. Zhang, R. Zhou, P. Wang, A. Mai-Prochnow, R. McConchie, W. Li, R. Zhou, E.W. Thompson, K. Ostrikov, P.J. Cullen, Degradation of cefixime antibiotic in water by atmospheric plasma bubbles: Performance, degradation pathways and toxicity evaluation, Chemical Engineering Journal (2020). https://doi.org/10.1016/j.cej.2020.127730.
[52] W.F.L.M. Hoeben, P.P. van Ooij, D.C. Schram, T. Huiskamp, A.J.M. Pemen, P. Lukeš, On the Possibilities of Straightforward Characterization of Plasma Activated Water, Plasma Chemistry and Plasma Processing 39(3) (2019) 597-626. https://doi.org/10.1007/s11090-019-09976-7.
[53] Q. Xiang, X. Liu, S. Liu, Y. Ma, C. Xu, Y. Bai, Effect of plasma-activated water on microbial quality and physicochemical characteristics of mung bean sprouts, Innovative Food Science & Emerging Technologies 52 (2019) 49-56. https://doi.org/10.1016/j.ifset.2018.11.012.
[54] K. Liu, Z. Yang, S. Liu, Study of the Characteristics of DC Multineedle-to-Water Plasma-Activated Water and Its Germination Inhibition Efficiency: The Effect of Discharge Mode and Gas Flow, IEEE Transactions on Plasma Science 48(4) (2020) 969-979. https://doi.org/10.1109/tps.2020.2980040.
[55] Y. Li, R. Zhou, F. Qi, D. Zhou, R. Zhou, J. Wan, Y. Xian, P.J. Cullen, X. Lu, K. Ostrikov, Plasma-enabled liquid ethanol conversion for hydrogen production: discharge characteristics and process control, Journal of Physics D: Applied Physics 53(17) (2020). https://doi.org/10.1088/1361-6463/ab71ac.
[56] H.S. Uhm, S.H. Ki, K.Y. Baik, E.H. Choi, Influence of oxygen on generation of reactive chemicals from nitrogen plasma jet, Sci Rep 8(1) (2018) 9318. https://doi.org/10.1038/s41598-018-27473-3.
[57] A. John, A. Brookes, I. Carra, B. Jefferson, P. Jarvis, Microbubbles and their application to ozonation in water treatment: A critical review exploring their benefit and future application, Critical Reviews in Environmental Science and Technology (2020) 1-43. https://doi.org/10.1080/10643389.2020.1860406.
[58] J. Li, J. Ahn, D. Liu, S. Chen, X. Ye, T. Ding, Evaluation of Ultrasound-Induced Damage to Escherichia coli and Staphylococcus aureus by Flow Cytometry and Transmission Electron Microscopy, Appl Environ Microbiol 82(6) (2016) 1828-1837. https://doi.org/10.1128/AEM.03080-15.
[59] K.H. Baek, H.I. Yong, J.H. Yoo, J.W. Kim, Y.S. Byeon, J. Lim, S.Y. Yoon, S. Ryu, C. Jo, Antimicrobial effects and mechanism of plasma activated fine droplets produced from arc discharge plasma on planktonic Listeria monocytogenes and Escherichia coli O157:H7, Journal of Physics D: Applied Physics 53(12) (2020). https://doi.org/10.1088/1361-6463/ab634d.
[60] Y. Li, J. Pan, G. Ye, Q. Zhang, J. Wang, J. Zhang, J. Fang, In vitro studies of the antimicrobial effect of non-thermal plasma-activated water as a novel mouthwash, Eur J Oral Sci 125(6) (2017) 463-470. https://doi.org/10.1111/eos.12374.
[61] Y. Tian, R. Ma, Q. Zhang, H. Feng, Y. Liang, J. Zhang, J. Fang, Assessment of the Physicochemical Properties and Biological Effects of Water Activated by Non-thermal Plasma Above and Beneath the Water Surface, Plasma Processes and Polymers 12(5) (2015) 439-449. https://doi.org/10.1002/ppap.201400082.

[62] C.M. Lin, C.P. Hsiao, H.S. Lin, J.S. Liou, C.W. Hsieh, J.S. Wu, C.Y. Hou, The Antibacterial Efficacy and Mechanism of Plasma-Activated Water Against Salmonella Enteritidis (ATCC 13076) on Shell Eggs, Foods 9(10) (2020). https://doi.org/10.3390/foods9101491.
[63] Y.-M. Zhao, M. Oliveira, C.M. Burgess, J. Cropotova, T. Rustad, D.-W. Sun, B.K. Tiwari, Combined effects of ultrasound, plasma-activated water, and peracetic acid on decontamination of mackerel fillets, Lwt 150 (2021). https://doi.org/10.1016/j.lwt.2021.111957.
[64] M. Ali, D.W. Sun, J.H. Cheng, O. Johnson Esua, Effects of combined treatment of plasma activated liquid and ultrasound for degradation of chlorothalonil fungicide residues in tomato, Food Chem 371 (2022) 131162. https://doi.org/10.1016/j.foodchem.2021.131162.
[65] K. Oehmigen, M. Hähnel, R. Brandenburg, C. Wilke, K.D. Weltmann, T. von Woedtke, The Role of Acidification for Antimicrobial Activity of Atmospheric Pressure Plasma in Liquids, Plasma Processes and Polymers 7(3-4) (2010) 250-257. https://doi.org/10.1002/ppap.200900077.
[66] M. Bafoil, A. Jemmat, Y. Martinez, N. Merbahi, O. Eichwald, C. Dunand, M. Yousfi, Effects of low temperature plasmas and plasma activated waters on Arabidopsis thaliana germination and growth, PLoS One 13(4) (2018) e0195512. https://doi.org/10.1371/journal.pone.0195512.
[67] P. Lukes, E. Dolezalova, I. Sisrova, M. Clupek, Aqueous-phase chemistry and bactericidal effects from an air discharge plasma in contact with water: evidence for the formation of peroxynitrite through a pseudo-second-order post-discharge reaction of H2O2and HNO2, Plasma Sources Science and Technology 23(1) (2014). https://doi.org/10.1088/0963-0252/23/1/015019.
[68] J.-L. Brisset, J. Pawlat, Chemical Effects of Air Plasma Species on Aqueous Solutes in Direct and Delayed Exposure Modes: Discharge, Post-discharge and Plasma Activated Water, Plasma Chemistry and Plasma Processing 36(2) (2015) 355-381. https://doi.org/10.1007/s11090-015-9653-6.
[69] P. Rahmadi, Y.R. Kim, Effects of different levels of ozone on ammonia, nitrite, nitrate, and dissolved organic carbon in sterilization of seawater, Desalination and Water Treatment 52(22-24) (2013) 4413-4422. https://doi.org/10.1080/19443994.2013.803702.
[70] M.J. Traylor, M.J. Pavlovich, S. Karim, P. Hait, Y. Sakiyama, D.S. Clark, D.B. Graves, Long-term antibacterial efficacy of air plasma-activated water, Journal of Physics D: Applied Physics 44(47) (2011). https://doi.org/10.1088/0022-3727/44/47/472001.
[71] J. Shen, Y. Tian, Y. Li, R. Ma, Q. Zhang, J. Zhang, J. Fang, Bactericidal Effects against S. aureus and Physicochemical Properties of Plasma Activated Water stored at different temperatures, Sci Rep 6 (2016) 28505. https://doi.org/10.1038/srep28505.
[72] M. Naitali, G. Kamgang-Youbi, J.M. Herry, M.N. Bellon-Fontaine, J.L. Brisset, Combined effects of long-living chemical species during microbial inactivation using atmospheric plasma-treated water, Appl Environ Microbiol 76(22) (2010) 7662-4. https://doi.org/10.1128/AEM.01615-10.
[73] Q. Zhang, Y. Liang, H. Feng, R. Ma, Y. Tian, J. Zhang, J. Fang, A study of oxidative stress induced by non-thermal plasma-activated water for bacterial damage, Applied Physics Letters 102(20) (2013). https://doi.org/10.1063/1.4807133.
[74] G. Kamgang-Youbi, J.M. Herry, T. Meylheuc, J.L. Brisset, M.N. Bellon-Fontaine, A. Doubla, M. Naitali, Microbial inactivation using plasma-activated water obtained by gliding electric discharges, Lett Appl Microbiol 48(1) (2009) 13-8. https://doi.org/10.1111/j.1472-765X.2008.02476.x.
[75] G. Kamgang-Youbi, J.M. Herry, J.L. Brisset, M.N. Bellon-Fontaine, A. Doubla, M. Naitali, Impact on disinfection efficiency of cell load and of planktonic/adherent/detached state: case of Hafnia alvei inactivation by plasma activated water, Appl Microbiol Biotechnol 81(3) (2008) 449-57. https://doi.org/10.1007/s00253-008-1641-9.
[76] D. Selgas, M. Luisa Marín, C. Pin, C. Casas, Attachment of bacteria to meat surfaces: A review, Meat Science 34(3) (1993) 265-273. https://doi.org/10.1016/0309-1740(93)90076-t.
[77] P.M. Fratamico, F.J. Schultz, R.C. Benedict, R.L. Buchanan, P.H. Cooke, Factors Influencing Attachment of Escherichia coli O157:H7 to Beef Tissues and Removal Using Selected Sanitizing Rinses (double dagger), J Food Prot 59(5) (1996) 453-459. https://doi.org/10.4315/0362-028X-59.5.453.
[78] M.M. Theron, J.F.R. Lues, Organic Acids and Meat Preservation: A Review, Food Reviews International 23(2) (2007) 141-158. https://doi.org/10.1080/87559120701224964.
[79] F.H. Grau, End Products of Glucose Fermentation by Brochothrix thermosphacta, Appl Environ Microbiol 45(1) (1983) 84-90. https://doi.org/10.1128/aem.45.1.84-90.1983.
[80] R.H. Dainty, C.M. Hibbard, Precursors of the major end products of aerobic metabolism ofBrochothrix thermosphacta, Journal of Applied Bacteriology 55(1) (1983) 127-133. https://doi.org/10.1111/j.1365-2672.1983.tb02656.x.
[81] R.H. Dainty, C.M. Hibbard, Aerobic metabolism of Brochothrix thermosphacta growing on meat surfaces and in laboratory media, J Appl Bacteriol 48(3) (1980) 387-96. https://doi.org/10.1111/j.1365-2672.1980.tb01027.x.

[82] K. Milios, E.H. Drosinos, P.E. Zoiopoulos, Carcass decontamination methods in slaughterhouses: a review, Journal of the Hellenic Veterinary Medical Society 65(2) (2017). https://doi.org/10.12681/jhvms.15517.
[83] R.O. Elder, J.E. Keen, G.R. Siragusa, G.A. Barkocy-Gallagher, M. Koohmaraie, W.W. Laegreid, Correlation of enterohemorrhagic Escherichia coli O157 prevalence in feces, hides, and carcasses of beef cattle during processing, Proc Natl Acad Sci U S A 97(7) (2000) 2999-3003. https://doi.org/10.1073/pnas.97.7.2999.
[84] M.D. Hardin, G.R. Acuff, L.M. Lucia, J.S. Oman, J.W. Savell, Comparison of Methods for Decontamination from Beef Carcass Surfaces, J Food Prot 58(4) (1995) 368-374. https://doi.org/10.4315/0362-028X-58.4.368.
[85] K. Kučerová, Z. Machala, K. Hensel, Transient Spark Discharge Generated in Various N2/O2 Gas Mixtures: Reactive Species in the Gas and Water and Their Antibacterial Effects, Plasma Chemistry and Plasma Processing 40(3) (2020) 749-773. https://doi.org/10.1007/s11090-020-10082-2.
[86] C.-h. Wang, Y. Wu, G.-f. Li, Inactivation of E. coli with plasma generated by bipolar pulsed discharge in a three-phase discharge plasma reactor, Journal of Electrostatics 66(1-2) (2008) 71-78. https://doi.org/10.1016/j.elstat.2007.08.002.
[87] K. Tachibana, J.-S. Oh, T. Nakamura, Oxidation processes of NO for production of reactive nitrogen species in plasma activated water, Journal of Physics D: Applied Physics 53(38) (2020). https://doi.org/10.1088/1361-6463/ab91eb.
[88] Z. Machala, B. Tarabova, K. Hensel, E. Spetlikova, L. Sikurova, P. Lukes, Formation of ROS and RNS in Water Electro-Sprayed through Transient Spark Discharge in Air and their Bactericidal Effects, Plasma Processes and Polymers 10(7) (2013) 649-659. https://doi.org/10.1002/ppap.201200113.
[89] Z. Liu, C. Zhou, D. Liu, T. He, L. Guo, D. Xu, M.G. Kong, Quantifying the concentration and penetration depth of long-lived RONS in plasma-activated water by UV absorption spectroscopy, AIP Advances 9(1) (2019). https://doi.org/10.1063/1.5037660.
[90] M.J. Pavlovich, T. Ono, C. Galleher, B. Curtis, D.S. Clark, Z. Machala, D.B. Graves, Air spark-like plasma source for antimicrobial NOxgeneration, Journal of Physics D: Applied Physics 47(50) (2014). https://doi.org/10.1088/0022-3727/47/50/505202.
[91] R. Burlica, M.J. Kirkpatrick, B.R. Locke, Formation of reactive species in gliding arc discharges with liquid water, Journal of Electrostatics 64(1) (2006) 35-43. https://doi.org/10.1016/j.elstat.2004.12.007.
[92] T. Shao, C. Zhang, Z. Fang, Y. Yu, D. Zhang, P. Yan, Y. Zhou, E. Schamiloglu, A Comparative Study of Water Electrodes Versus Metal Electrodes for Excitation of Nanosecond-Pulse Homogeneous Dielectric Barrier Discharge in Open Air, IEEE Transactions on Plasma Science 41(10) (2013) 3069-3078. https://doi.org/10.1109/tps.2013.2279254.
[93] N. Lu, J. Li, Y. Wu, S. Masayuki, Treatment of Dye Wastewater by Using a Hybrid Gas/Liquid Pulsed Discharge Plasma Reactor, Plasma Science and Technology 14(2) (2012) 162-166. https://doi.org/10.1088/1009-0630/14/2/15.
[94] M. Schmidt, V. Hahn, B. Altrock, T. Gerling, I.C. Gerber, K.-D. Weltmann, T. von Woedtke, Plasma-Activation of Larger Liquid Volumes by an Inductively-Limited Discharge for Antimicrobial Purposes, Applied Sciences 9(10) (2019). https://doi.org/10.3390/app9102150.
[95] K. Kutasi, D. Popović, N. Krstulović, S. Milošević, Tuning the composition of plasma-activated water by a surface-wave microwave discharge and a kHz plasma jet, Plasma Sources Science and Technology 28(9) (2019). https://doi.org/10.1088/1361-6595/ab3c2f.
[96] T. Royintarat, E.H. Choi, D. Boonyawan, P. Seesuriyachan, W. Wattanutchariya, Chemical-free and synergistic interaction of ultrasound combined with plasma-activated water (PAW) to enhance microbial inactivation in chicken meat and skin, Sci Rep 10(1) (2020) 1559. https://doi.org/10.1038/s41598-020-58199-w.
[97] A. Kilonzo-Nthenge, S. Liu, S. Yannam, A. Patras, Atmospheric Cold Plasma Inactivation of Salmonella and Escherichia coli on the Surface of Golden Delicious Apples, Front Nutr 5 (2018) 120. https://doi.org/10.3389/fnut.2018.00120.
[98] G.G. Balan, I. Rosca, E.L. Ursu, F. Doroftei, A.C. Bostanaru, E. Hnatiuc, V. Nastasa, V. Sandru, G. Stefanescu, A. Trifan, M. Mares, Plasma-activated water: a new and effective alternative for duodenoscope reprocessing, Infect Drug Resist 11 (2018) 727-733. https://doi.org/10.2147/IDR.S159243.
[99] Y.M. Zhao, S. Ojha, C.M. Burgess, D.W. Sun, B.K. Tiwari, Inactivation efficacy and mechanisms of plasma activated water on bacteria in planktonic state, J Appl Microbiol 129(5) (2020) 1248-1260. https://doi.org/10.1111/jam.14677.
[100] M. Huang, H. Zhuang, J. Wang, W. Yan, J. Zhao, J. Zhang, Inactivation Kinetics of Salmonella typhimurium and Staphylococcus aureus in Different Media by Dielectric Barrier Discharge Non-Thermal Plasma, Applied Sciences 8(11) (2018). https://doi.org/10.3390/app8112087.
[101] R. Zhou, R. Zhou, P. Wang, Y. Xian, A. Mai-Prochnow, X. Lu, P.J. Cullen, K. Ostrikov, K. Bazaka, Plasma-activated water: generation, origin of reactive species and biological applications, Journal of Physics D: Applied Physics 53(30) (2020). https://doi.org/10.1088/1361-6463/ab81cf.

[102] A. Wright, M. Taglioli, F. Montazersadgh, A. Shaw, F. Iza, H.C.H. Bandulasena, Microbubble-enhanced DBD plasma reactor: Design, characterisation and modelling, Chemical Engineering Research and Design 144 (2019) 159-173. https://doi.org/10.1016/j.cherd.2019.01.030.
[103] N. Misra, O. Schlüter, P. Cullen, Cold Plasma in Food and Agriculture: Fundamentals and Applications, Elsevier Science2016.
[104] K. Tachibana, T. Nakamura, Comparative study of discharge schemes for production rates and ratios of reactive oxygen and nitrogen species in plasma activated water, Journal of Physics D: Applied Physics 52(38) (2019). https://doi.org/10.1088/1361-6463/ab2529.
[105] J. Sun, D. Alam, R. Daiyan, H. Masood, T. Zhang, R. Zhou, P.J. Cullen, E.C. Lovell, A. Jalili, R. Amal, A hybrid plasma electrocatalytic process for sustainable ammonia production, Energy & Environmental Science 14(2) (2021) 865-872. https://doi.org/10.1039/d0ee03769a.
[106] H. Shi, H. Jiang, Y. Liu, R. Chen, Bubble dynamics and mass transfer characteristics from an immersed orifice plate, Journal of Chemical Technology & Biotechnology 95(6) (2020) 1729-1738. https://doi.org/10.1002/jctb.6370.
[107] E. Shiomitsu, T. Sakoda, Characteristics of an Underwater Plasma Source with a Porous Glass Membrane, Electronics and Communications in Japan 98(12) (2015) 72-79. https://doi.org/10.1002/ecj.11772.
[108] Y. Hayashi, N. Takada, Wahyudiono, H. Kanda, M. Goto, Hydrogen Peroxide Formation by Electric Discharge with Fine Bubbles, Plasma Chemistry and Plasma Processing 37(1) (2016) 125-135. https://doi.org/10.1007/s11090-016-9767-5.
[109] X. Wang, J. Luo, Y. Huang, J. Mei, Y. Chen, Degradation of pharmaceutical contaminants by bubbling gas phase surface discharge plasma combined with g-C3N4 photocatalysis, Environmental Science: Water Research & Technology 7(3) (2021) 610-621. https://doi.org/10.1039/d0ew00985g.
[110] M. Wartel, F. Faubert, I.D. Dirlau, S. Rudz, N. Pellerin, D. Astanei, R. Burlica, B. Hnatiuc, S. Pellerin, Analysis of plasma activated water by gliding arc at atmospheric pressure: Effect of the chemical composition of water on the activation, Journal of Applied Physics 129(23) (2021). https://doi.org/10.1063/5.0040035.
[111] C.-M. Lin, C.-P. Hsiao, H.-S. Lin, J.S. Liou, C.-W. Hsieh, J.-S. Wu, C.-Y. Hou, The Antibacterial Efficacy and Mechanism of Plasma-Activated Water Against Salmonella Enteritidis (ATCC 13076) on Shell Eggs, Foods 9(10) (2020). https://doi.org/10.3390/foods9101491.
[112] A. Soni, J. Choi, G. Brightwell, Plasma-Activated Water (PAW) as a Disinfection Technology for Bacterial Inactivation with a Focus on Fruit and Vegetables, Foods 10(1) (2021). https://doi.org/10.3390/foods10010166.
[113] Y. Bai, A. Idris Muhammad, Y. Hu, S. Koseki, X. Liao, S. Chen, X. Ye, D. Liu, T. Ding, Inactivation kinetics of Bacillus cereus spores by Plasma activated water (PAW), Food Res Int 131 (2020) 109041. https://doi.org/10.1016/j.foodres.2020.109041.
[114] K. Hadinoto, J.B. Astorga, H. Masood, R. Zhou, D. Alam, P.J. Cullen, S. Prescott, F.J. Trujillo, Efficacy optimization of plasma-activated water for food sanitization through two reactor design configurations, Innovative Food Science & Emerging Technologies 74 (2021). https://doi.org/10.1016/j.ifset.2021.102867.
[115] J. Qian, L. Yan, K. Ying, J. Luo, H. Zhuang, W. Yan, J. Zhang, Y. Zhao, Plasma-activated water: A novel frozen meat thawing media for reducing microbial contamination on chicken and improving the characteristics of protein, Food Chem 375 (2022) 131661. https://doi.org/10.1016/j.foodchem.2021.131661.
[116] J. Qian, C. Wang, H. Zhuang, M.M. Nasiru, J. Zhang, W. Yan, Evaluation of meat-quality and myofibrillar protein of chicken drumsticks treated with plasma-activated lactic acid as a novel sanitizer, Lwt 138 (2021). https://doi.org/10.1016/j.lwt.2020.110642.
[117] Y. Zhao, Z. Zhao, R. Chen, E. Tian, D. Liu, J. Niu, W. Wang, Z. Qi, Y. Xia, Y. Song, Plasma-Activated Water Treatment of Fresh Beef: Bacterial Inactivation and Effects on Quality Attributes, IEEE Transactions on Radiation and Plasma Medical Sciences 4(1) (2020) 113-120. https://doi.org/10.1109/trpms.2018.2883789.
[118] https://www.mla.com.au/globalassets/mla-corporate/research-and-development/program-areas/food-safety/documents/food-safety-intervention/organic-acids.pdf.

9.0 Appendices

9.1 Parameters and Goodness of Fit for Log-Linear Model and Weibull Model.

Table S1

Parameters and goodness of fit for log-linear model and Weibull model by the pin-to-liquid discharge.

Microbe	***E. coli* 0157:H7**					***S.* Typhimurium**				
Microbial Model	**Log Linear**		**Weibull**			**Log Linear**		**Weibull**		
Model Parameter	k_{max} (x10^{-3})	$RMSE$ (x10^{-2})	δ	p	$RMSE$ (x10^{-2})	k_{max} (x10^{-3})	$RMSE$ (x10^{-2})	δ	p	$RMSE$ (x10^{-2})
1 000Hz, GO										
0S.m^{-1}	5.61	23.6	599	1.77	13.3	8.24	8.20	323	1.12	5.41
2 000Hz, GO										
0S.m^{-1}	18.2	25.1	190	1.42	14.4	33.97	21.2	87.6	1.26	17.8
0.02S.m^{-1}	20.8	26.2	165	1.50	6.47	39.00	30.0	83.9	1.33	24.2
0.2S.m^{-1}	21.2	25.0	162	1.48	4.36	40.13	18.0	70.4	1.16	16.0
2 000Hz, GI										
0.02S.m^{-1}	15.1	34.4	250	2.34	8.82	35.40	12.7	79.8	1.18	4.66
0.2S.m^{-1}	33.2	42.8	117	6.31	26.4	58.66	12.7	67.8	1.42	4.66

Table S2

Parameters and goodness of fit for log-linear model and Weibull model by the plasma-bubble generator.

Microbe	***E. coli* 0157:H7**					***S.* Typhimurium**				
Microbial Model	**Log Linear**		**Weibull**			**Log Linear**		**Weibull**		
Model Parameter	k_{max} (x10^{-4})	$RMSE$ (x10^{-2})	δ	p	$RMSE$ (x10^{-2})	k_{max} (x10^{-4})	$RMSE$ (x10^{-2})	δ	p	$RMSE$ (x10^{-2})
GO, 0.2 L.min^{-1}, 0 S.m^{-1}										
1 000 Hz	9.10	3.33	4419	0.61	2.14	9.30	3.20	5974	0.49	3.62
2 000 Hz	12.3	5.55	2187	0.79	1.18	14.9	7.28	1593	0.93	4.39
1 000 Hz, GO, 0.4 L.min^{-1}										
0S.m^{-1}	7.72	39.2	1907	1.67	0.99	17.8	5.53	1295	0.99	0.71
2 000Hz, GO, 0.8 L.min^{-1}										
0 S.m^{-1}	9.46	2.73	1488	2.13	1.55	34.9	2.00	727	1.31	2.22
0.02 S.m^{-1}	11.2	2.91	2088	0.97	3.54	43.0	9.78	585	1.17	9.55
0.2 S.m^{-1}	24.0	13.6	961	2.05	3.83	74.2	17.3	405	1.30	6.72
2 000Hz, GI, 0.8 L.min^{-1}										
0.02S.m^{-1}	8.73	0.70	2878	0.92	0.33	35.9	9.11	643	1.00	11.2
0.2S.m^{-1}	20.3	3.19	1124	1.08	3.55	30.9	7.25	765	1.09	8.50